ADSORPTION OF PB (II) IONS FROM WATER USING MAGNETICALLY MODIFIED BIOCHARS OBTAINED FROM MICROWAVE-ASSISTED PYROLYSIS

by

Patrick Muesi Godwin

M.Eng in Chemical Engineering, The University of Manchester, 2017

A Thesis Submitted in Partial Fulfillment of

the Requirements for the Degree of

Master of Science in Engineering

in the Graduate Academic Unit of Chemical Engineering

Supervisors: Huining Xiao, PhD, Chemical Engineering

Muhammad T. Afzal, PhD, Mechanical Engineering

Examining Board: Brian Lowery, PhD, Chemical Engineering (Chair)

Guida Bendrich, PhD, Chemical Engineering

Huining Xiao, PhD, Chemical Engineering

Muhammad T. Afzal, PhD, Mechanical Engineering

Kripa S. Singh, PhD, Civil Engineering

This thesis is accepted by the

Dean of Graduate Studies

THE UNIVERSITY OF NEW BRUNSWICK

June 2020

ABSTRACT

In this study, biochars were produced from biomass at pilot scale in a microwave-assisted pyrolysis process. These pyrolyzed biochars were magnetically modified to improve their adsorption performance and facilitate the recovery of the spent biochars from solution. The magnetic chars were investigated as a potential renewable bio-sorbents for removing lead ions from aqueous solution in a batch-mode experiment.

The biochar samples from microwave pyrolysis of 1.5 kg hemp stalks and maple wood chips biomass at a temperature range of 500 - 700 ˚C were first impregnated with H_2O_2 (30%) solution and then magnetized by mixing aqueous Fe^{3+}/Fe^{2+} solution with biochar suspensions, followed by NaOH treatment.

The synthesized magnetic adsorbents were characterized. The effects of temperature, pH, dosage, contact time and initial concentration of Pb (II) solution on adsorption were examined. Adsorption kinetics and isotherm of the modified biochars were modelled and their adsorption performance after 5 regeneration cycles quantified. The adsorbents recovery from solution with a low magnetic field was investigated. The prepared magnetic biochars demonstrated a potential as renewable adsorbents in treating lead ions-contaminated water.

Keywords: Microwave-pyrolysis; Magnetic biochar; hemp; maple; adsorbent; water treatment; heavy metal ions.

DEDICATION

This thesis is dedicated to the Almighty God and my beloved mother!

ACKNOWLEDGEMENTS

Firstly, my utmost gratitude goes to my supervisors Dr. Huining Xiao and Dr. Muhammad T. Afzal for their guidance at every stage of the project. Your supports enabled me to enhance my scientific research capability. I am truly grateful for the experience and invaluable knowledge you have imparted me with during this study.

I am equally indebted and thankful to Dennis Connor for his unwavering support in the analysis of the samples with ICP-OES. Your guidance and unusual patience facilitated the completion of the adsorption study.

Additionally, special thanks go to Steven Cogswell for his instruction and assistance with performing SEM imaging.

Finally, this project could not have been possible without the funding support from Natural Sciences and Engineering Research Councils (NSERC) of Canada. Thank you for the financial support.

Table of Contents

List of Tables

List of Figures

List of Symbols, Nomenclature or Abbreviations

BC	Biochar
BET	Brunauer-Emmett-Teller
EDS	Energy-dispersive X-ray spectroscopy
EDTA-2Na	Ethylenediaminetetraacetic acid disodium salt
FT-IR	Fourier transform infrared spectroscopy
$FeCl_3$	Iron (III) Chloride
$FeCl_3 \cdot 6H_2O$	Iron (III) Chloride Hexahydrate
$FeSO_4.7H_2O$	Iron (II) sulfate heptahydrate
$Fe_2(SO_4)_3$	Iron (III) sulfate
Fe_3O_4	Iron (II, III) oxide
H_2O_2	Hydrogen peroxide
H_2SO_4	Sulphuric acid
HNO_3	Nitric acid
H_3PO_4	Phosphoric acid
ICP-OES	Inductively Coupled Plasma Optical Emission Spectrometer
KBr	Potassium Bromide
$KMnO_4$	Potassium Permanganate
KOH	Potassium Hydroxide
MHBC	Magnetic Hemp Biochar
MMBC	Magnetic Maple Biochar
MSW	Municipal Solid Waste
NaOH	Sodium Hydroxide
$Na_2S_2O_4$	Sodium dithionite
$(NH_4)_2S_2O_8$	Ammonium persulfate
$Pb(NO_3)_2$	Lead nitrate
O_3	Ozone
PFO	Pseudo First Order
PSO	Pseudo Second Order
SEM	Scanning electron microscopy
TGA	Thermo Gravimetric Analyzer
VSM	Vibrating sample magnetometry
XRD	X-Ray Powder Diffraction

Chapter 1 Introduction

1.1. Research Background

Heavy metals are discharged from different industries including mining, metal finishing, electroplating, glass, textiles, ceramics, and storage batteries. Recently, there has been growing concerns over water pollution by heavy metals released from industrial effluents due to the toxic effects of their ions on organisms and their accumulation in biota. Among these heavy metals, lead have received considerable attention due to their toxicity. The presence of these metal ions in water endangers human beings and aquatic lives because they accumulate in the food chains [1]. Therefore, there is the need to purify and recycle wastewater contaminated by heavy metal ions to secure alternative sources of water [2] and to protect our food chains [1].

Several treatment technologies have been suggested to remove these heavy metal ions from contaminated wastewater including adsorption, ion exchange, chemical precipitation, membrane technologies, reverse osmosis and electrochemical treatment [3]. Among these technologies, adsorption is a universal, most convenient and fast method to remove heavy metals from contaminated solutions efficiently at a low cost [4,5]. The major advantages of this treatment technology are its low residue generation and the potential to recover and recycle the used adsorbent [6]. Additionally, bio sorbents are not only environmentally friendly but are also readily available in abundant quantities. A very well-known bio sorbent is biochar. Different kinds of adsorbents (synthetic products and natural materials) have been developed [7]. Ali et. al [2] has shown that carbon-based adsorbents such as activated carbon proved to be the very effective in the adsorption of organic and inorganic pollutants from contaminated water. Although activated carbon is excellent for sorption of

contaminants from water, it is however limited due to its low selectivity and high cost of preparation, whereas it is relatively less costly to prepare "sustainable" biochar. Biochar has attracted attention in recent years as a relatively cheaper bio sorbent with numerous promising potential environmental applications including soil improvement, water treatment and carbon sequestration [8]. Recent studies have shown that biochar as a bio sorbent can be employed as a useful material to sorb heavy metal ions from contaminated water and also as a remedy for immobilization of metal ions in metal-contaminated soil [9–11].

Biochar is a fine-grained, porous and carbon-rich material produced from the thermal degradation of organic materials under oxygen-limited conditions. Biochar has also been proven to be an effective sorbent for the sorption of a wide variety of inorganic and organic pollutants from aqueous solutions. Their large sorption capacity is connected to their highly-porous structure and surface area which contains various functional groups (e.g. hydroxyl, carboxyl, phenolic groups) hence, it has a very strong affinity for heavy metal ions [12–14]. Until recently, the traditional and widely used carbon-based adsorbent for water treatment has been activated carbon. Therefore, for biochar to compete favorably for industrial application, researchers are left with the challenge of ensuring that biochar is the most effective bio sorbents with specific chemical properties. Hence, recent research on biochar has paid attention to their modification and characterization to satisfy the growing demands for cleaner water [15].

Since biochar is a carbonaceous material whose surface is composed of surface functional groups bonded to 'fused' aromatic rings, it is expected that they would possess similar chemical properties to those of aromatic hydrocarbon [16]. Hence, the

chemical reactions applicable to aromatic hydrocarbons would be expected to apply to biochar. The existence of these functional groups on the biochar matrix therefore means they can be altered by chemical or physical methods to manufacture adsorbents that are tailored for specific functions. For example, when adsorption occur in liquid phase, if the adsorbent's surface contains oxygen-containing functional groups, water molecules are preferentially adsorbed to these functional groups to form complexes, thereby obstructing molecules of the target adsorbates from adsorbing onto the adsorbent [16]. In cases like this, it is therefore important to improve the affinity of the surface to targeted adsorbates by proper surface modifications that alters the chemical structure of the adsorbent surface. There has been extensive studies on the removal of heavy metal ions from water using unmodified biochar produced by conventional pyrolysis, capitalizing on the fast adsorption kinetics, high surface area and the nanopores structure of biochar materials [17]. However, metal ions adsorption from aqueous solutions is believed to be fundamentally a function of the nature and quantity of the biochar surface functional groups, rather than just the porosity and surface area of the biochar [18].

One of the major challenges with practical water treatment is the difficulty encountered in isolating and recycling the spent adsorbent from aqueous solution by the traditional methods (filtration and centrifugation). Magnetic separation method has been demonstrated to be a potential technique for solid-liquid phase separation [19]. Using an external/internal magnetic field to isolate the magnetic bio-sorbent from the aqueous solution was convenient. However, to the best of our knowledge, very few studies have investigated the preparation and application of magnetically modified bio sorbent for water treatment. In these cases, the biochars were produced by conventional pyrolysis. There has not been any study of the potential applications of

biochars produced by microwave-assisted pyrolysis for water treatment. Thus, in this study, biochars were produced via microwave-assisted pyrolysis of biomass at pilot scale (1.50 kg reactor feed). These biochars were magnetized before investigating their potential applications for treatment of Pb (II) ions-contaminated water.

Biochars (BC) obtained from microwave pyrolysis of maple wood chips and hemp stalks were modified chemically followed by magnetization in two simple steps: (i) oxidation of the BC using H_2O_2 to improve its adsorption capacity for heavy metal ions. (ii) Preparation of the magnetic modified BC by co-precipitation to load the magnetic particles onto the surface of the modified BC to facilitate the separation of used biochar from aqueous solution. The as-prepared bio-sorbent was characterized and used to adsorb Pb (II) ions from a synthetic water system. Adsorption isotherm, pH dependence, sorption and desorption kinetics of Pb (II) ions on the magnetic modified biochar was studied. An effective method of recovery of the spent biochars using a simple magnetic field was also investigated.

1.2. Objectives

The goals of this research were:

i. Understand the effects of pH, contact time, temperature, heavy metal ions concentration and the adsorbent dose on the adsorption capacity of magnetically modified microwave pyrolyzed biochar.

ii. Carry out a comparable study on the adsorption capacities of biochar from two different biomass; maple wood chips (hardwood biomass) and hemp stalks (agricultural biomass).

iii. Establish a proper procedure for the separation and recovery of the metal loaded biochars from the aqueous solution.

1.3. Significance of study

The outcome of this research provides an invaluable tool in environmental sustainability and recovery applications. As the world intensifies the emphasis on sustainability, biochar and its application are highly likely to play an increasingly vital role in water treatment.

The contributions of this research are as follows:

- Provide a better alternative to activated carbon as a critical tool in upholding water quality in industrial settings.
- Produce a cost effective and eco-friendlier adsorbent with a potential higher adsorption capacity and selectivity for heavy metal pollutants.
- Enhance the recovery and reusability of metal loaded biochar via magnetic modification.
- Provide a deeper insight into the adsorption behaviour of heavy metal ions in aqueous solutions.

1.4. Outline of thesis

In chapter 2, modified biochar is reviewed in its preparation, functionality, application in water treatment and regeneration. The nature of precursor materials, preparatory conditions and modification methods are key factors influencing BC properties. This section examines the different methods of preparing biochar such as slow pyrolysis, fast pyrolysis and microwave-assisted pyrolysis. Furthermore, appropriate method of biochar modification for enhancing the adsorption of different contaminants from

water are discussed. Finally, the section ends with the discussion of biochar application for water treatment and the recovery of spent biochar for re-use.

In chapter 3, biochar produced by microwave-assisted pyrolysis using hemp stalks biomass was investigated. Magnetic modification of the biochar by two simple step process discussed. The magnetic char was investigated for its potential application as a renewable adsorbent for removing lead ions from aqueous solution in a batch-mode experiment. The effects of temperature, pH, contact time and initial concentration of Pb (II) solution on adsorption were examined. The adsorption performance of biochar after 5 regeneration cycles was quantified as well as the recovery of the spent biochar using simple magnetic field.

Chapter 4 evaluates and compares two microwave pyrolyzed biochars produced from agricultural biomass (shredded hemp stalk) vs woody biomass (maple wood chips) for the removal of Pb (II) from aqueous solution in a batch adsorption study. The magnetic biochars characteristics and the effects of pH, adsorbent dose, temperature, contact time and initial concentration of Pb (II) solution on their adsorption performance discussed. Factors such as higher polarity index, pH and zeta potential which contributed to a higher adsorption efficiency of agricultural biochar are discussed in depth. This section ends with the discussion of the kinetics and the isotherms of the adsorption behavior of the magnetic biochars.

Finally, the thesis summary and recommendations for future work are presented in chapter 5.

1.5. Reference

[1] Wang N-X, Zhang X-Y, Wu J, Xiao L, Yin Y, Miao A-J, et al. Effects of microcystin-LR on the metal bioaccumulation and toxicity in Chlamydomonas reinhardtii. Water Res 2012;46:369–77. doi:10.1016/J.WATRES.2011.10.035.

[2] Ali I. The Quest for Active Carbon Adsorbent Substitutes: Inexpensive Adsorbents for Toxic Metal Ions Removal from Wastewater. Sep Purif Rev 2010;39:95–171. doi:10.1080/15422119.2010.527802.

[3] Demirbas A. Heavy metal adsorption onto agro-based waste materials: A review. J Hazard Mater 2008;157:220–9. doi:10.1016/J.JHAZMAT.2008.01.024.

[4] Bailey SE, Olin TJ, Bricka RM, Adrian DD. A review of potentially low-cost sorbents for heavy metals. Water Res 1999;33:2469–79. doi:10.1016/S0043-1354(98)00475-8.

[5] Dupont L, Guillon E. Removal of hexavalent chromium with a lignocellulosic substrate extracted from wheat bran. Environ Sci Technol 2003;37:4235–41. doi:10.1021/es0342345.

[6] Yu J-X, Wang L-Y, Chi R-A, Zhang Y-F, Xu Z-G, Guo J. Competitive adsorption of Pb2+ and Cd2+ on magnetic modified sugarcane bagasse prepared by two simple steps. Appl Surf Sci 2013;268:163–70. doi:10.1016/J.APSUSC.2012.12.047.

[7] Gupta VK, Al Khayat M, Singh AK, Pal MK. Nano level detection of Cd(II) using poly(vinyl chloride) based membranes of Schiff bases. Anal Chim Acta 2009;634:36–43. doi:10.1016/J.ACA.2008.11.065.

[8] Xue Y, Gao B, Yao Y, Inyang M, Zhang M, Zimmerman AR, et al. Hydrogen peroxide modification enhances the ability of biochar (hydrochar) produced from hydrothermal carbonization of peanut hull to remove aqueous heavy metals: Batch and column tests. Chem Eng J 2012;200–202:673–80. doi:10.1016/j.cej.2012.06.116.

[9] Chen X, Chen G, Chen L, Chen Y, Lehmann J, McBride MB, et al. Adsorption of copper and zinc by biochars produced from pyrolysis of hardwood and corn straw in aqueous solution. Bioresour Technol 2011;102:8877–84. doi:10.1016/J.BIORTECH.2011.06.078.

[10] Xu X, Cao X, Zhao L, Wang H, Yu H, Gao B. Removal of Cu, Zn, and Cd from aqueous solutions by the dairy manure-derived biochar. Environ Sci Pollut Res 2013;20:358–68. doi:10.1007/s11356-012-0873-5.

[11] Inyang M, Gao B, Yao Y, Xue Y, Zimmerman AR, Pullammanappallil P, et al. Removal of heavy metals from aqueous solution by biochars derived from anaerobically digested biomass. Bioresour Technol 2012;110:50–6. doi:10.1016/J.BIORTECH.2012.01.072.

[12] Mohan D, Pittman CU, Bricka M, Smith F, Yancey B, Mohammad J, et al. Sorption of arsenic, cadmium, and lead by chars produced from fast pyrolysis of wood and bark during bio-oil production. J Colloid Interface Sci 2007;310:57–73. doi:10.1016/J.JCIS.2007.01.020.

[13] Cao X, Ma L, Gao B, Harris W. Dairy-Manure Derived Biochar Effectively Sorbs Lead and Atrazine. Environ Sci Technol 2009;43:3285–91. doi:10.1021/es803092k.

[14] Park JH, Choppala GK, Bolan NS, Chung JW, Chuasavathi T. Biochar reduces the bioavailability and phytotoxicity of heavy metals. Plant Soil 2011;348:439–51. doi:10.1007/s11104-011-0948-y.

[15] Chingombe P, Saha B, Wakeman RJ. Surface modification and characterisation of a coal-based activated carbon. Carbon N Y 2005;43:3132–43. doi:10.1016/J.CARBON.2005.06.021.

[16] Abe M, Kawashima K, Kozawa K, Sakai H, Kaneko K. Amination of activated carbon and adsorption characteristics of its aminated surface. Langmuir 2000;16:5059–63. doi:10.1021/la990976t.

[17] Chaukura N, Gwenzi W, Mupatsi N, Ruziwa DT, Chimuka C. Comparative Adsorption of Zn2+from Aqueous Solution Using Hydroxylated and Sulphonated Biochars Derived from Pulp and Paper Sludge. Water Air Soil Pollut 2017;228. doi:10.1007/s11270-016-3191-6.

[18] Yantasee W, Lin Y, Alford KL, Busche BJ, Fryxell GE, Engelhard MH. Electrophilic aromatic substitutions of amine and sulfonate onto fine-grained activated carbon for aqueous-phase metal ion removal. Sep Sci Technol 2004;39:3263–79. doi:10.1081/SS-200033140.

[19] Chang YC, Chang SW, Chen DH. Magnetic chitosan nanoparticles: Studies on chitosan binding and adsorption of Co(II) ions. React Funct Polym 2006;66:335–41. doi:10.1016/j.reactfunctpolym.2005.08.006.

Chapter 2 Literature Review

2.1. Biochar Preparation

The physical and chemical properties of biochar depend primarily on the types of feedstock and pyrolysis conditions i.e., temperature, residence time, reactor type and heating rate. Conventional carbonization/slow pyrolysis, fast pyrolysis, flash carbonization, gasification and microwave assisted pyrolysis are the main thermochemical processes that are commonly used to produce biochar [1]. It has been demonstrated that the biochar produced at high temperature (circa 600℃−700℃) possesses fewer H and O functional groups due to dehydration and deoxygenation of the biomass but shows highly aromatic nature with well-organized C layers and has lower ion exchange capabilities [2,3]. On the other hand, the biochar produced at lower temperature (circa 300℃−400℃) shows varied organic characters, including aliphatic and cellulose type structures and contain more C—H and C==C functional groups [4]. It is this complex and heterogenous physical and chemical composition of biochar that provides its excellent properties of contaminants removal via sorption [5].

2.1.1. Feedstocks

The feedstock for both conventional and microwave-assisted pyrolysis is biomass. During pyrolysis, the proportion of cellulose, hemi-cellulose and lignin content determine the ratios of bio-oil, gas and biochar in pyrolysis products. It has been demonstrated that feedstocks with low lignin content produce the highest biochar yield when pyrolyzed at moderate temperatures (circa 500℃) [6]. Therefore, choice of pyrolysis feedstocks may be determined by the desired balance between the different pyrolysis products (biochar, bio-oil, gas). Biomass is any living or recently living biological material with the potential as a source of energy [7]. Biomass is believed to

have the potential to become one of the major sources of energy in the next century [8]. The biomass as a source of energy is carbon- neutral, renewable, readily available in nature, relatively lower sulphur content, and have the potential to be the best alternative to fossil fuel resources. Replacing fossil fuel with biomass as a source of energy can lead to reduction in pollution and global warming, alleviate the energy crisis and contribute to-wards sustainable development [9,10]. Biomass resources can be grouped into three major categories: virgin resources, residues and municipal solid waste [7]. The virgin resources include forest resources and oilseed/cereal crops. The residues may be wood residues, agricultural residues and wastes as well as livestock residues. Municipal solid waste (MSW) could be residential or non-residential. With a suitable conversion process, these categories of biomass can be promising sources of energy for the future. The municipal solid wastes, forest and agricultural residues are promising substitutes for microwave pyrolysis processes.

Extensive studies utilising these lignocellulosic feedstocks including virgin resources and residues have been reported. Detailed research using wood, wood pellets, tea waste, coffee hulls, sewage sludge, wheat straw, rice straw, macro- and microalgae, corn Stover demonstrated excellent potentials as feedstocks for pyrolysis process [11-16].

2.1.2. Conventional Pyrolysis

This is the traditional heating system in which heat is transferred from an external source to the biomass through conduction, radiation and convection. In this method, the heat/temperature at the surface of the feedstock is very high and decreases towards the centre of the feedstock. In conventional pyrolysis process, the major process variables are that; 1) the heating rate is low, and (2) the vapor residence time is long [1]. This method has been used to produce charcoal for several years. During this

pyrolysis, there are some identified variables that determine the efficiency and yield of the process. These parameters are; pressure and moisture content of the feedstock [17].

The maximum temperature attained during conventional pyrolysis process is called the peak temperature. It has been reported that an increase in the peak temperature leads to an increase in the biochar fixed content [1]. The operating pressure of the pyrolysis process has significant impact on the properties of the produced bio-char. For a study carried out on the pyrolysis of different biomass feedstocks (eucalyptus wood, radiata pine, sugar cane bagasse) [18], it was found that increasing the operating pressure results in a decrease in the total surface area of the char. Similar results were also reported during a slow pyrolysis of Miscanthus [19]. They observed a significant decrease in BET surface area of char from 161.7 m^2/g at 0.1 MPa to 0.137 m^2/g at 2.6 MPa. The researchers attribute these observations to the blocking of the char pores by deposits from the tar due to high pressure. Reported studies on the effects of moisture content of the biomass feedstocks indicated that high moisture content enhances the yields of charcoal at high pressures. Hence, most biomass with high moisture contents are particularly attractive for biochar production via conventional pyrolysis [1]. This pyrolysis technique is comparatively inefficient and slow and is also dependent on the biomass' thermal conductivity and the convection current of the system.

2.1.3. Microwave Assisted Pyrolysis

Pyrolysis of biomass by microwave involves energy conversion instead of mere heating. In this technique, electromagnetic energy is converted to thermal energy by dielectric heating [7]. Furthermore, the heat is generated throughout the biomass volume instead of an external source. Contrary to the conventional pyrolysis, the

temperature at the centre of the feedstock is higher than the materials surface and surrounding as shown in **Figure 2-1.**

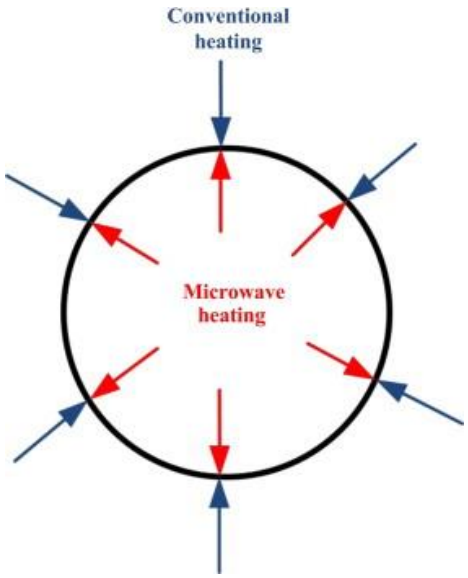

Figure 2-1 *Microwave and conventional heating nature [7]*

The microwave assisted pyrolysis technique is among the most promising techniques of accelerating and enhancing chemical reactions. Because of the efficient heat transfer profile, the chemical reactions are completed within a shorter time and efficiently as compared with other thermo-chemical processes [20-22]. The advantages of this technique over other methods of pyrolysis are that it speeds up the chemical reactions and reduces the residence time, hence saves energy.

2.1.4. Microwave Assisted Pyrolysis System

The biochars were produced in a custom-built insulated cylindrical stainless steel 309 reactor using the set-up shown in **Figure. 2-2**. The configuration of the microwave system and its operation were as detailed by Salema et al. [23] and Nhunchhen et al. [24]. Briefly described, the SS 309 reactor has a top lid with three openings for nitrogen supply and temperature measurement using two K-type thermocouples. There is a little

hole in the reactor bottom lid connected to a high temperature flexible hose for collection of flue gas. The inner diameter and height of the reactor is 35.5 cm x 53.3 cm respectively and contains a perforated circular plate at the base that holds the biomass sample for pyrolysis and allows flue gas to pass through. The reactor was connected to a 3kW and 2.45 GHz microwave supply system acquired from Muegge GmbH, Germany. The microwave generating system is made up of the power source (MX3000D-152 KL), a magnetron head with isolator (MH3000Se250BB), a stub-tuner (MW2009A-260ED), and a microwave guide (WR 340). The pyrolysis carrier gas (nitrogen) flowing through the reactor from the top was supplied from a nitrogen generator (VWR model CA26000-014) which converts pressurized air into nitrogen with 97.5% purity. The nitrogen flow purge the reactor of the generated volatiles or flue gas through the bottom of the reactor to the condenser. The flue gas was water-cooled in the condenser to collect bio-oils while the non-condensable gases are safely vented off via the fume hood. Two K-type thermocouples in direct contact with the biomass inside the reactor were connected to an 8 channel Pico data logger (Pico Technology, Cambridge shire, U.K.) to provide a real-time pyrolysis temperature that was recorded with a personal computer. Any microwave leakage during the experiment was monitored with a leakage detector (Electron Microscopy Science Model 72083-00).

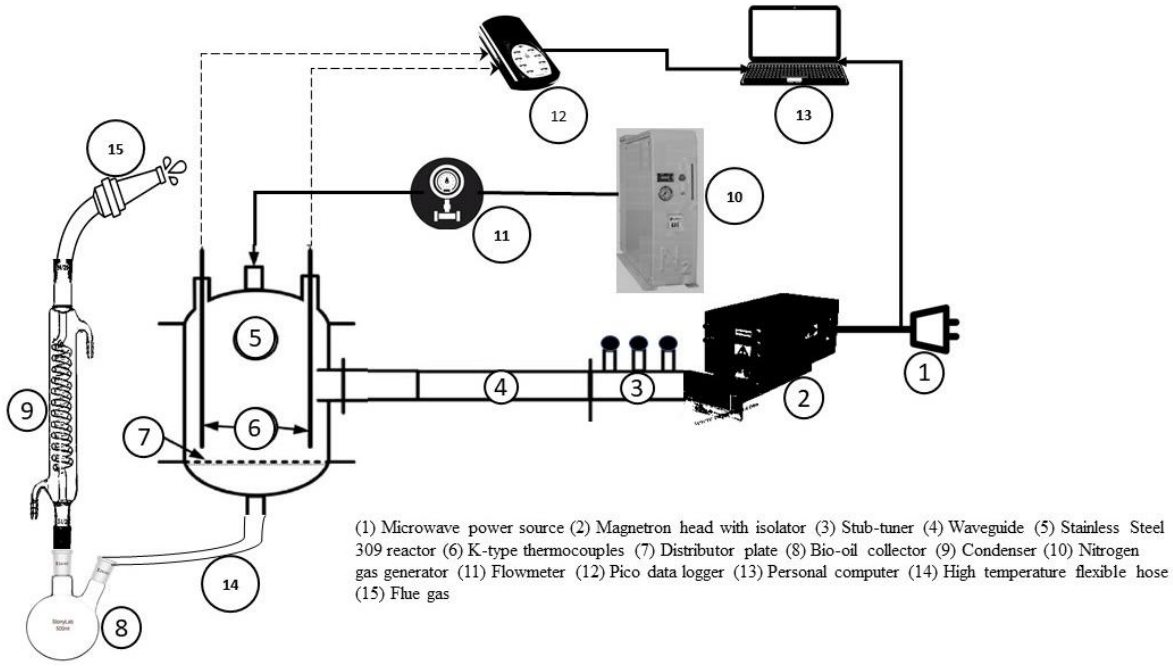

Figure 2-2: Schematics of MW Pyrolysis system at UNB, Canada.

2.2. Modification of Biochar for Water Treatment

Though the biochar has an excellent capability to adsorb heavy metal ions from metal contaminated solutions, this capacity is relatively lower in comparison with other known bio-sorbents such as activated carbon. Hence, despite several scientific researches on the biochar applications, recent researches have been focused primarily on the modification of the biochar with good surface properties and novel structures to enhance its environmental benefits and remediation efficacy. For instance, efforts have been made to increase its porosity, surface area and/or surface functional groups. There are several approaches to modify the biochar which can be divided into four main categories, i.e., chemical modifications, physical modifications, magnetic modifications and impregnation with mineral oxides. This review is focused on the chemical and magnetic modifications and their application to the treatment of heavy metal contaminated water.

2.2.1. Chemical modifications

Biochar modification by chemical methods involves both one-step modification or two-step modification process. In one-step process, both the carbonization and activation are achieved simultaneously in the presence of the activating chemical agent. On the other hand, in two -step process, the biomass feedstock is first carbonized followed by an activation using the relevant chemical agent or pre-treatment of feedstock before the process of carbonization. There are several methods of modifying biochar chemically (**Figure 2-3**). However, for this thesis, only the major and commonly used methods are identified.

2.2.1.1. Acid/Base Treatment and Chemical Oxidation of Biochars

Acidic/alkaline modification of the biochar can cause significant changes to the biochar physico-chemical properties. The biochar modification leads to more acidic functional groups on its surface; for instance, rising per-centage of oxygen results in increased O/C and H/C molar ratios with sulfuric acid treatment. The increases in O/C and H/C ratios signified the occurrence of a decrease in hydrophobicity [5]. It has been shown that nitric acid treatment breaks the pore wall and expands micropores into meso- or macro pores, hence the obtained acidic modified biochar possesses more acidic functional groups such as the carboxylic, ketonic, hydroxyl and other moieties containing oxygen [25]. The resulting increase in polarity of acid modified biochar can lead to chemisorption of pollutants from wastewater. Alkaline treatment produces biochar with (H/C), higher N/C ratio with lower value of O/C compared to acid modified biochar [26]. Low O/C ratio signifies the decline in the hydrophilic nature of basic modified biochar when aromaticity increased. An increase in oxygen and nitrogen and decrease in carbon in modified biochar results in crosslinking reaction of the biochar surface and the modifying agents [27]. The increase N/C ratio signifies

that more groups containing nitrogen to which the basic properties of the biochar are attributed are present on the modified biochar surface. This enhances the sorption of negatively charged ions and organic pollutants form wastewater. Furthermore, biochar oxidation using hydrogen peroxide (H_2O_2), Potassium Permanganate ($KMnO_4$), ammonium persulfate [$(NH_4)_2S_2O_8$] and ozone (O_3) have been used to modify surface functional groups [3,28,29].

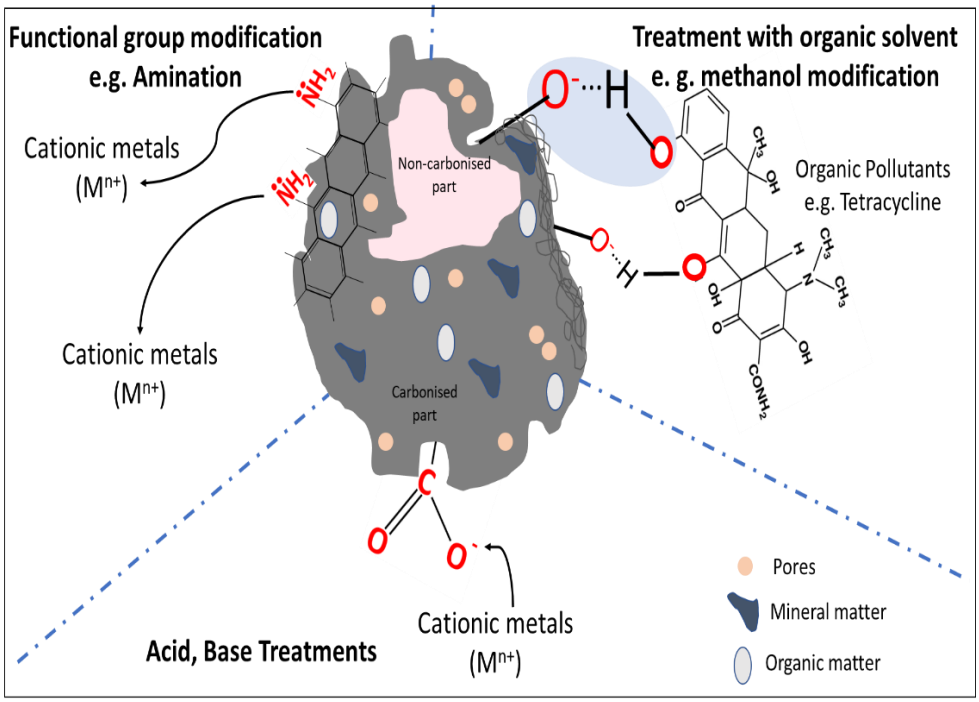

Figure 2-3 *Chemical Modification of Biochar*

2.2.1.2. Modification of Functional Groups (Carboxylation and Amination)

The biochar surface functional groups and its hydrophilicity can be modified chemically to meet targeted requirements such as pollutants adsorption from contaminated wastewater and amendment of contaminated soil [30]. It has been reported that biochar produced at low temperature (250℃−400℃) has more C==C and C—H functional groups. Furthermore, acidic functional groups such as carbonyl, carboxylic, phenolic and lactonic groups have been introduced onto the bio-char surface at relatively low temperature by chemical oxidation using H_2O_2, $KMnO_4$,

HNO_3, H_3PO_4 or HNO_3/H_2SO_4 mixture [22,31,32]. Surface carboxylation is mainly achieved by single-step oxidation.

In addition to functional groups containing oxygen, nitrogen-containing functionalities such as (imide, amide, lactane, pyridinic and pyrrolic groups) have significant impact on environmental remediation due to their high affinity for complexation, especially for heavy metal ions such as Cd^{2+}, Cu^{2+}, Zn^{2+}, Pb^{2+} [31,33]. The N-containing functionalities is typically introduced onto the biochar surface by nitration followed by reduction [34,35]. The HNO_3 dissociates to form an intermediate nitronium (NO^{2+} ions) which is very active. This attacks the aromatic/benzene rings resulting in nitrated product ($-NO_2$) on the biochar surface. The nitration of the bio-char surfaces is limited by the slow rate of nitration and small quantities of NO^{2+} [33], hence, concentrated H_2SO_4 is usually added simultaneously to enhance the formation of nitronium ions. It has been demonstrated that the nitration occurs via electrophilic aromatic substitution reaction where the nitro group is introduced onto the aromatic rings in biochar [34]. The nitro functional groups are then reduced to amino groups using acidified sodium dithionite ($Na_2S_2O_4$) as a reducing agent [34,35]. The surface amination introduces the amino functional groups that provide the basic properties and strong affinities of biochar to metal ions in contaminated wastewater.

Zhou et al. [36] used Chitosan to introduce the amine functional groups onto bamboo biochar surfaces to enhance its adsorption capability for heavy metal ions like Pb^{2+}, Cu^{2+} and Cd^{2+}. They demonstrated that coating biochar surface with chitosan can also improve the bio-char capacity as a soil amendment or adsorbent and deduced that chitosan-modified biochar can be used as a low-cost, effective and environmental-friendly adsorbent to remediate heavy metal contaminated environment. The amine

groups in chitosan forms a very strong chemical bond with heavy metal ions, hence it enhances heavy metal ions uptake from wastewater [37].

Xue et al. [38] modified the surface of peanut hull biochar using hydrogen peroxide (H_2O_2). The study demonstrated an increase in the O-containing functional groups, especially carboxylic group which improves the biochar capacity to adsorb metal ions like Cd^{2+}, Ni^{2+} and Pb^{2+}. It was observed that the modified biochar exhibited improved Pb^{2+} ion adsorption capability with an adsorption capacity of 22.82 mg/g. This adsorption capacity compares with the capacity of commercial bio-sorbent such as activated carbon and over 20 times more than the adsorption capacity of pristine biochar (0.88 mg/g). The modified biochar was employed in packed column as a filter media, and it was observed that it filters lead even more than a pristine biochar. The modified biochar capacity for lead removal in packed column was found to be nearly 20 times the capacity of unmodified biochar. For a multi-metal solution, the column containing modified biochar was still very efficient in removing lead and other heavy metal ions (i.e., Ni^{2+}, Cu^{2+}, and Cd^{2+}) from water flow. Model results for the multi-metal system showed that the adsorption sequence for the heavy metal ions by the modified biochar were in the order of $Pb^{2+} > Cu^{2+} > Cd^{2+} > Ni^{2+}$. They concluded that H_2O_2-modified biochar could be a cheap, effective and environmentally friendly or sustainable sorbent for several environmental applications, especially for heavy metal immobilization.

Yang and Jiang [34] reported the amino-modification of biochar to improve its adsorption capacity for Cu^{2+} ions from wastewater. The biochar modification was to make it a selective and highly efficient adsorbent for Cu^{2+} ions by nitration using HNO_3/H_2SO_4 mixture, followed by reduction using a mixture of $H_2SO_4/N_2S_2O_4$ as a reducing agent. Their characterisation results suggested that the amino groups were

chemically bond to the surface functional groups of the biochar. Their experimental results indicated that the modified biochar was highly efficient in the adsorption of Cu^{2+} ions. The bed volume and adsorption capacity of the amino-modified biochar were eight-and five-folds of the pristine biochar respectively. They concluded that the amino-modified biochar was endowed with high ion selectivity and pH stability due to the strong complexation between the Cu^{2+} ions and the amino functional groups.

Liu et al. [39] investigated the sorption of tetracycline from aqueous solution using biochar modified with KOH and H_2SO_4. Their characterisation results indicated that the biochar treated with alkali has larger surface area in comparison with those of pristine biochar and biochar treated with acid, and correspondingly shows a better adsorption capacity (58.8 mg/g) than the other two bio-chars. The KOH modification increased O-containing functional groups (O—H, C—H, C==O and COOH) on biochar surface and thus improved tetracycline adsorption. At neutral pH, O-containing functional groups on the surface of alkali modified biochar facilitated the formation of H_2 bonding with tetracycline molecules thus improved its adsorption by the KOH modified biochar [33]. It was concluded that the biochar can remove tetracycline from wastewater effectively. Furthermore, alkali modification of the BC can improve the biochar adsorption capacity. The adsorption is primarily due to hydrogen bonding and π-π interactions.

2.2.1.3. Treatment with Organic Solvents

Another method of achieving high carboxylic functional groups on biochar surface is by modifying the biochar using acidified methanol which is inexpensive. The bio-char modification by methanol involves esterification, followed by direct reaction involving the biochar carbonyl groups and methanol [40].

Jing et al. [40] investigated the adsorption performance of tetracycline (TC) in aqueous solutions by methanol-modified biochar. They modified rice husk biochar by methanol to enhance the TC adsorption capacities and reduce the inherent organic compound content in the biochar. Their results indicated that methanol-modified biochar showed approximately 45.6% enhancement of adsorption capacity in 12h and 17.2% in equilibrium time compared with pristine biochar. Furthermore, they observed that the hydroxyl and ester functional groups (O-containing groups) were more on methanol-modified biochar than pristine biochar which affects π-π electron-donor-acceptor interactions between the biochar surface and the TC.

2.2.2. Magnetic Modifications

It has been sufficiently demonstrated that biochar has the potential of being an effective sorbent for treating heavy metal contaminated water and wastewater due to its multi-functional properties. However, the separation of the powdered biochar from the aqueous matrix after the contaminant adsorption is very difficult which makes the use of the biochar for wastewater treatment less attractive. Therefore, researchers have made attempts to develop magnetic biochar sorbents to ensure a better and effective separation of the biochar particles after the wastewater treatment process [41-44]. Furthermore, it is known that the surface of the biochar has a net negative charge [45]; therefore, adsorption of anionic pollutants, e.g., As (III) or As (V) is somewhat low [45,46]. Hence, researchers have developed several methods for the adsorption of anionic contaminants by magnetically modifying biochar to enhance its adsorption capacities for anionic contaminants [47,48].

Generally, there are some common techniques employed to produce magnetic biochar such as pyrolysis and co-precipitation method. These methods are utilized by many researchers to produce high quality and high yield of magnetic biochar.

2.2.2.1. Magnetic Modification of Biochar by Pyrolysis

A typical pyrolysis process can be divided into three types such as conventional pyrolysis, fast pyrolysis and flash pyrolysis depending on the operating conditions [49]. The conventional pyrolysis process takes place under a slow heating rate which allows the production of solid, liquid, and gaseous product in compelling portions. As for laboratory scale, the pyrolysis process is generally done either through conventional heating or microwave heating.

Several papers have appeared where fast or slow pyrolysis (conventional heating) biochars were magnetized, characterized and applied to wastewater treatment [39,41,43,50-53].

Chen B L et al. [47] used orange peel, biomass waste to produce three novel magnetic biochars (MOP250, MOP400, MOP700) by employing the orange peel as the raw material in the presence of $FeCl_3 \cdot 6H_2O$ and $FeCl_3$ in which the biomass mixture was pyrolyzed under different temperatures (250℃, 400℃ and 700℃) at 5 ℃/min for 6 h. The produced magnetic biochar was used to adsorb organic pollutants and phosphate from wastewater. The introduction of Fe_2O_3 as the source of magnet for the biochar was signified by the higher ash contents and lower carbon contents of the produced biochar. The surface areas of the produced magnetic biochar were determined to be 41.2, 23.4 and 19.4 m^2/g with respect of MOP250, MOP400 and MOP700. These results showed that higher temperature leads to a reduction in the surface area due to the destruction of the biochar pores. It was found that the MOP400 consisted of amorphous biochar and nano-size magnetite particles, and hence showed hybrid sorption capacity to adequately sorb phosphate and organic pollutants from water. For adsorption of organic pollutants, MOP400 showed the highest sorption capacity, which was very much higher than the non-magnetic biochar (OP400). For phosphate

adsorption, magnetically modified biochars, particularly MOP250, showed much higher adsorption capacity than the unmodified biochars companion. They concluded that the magnetically modified biochar sorbent has the potential to adsorb phosphates and organic contaminants from wastewater simultaneously.

Liu et al. [39] investigated Arsenate sorption from water using Fe_3O_4-loaded biochar prepared from waste biomass (pinewood sawdust) in the presence of $FeCl_3$ as the metallic solution to provide the magnetic effect on the magnetic biochar produced. The important point of the synthetic method was that the carbonization, activation and Fe_3O_4 loading were achieved simultaneously. The pyrolysis process was done in the horizontal pyrolysis reactor in an electrical furnace with the flow of N_2 gas at 600 ℃ for about 3 h. This pyrolysis method was able to produce Fe_3O_4-loaded magnetic biochar that has a spinel structure (maghemite, γ-Fe $_2O_3$ or magnetite, Fe_3O_4) which signifies that γ-Fe_2O_3 has been reduced to Fe_3O_4. The characteristic of this composite was carried out and used as a sorbent for arsenate sorption from wastewater. Experimental results demonstrated that the Fe_3O_4 particles were deposited uniformly on the composite surface. The surface area of the composite was as high as 349 m^2/g, pore volume of 0.20 cm^3/g and iron of 39 wt.% for arsenate adsorption.

Wang S S et al. [43] studied arsenic removal by a magnetically modified biochar produced using natural hematite and pinewood. To prepare this magnetic biochar, a mixture of pinewood biomass and hematite were pyrolyzed in a tube furnace under nitrogen gas flow at 600 ℃ for 1 h. When compared to the pristine biochar, the hematite-modified biochar had both stronger magnetic behaviour and exhibited much higher capacity to adsorb As from water, possibly due to the γ-Fe_2O_3 particles on the surface of the carbon serving as sites for sorption via electrostatic interactions. It was concluded that the magnetised biochar can be used for As pollutant sorption from

aqueous solution since the used biochar can be recovered easily using external magnets.

On the contrary, only a very few articles have been published on the use of microwave assisted pyrolyzed biochar for magnetic modification [54-58].

Meng et al. [58] used chitosan as the raw material to produce $MnFe_2O_4$-loaded magnetic biochar by a novel single-step microwave assisted hydrothermal method at a microwave heating temperature of 120℃ for 10 min. The magnetic biochars were used to sorb Cu^{2+} ions from synthetic wastewater. Several experimental variables such as contact time, pH value and initial Cu^{2+} ions concentration which affect the adsorption behaviour or efficiency of the modified biochars were investigated. Experimental results demonstrated adsorption efficiency increases with solution pH value and contact time. Particularly, it was reported that adsorption efficiency can be as high as 100% and 96.7% after 500 min of sorption at pH value of 6.5 for the solutions when the initial Cu^{2+} ions concentration was 50 mg/L and 100 mg/L respectively. In conclusion, this work suggests that magnetic nanoparticles can be helpful for the adsorption of Cu^{2+} ions from wastewater.

Zhang Z S et al. [59] employed bamboo charcoal (BC) as a raw material to synthesize iron-modified bamboo charcoal (Fe-MBC) by impregnating the BC in HNO_3 and $FeCl_3$ solutions simultaneously. This is followed by microwave heating with a frequency of 2.45 GHz and an output power of 640 W for 6 min under an inert gas (nitrogen) flow of 10 mL/min. The magnetic biochar was used to adsorb Pb (II) ions contaminants from water. When compared to pristine biochar, the Iron bamboo magnetic biochar exhibited rougher surfaces. Furthermore, it was observed that increasing the concentration of $FeCl_3$ created better cluster of iron oxide on the

magnetic biochar surfaces. Also, increasing the concentration of $FeCl_3$ produced the maximum BET surface area of 298.732 m^2/g and a total pore volume of 0.273 cm^3/g which demonstrated that the pores were well widened and not blocked by the available Fe_2O_3 particles. They concluded these results have vital implications for the design of effective and low-cost adsorbent for the sorption of Pb (II) ions from aqueous solutions.

Wang et al. [60] investigated the sorption of Cr (VI) ions from wastewater using a microwave assisted prepared bamboo charcoal-based iron-containing sorbents. Bamboo charcoal-based, iron-containing adsorbent (Fe-BC) was synthesized by employing bamboo charcoal as a supporting medium for the ferric iron. The impregnation was achieved using a mixture of $Fe_2(SO_4)_3$ and H_2SO_4 simultaneously, before microwave heating. The experimental results demonstrated that the iron impregnation led to a decrease of total pore volume, the BET specific surface area and average mesoporous diameter. The microwave heating was carried out with power output of 640 W and 2.45 GHz frequency for 6 min under a nitrogen flow rate of 10 mL/min. The Fe-BC was observed to be well-crystallized with a BET surface area of 49 m^2/g which is relatively lower than that of the pristine biochar (64 m^2/g) likely due to the pores of the biochar been blocked by iron oxide. It was concluded that Fe-BC can be used as a useful sorbent for Cr (VI) sorption and in fixed bed filtration due to its high affinity toward Cr (VI) because of the iron oxide functional groups.

Wang et al. [61] used bamboo charcoal as raw material to produce bamboo based-cobalt coated magnetic biochar (Co-MBC). The process utilized $Co(NO_3)_2 \cdot 6H_2O$ as the precursor of cobalt oxide fusion into the biochar pores before the mixture was heated in a modified micro-wave with a power output of 640 W and 2.45 GHz frequency for 6 min under a nitrogen flow rate of 10 mL/min. On the other hand, the

Co-MBC synthesized via this study have a relatively higher BET surface area of value 263 m^2/g in comparison with the unmodified biochar (15 m^2/g) possibly because of the pores that developed from the micro-wave heating. The desorption study carried out showed that the Co-MBC have a regeneration and reusability.

2.2.2.2. Magnetic Modification of Biochar by Co-precipitation

Coprecipitation is a phenomenon whereby impurities in the form of solutes precipitate out from a solution via an agent or carrier that encourages the solutes to attach itself with the agent or carrier rather than remaining dissolved in the solution. This process is widely known as the simplest method in the preparation of magnetic particles [49]. This method has been widely used by researchers in the preparation of magnetic biochar because it is simple. Researchers have introduced various manipulated variables to achieve the necessary dimension and properties of magnetic particles produced. With this method, researchers have control over the size of the magnetic particles produced and several research works have been published where magnetic biochar was produced using different biomass.

Saravanan et al. [62] used gum kondagogu (GK) to produce GK-modified magnetic iron oxide particles by co-precipitating Fe^{2+} and Fe^{3+} ions in the ratio of 2:1 using ammonia solution in the presence of GK biomacromolecules. It was observed that the magnetic biochar was stable thermally compared to pristine GK. The magnetic biochars have aggregate structure that is spherical in shape and embedded with iron oxide particles which exhibited ferromagnetic properties with Ms value of 60 emu/g.

Jiang et al. [63] produced magnetic chitosan–graphene oxide (MCGO) via the chemical precipitation of Fe^{2+} and Fe^{3+} ions and used it to remove dye (methyl orange, MO) from water. The maximum adsorption capacity of MCGO for MO was 398.08 mg/g. This study showed that the MCGO offered enormous potential applications for

water treatment. Similarly, Yu et al. [64] investigated the competitive adsorption of Pb^{2+} and Cd^{2+} ions from solutions using modified sugarcane bagasse modified by magnetic method by two simple steps. The magnetic modified sugarcane bagasse (MSCB) was produced via the chemical precipitation of Fe^{2+} and Fe^{3+} (obtained from $FeCl_3$ and $FeSO_4$). The studies showed that the adsorption capabilities of the modified sorbent for Pb^{2+} and Cd^{2+} ions were 1.2 and 1.1 mmol/g respectively. This result demonstrated that Pb^{2+} ions in solution inhibited the adsorption of Cd^{2+} ions. The inhibition was found to be proportional to the initial concentration ratio of Pb^{2+} and Cd^{2+}. They concluded that the produced magnetic sorbent can be used in treating heavy metal contaminated water. Devi and Saroha [65] produced zero-valent iron magnetic biochar composites (ZVI-MBC) using biochar from paper mill sludge. In the synthesis, $NaBH_4$ solution was employed to reduce $FeSO_4$ to Fe (0). The magnetic biochar was used to treat real and synthetic effluent contaminated with pentachlorophenol (PCP). Analysis showed that the BET surface area and micropore volume of ZVI-MBC were found to be 101.23 m^2/g and 0.029 cm^3/g while the BET surface area and micropore volume of paper mill-based pristine biochar was 67 m^2/g and 0.026 cm^3/g respectively. This work suggests that the binding of the ZV Iron onto the surface of biochar presented increased surface area for adsorption.

2.3. Application of Magnetic Biochar for Adsorption of Heavy Metal Ions from Water

Researchers have made attempts to develop magnetic biochar adsorbents to ensure a better and effective separation of the biochar particles after the water treatment process [42,43,47]. Generally, magnetic biochars are produced by pyrolysis and co-precipitation method. The co-precipitation method adopted in this work has been used by many studies to produce high quality and high yield magnetic biochars. Scholars

have introduced various manipulated variables to achieve the necessary dimension and properties of magnetic particles produced. In the work of Saravanan et. al [62], it was observed that magnetic biochar was thermally stable compared to pristine biomass. The spherical and aggregate structured magnetic biochar was embedded with iron oxide particles and exhibited ferromagnetic properties with M_s value of 60 emu/g. Magnetic biochar with a very high adsorption capacity for methyl orange, 398.08 emu/g was reported by Jiang et. al [63]. Furthermore, Yuwei and Jianlong [66] studies showed that magnetic biochar with M_s 36 emu/g exhibited super-paramagnetic properties with an adsorption capacity of 35.5 emu/g.

So far, only few published papers have applied magnetised biochar for heavy metal ions adsorption from water. Heavy metals such as zinc [54], lead and cadmium [42,64,67,68], tin [55], chromium [69], and copper [70] were adsorbed from contaminated water by the application of magnetic biochar as adsorbent in a simple adsorption process. The reported studies employed biochar prepared by conventional pyrolysis and not microwave assisted pyrolyzed biochar.

2.4. Bio-adsorbents for Water Treatment

Another useful adsorbent under investigation globally for water treatment is bio adsorbent as extensively studied by Li et al. [71-73]. By-products from agroindustry are not only cheap and readily available but are also renewable. Heavy metal ions have been successfully removed from aqueous solution using potato peels and guava leaves.

These bio-sorbents also have applications in soil remediation and have shown the potential for environmental protection. Potato peels and grass clippings co-composting with eggshell and rice husks also have application as bio-sorbent for treating Pb (II) ions contaminated water. Cellulose-based materials have been demonstrated to be a

potential bio-adsorbent for removing Pb (II) ions from aqueous solutions by Li et al. [71]. New physical and chemical properties have been introduced into this cellulose via surface graft modifications to develop “smart” adsorbents based on cellulose.

2.5. References

[1] Manyà JJ. Pyrolysis for biochar purposes: A review to establish current knowledge gaps and research needs. Environ Sci Technol 2012;46:7939–54. doi:10.1021/es301029g.

[2] Ahmad M, Rajapaksha AU, Lim JE, Zhang M, Bolan N, Mohan D, et al. Biochar as a sorbent for contaminant management in soil and water: A review. Chemosphere 2014;99:19–33. doi:10.1016/j.chemosphere.2013.10.071

[3] Uchimiya M, Chang S, Klasson KT. Screening biochars for heavy metal retention in soil: Role of oxygen functional groups. J Hazard Mater 2011;190:432–41. doi:10.1016/j.jhazmat.2011.03.063.

[4] Glaser B, Lehmann J, Zech W. Ameliorating physical and chemical properties of highly weathered soils in the tropics with charcoal - A review. Biol Fertil Soils 2002;35:219–30. doi:10.1007/s00374-002-0466-4.

[5] Vithanage M, Rajapaksha AU, Ahmad M, Uchimiya M, Dou X, Alessi DS, et al. Mechanisms of antimony adsorption onto soybean stover-derived biochar in aqueous solutions. J Environ Manage 2015;151:443–9. doi:10.1016/j.jenvman.2014.11.005.

[6] Fushimi C, Araki K, Yamaguchi Y, Tsutsumi A. Effect of heating rate on steam gasification of biomass. 2. Thermogravimetric-mass spectrometric (TG-MS) analysis of gas evolution. Ind Eng Chem Res 2003;42:3929–36. doi:10.1021/ie0300575.

[7] Motasemi F, Afzal MT. A review on the microwave-assisted pyrolysis technique. Renew Sustain Energy Rev 2013;28:317–30. doi:10.1016/J.RSER.2013.08.008

[8] Oran Berndes G, Hoogwijk M, Van Den Broek R. The contribution of biomass in the future global energy supply: a review of 17 studies. Biomass and Bioenergy 2003;25:1–28. doi:10.1016/S0961-9534(02)00185-X

[9] Hall ' DO. Biomass energy in industrialised countries-a view of the future. Fores Manag For Ecol Manag Hall/ For Ecol Manag 1997;91:17–45.

[10] Panwar NL, Kaushik SC, Kothari S. Role of renewable energy sources in environmental protection: A review. Renew Sustain Energy Rev 2010;15:1513–24. doi:10.1016/j.rser.2010.11.037.

[11] Yagmur E, Ozmak M, Aktas Z. A novel method for production of activated carbon from waste tea by chemical activation with microwave energy. Fuel 2008;87:3278–85. doi:10.1016/J.FUEL.2008.05.005.

[12] Domínguez A, Menéndez JA, Fernández Y, Pis JJ, Nabais JMV, Carrott PJM, et al. Conventional and microwave induced pyrolysis of coffee hulls for the production of a hydrogen rich fuel gas. J Anal Appl Pyrolysis 2007;79:128–35. doi:10.1016/J.JAAP.2006.08.003.

[13] Budarin VL, Clark JH, Lanigan BA, Shuttleworth P, Breeden SW, Wilson AJ, et al. The preparation of high-grade bio-oils through the controlled, low temperature microwave activation of wheat straw. Bioresour Technol 2009;100:6064–8. doi:10.1016/J.BIORTECH.2009.06.068.

[14] Huang YF, Kuan WH, Lo SL, Lin CF. Hydrogen-rich fuel gas from rice straw via microwave-induced pyrolysis. Bioresour Technol 2010;101:1968–73. doi:10.1016/J.BIORTECH.2009.09.073.

[15] Budarin VL, Zhao Y, Gronnow MJ, Shuttleworth PS, Breeden SW, Macquarrie DJ, et al. Microwave-mediated pyrolysis of macro-algae. Green Chem 2011;13:2330. doi:10.1039/c1gc15560a.

[16] Miura M, Kaga H, Sakurai A, Kakuchi T, Takahashi K. Rapid pyrolysis of wood block by microwave heating. J Anal Appl Pyrolysis 2004;71:187–99. doi:10.1016/S0165-2370(03)00087-1.

[17] Antal MJ, Grønli M. The Art, Science, and Technology of Charcoal Production †. Ind Eng Chem Res 2003;42:1619–40. doi:10.1021/ie0207919

[18] Cetin E, Moghtaderi B, Gupta R, Wall TF. Influence of pyrolysis conditions on the structure and gasification reactivity of biomass chars. Fuel 2004;83:2139–50. doi:10.1016/j.fuel.2004.05.008.

[19] Melligan F, Auccaise R, Novotny EH, Leahy JJ, Hayes MHB, Kwapinski W. Pressurised pyrolysis of Miscanthus using a fixed bed reactor. Bioresour Technol 2011;102:3466–70. doi:10.1016/j.biortech.2010.10.129

[20] Lidström P, Tierney J, Wathey B, Westman J. Microwave assisted organic synthesis—a review. Tetrahedron 2001;57:9225–83. doi:10.1016/S0040-4020(01)00906-1.

[21] Salema A A, Afzal M T, Bennamoun L. Pyrolysis of corn stalk biomass briquettes in a scaled-up microwave technology. Bioresource Technology, 2017:233: 353–362. DOI: 10.1016/j.biortech.2017.02.113.

[22] Nhuchhen D R, Afzal M T, Dreise T, et al., Characteristics of biochar and bio-oil produced from wood pellets pyrolysis using a bench scale fixed bed, microwave reactor. Biomass and Bioenergy, 2018:119: 293–303. DOI: 10.1016/j.biombioe. 2018.09.035

[23] Salema AA, Afzal MT, Bennamoun L. Pyrolysis of corn stalk biomass briquettes in a scaled-up microwave technology. Bioresour Technol 2017;233:353–62. doi:10.1016/j.biortech.2017.02.113.

[24] Nhuchhen DR, Afzal MT, Dreise T, Salema AA. Characteristics of biochar and bio-oil produced from wood pellets pyrolysis using a bench scale fixed bed, microwave reactor. Biomass and Bioenergy 2018;119:293–303. doi:10.1016/j.biombioe.2018.09.035.

[25] Hadjittofi L, Prodromou M, Pashalidis I. Activated biochar derived from cactus fibres â€“ Preparation, characterization and application on Cu(II) removal from aqueous solutions 2014. doi:10.1016/j.biortech.2014.03.073.

[26] Ahmed MB, Zhou JL, Ngo HH, Guo W, Chen M. Progress in the preparation and application of modified biochar for improved contaminant removal from water and wastewater. Bioresour Technol 2016;214:836–51. doi:10.1016/j.biortech.2016.05.057.

[27] Ma Y, Liu W-J, Zhang N, Li Y-S, Jiang H, Sheng G-P. Polyethylenimine modified biochar adsorbent for hexavalent chromium removal from the aqueous solution 2014. doi:10.1016/j.biortech.2014.07.014.

[28] Cho HH, Wepasnick K, Smith BA, Bangash FK, Fairbrother DH, Ball WP. Sorption of aqueous Zn[II] and Cd[II] by multiwall carbon nanotubes: The relative roles of oxygen-containing functional groups and graphenic carbon. Langmuir 2010;26:967–81. doi:10.1021/la902440u.

[29] Tan Z, Qiu J, Zeng H, Liu H, Xiang J. Removal of elemental mercury by bamboo charcoal impregnated with H2O2. Fuel 2011;90:1471–5. doi:10.1016/j.fuel.2010.12.004.

[30] Yakout SM, El A, Daifullah HM, El-Reefy SA. PORE STRUCTURE CHARACTERIZATION OF CHEMICALLY MODIFIED BIOCHAR DERIVED FROM RICE STRAW. Environ Eng Manag J 2015;14:473–80.

[31] Shafeeyan MS, Daud WMAW, Houshmand A, Shamiri A. A review on surface modification of activated carbon for carbon dioxide adsorption. J Anal Appl Pyrolysis 2010;89:143–51. doi:10.1016/j.jaap.2010.07.006.

[32] Stavropoulos GG, Samaras P, Sakellaropoulos GP. Effect of activated carbons modification on porosity, surface structure and phenol adsorption. J Hazard Mater 2008;151:414–21. doi:10.1016/J.JHAZMAT.2007.06.005.

[33] Rajapaksha AU, Chen SS, Tsang DCW, Zhang M, Vithanage M, Mandal S, et al. Engineered/designer biochar for contaminant removal/immobilization from soil and water: Potential and implication of biochar modification. Chemosphere 2016;148:276–91. doi:10.1016/j.chemosphere.2016.01.043.

[34] Yang G-X, Jiang H. Amino modification of biochar for enhanced adsorption of copper ions from synthetic wastewater. Water Res 2014;48:396–405. doi:10.1016/J.WATRES.2013.09.050.

[35] Chingombe P, Saha B, Wakeman RJ. Surface modification and characterisation of a coal-based activated carbon. Carbon N Y 2005;43:3132–43. doi:10.1016/J.CARBON.2005.06.021

[36] Zhou Y, Gao B, Zimmerman AR, Fang J, Sun Y, Cao X. Sorption of heavy metals on chitosan-modified biochars and its biological effects. Chem Eng J 2013;231:512–8. doi:10.1016/j.cej.2013.07.036.

[37] Yong SK, Bolan NS, Lombi E, Skinner W, Guibal E. Sulfur-containing chitin and chitosan derivatives as trace metal adsorbents: A review. Crit Rev Environ Sci Technol 2013;43:1741–94. doi:10.1080/10643389.2012.671734.

[38] Xue Y, Gao B, Yao Y, Inyang M, Zhang M, Zimmerman AR, et al. Hydrogen peroxide modification enhances the ability of biochar (hydrochar) produced from hydrothermal carbonization of peanut hull to remove aqueous heavy metals: Batch and column tests. Chem Eng J 2012;200–202:673–80. doi:10.1016/j.cej.2012.06.116.

[39] Liu Z, Zhang FS, Sasai R. Arsenate removal from water using Fe3O4-loaded activated carbon prepared from waste biomass. Chem Eng J 2010;160:57–62. doi:10.1016/j.cej.2010.03.003

[40] Jing X-R, Wang Y-Y, Liu W-J, Wang Y-K, Jiang H. Enhanced adsorption performance of tetracycline in aqueous solutions by methanol-modified biochar 2014. doi:10.1016/j.cej.2014.03.006.

[41] Chen B, Chen Z, Lv S. A novel magnetic biochar efficiently sorbs organic pollutants and phosphate 2011. doi:10.1016/j.biortech.2010.08.067.

[42] Mohan D, Kumar H, Sarswat A, Alexandre-Franco M, Pittman CU, Mohan D. Cadmium and lead remediation using magnetic oak wood and oak bark fast pyrolysis bio-chars. Chem Eng J 2014;236:513–28. doi:10.1016/j.cej.2013.09.057.

[43] Wang S, Gao B, Zimmerman AR, Li Y, Ma L, Harris WG, et al. Removal of arsenic by magnetic biochar prepared from pinewood and natural hematite. Bioresour Technol 2015;175:391–5. doi:10.1016/j.biortech.2014.10.104.

[44] Zhang M, Gao B, Varnoosfaderani S, Hebard A, Yao Y, Inyang M. Preparation and characterization of a novel magnetic biochar for arsenic removal 2013. doi:10.1016/j.biortech.2012.11.132.

[45] Mukherjee A, Zimmerman AR, Harris W. Surface chemistry variations among a series of laboratory-produced biochars 2011. doi:10.1016/j.geoderma.2011.04.021.

[46] Beesley L, Marmiroli M. The immobilisation and retention of soluble arsenic, cadmium and zinc by biochar 2011. doi:10.1016/j.envpol.2010.10.016.

[47] Chen B, Chen Z, Lv S. A novel magnetic biochar efficiently sorbs organic pollutants and phosphate. Bioresour Technol 2011;102:716–23. doi:10.1016/J.BIORTECH.2010.08.067.

[48] Zhang M, Gao B. Removal of arsenic , methylene blue , and phosphate by biochar / AlOOH nanocomposite. Chem Eng J 2013;226:286–92. doi:10.1016/j.cej.2013.04.077.

[49] Thines KR, Abdullah EC, Mubarak NM, Ruthiraan M. Synthesis of magnetic biochar from agricultural waste biomass to enhancing route for waste water and polymer application: A review. Renew Sustain Energy Rev 2017;67:257–76. doi:10.1016/j.rser.2016.09.057.

[50] Zhang M, Gao B. Removal of arsenic , methylene blue , and phosphate by biochar / AlOOH nanocomposite. Chem Eng J 2013;226:286–92. doi:10.1016/j.cej.2013.04.077.

[51] Zhu X, Liu Y, Luo G, Qian F, Zhang S, Chen J. Facile fabrication of magnetic carbon composites from hydrochar via simultaneous activation and magnetization for triclosan adsorption. Environ Sci Technol 2014;48:5840–8. doi:10.1021/es500531c.

[52] Theydan SK, Ahmed MJ. Adsorption of methylene blue onto biomass-based activated carbon by FeCl 3 activation: Equilibrium, kinetics, and thermodynamic studies. J Anal Appl Pyrolysis 2012;97:116–22. doi:10.1016/j.jaap.2012.05.008.

[53] Mun SP, Cai Z, Zhang J. Magnetic separation of carbon-encapsulated Fe nanoparticles from thermally-treated wood char. Mater Lett 2013;96:5–7. doi:10.1016/j.matlet.2013.01.006.

[54] Wang W, Wang X, Wang X, Yang L, Wu Z, Xia S, et al. Cr(VI) removal from aqueous solution with bamboo charcoal chemically modified by iron and cobalt with the assistance of microwave. J Environ Sci (China) 2013;25:1726–35. doi:10.1016/S1001-0742(12)60247-2.

[55] Mubarak NM, Alicia RF, Abdullah EC, Sahu JN, Haslija ABA, Tan J. Statistical optimization and kinetic studies on removal of Zn2+ using functionalized carbon nanotubes and magnetic biochar. J Environ Chem Eng 2013;1:486–95. doi:10.1016/J.JECE.2013.06.011.

[56] Wang Y, Wang X, Wang X, Liu M, Wu Z, Yang L, et al. Adsorption of Pb(II) from aqueous solution to Ni-doped bamboo charcoal. J Ind Eng Chem 2013;19:353–9. doi:10.1016/j.jiec.2012.08.024.

[57] Ruthiraan M, Mubarak NM, Thines RK, Abdullah EC, Sahu JN, Jayakumar NS, et al. Comparative kinetic study of functionalized carbon nanotubes and magnetic biochar for removal of Cd2+ ions from wastewater. Korean J Chem Eng 2015;32:446–57. doi:10.1007/s11814-014-0260-7.

[58] Meng Y, Chen D, Sun Y, Jiao D, Zeng D, Liu Z. Adsorption of Cu2+ ions using chitosan-modified magnetic Mn ferrite nanoparticles synthesized by microwave-assisted hydrothermal method. Appl Surf Sci 2015;324:745–50. doi:10.1016/j.apsusc.2014.11.028

[59] Zhang Z, Wang X, Wang Y, Xia S, Chen L, Zhang Y, et al. Pb(II) removal from water using Fe-coated bamboo charcoal with the assistance of microwaves. J Environ Sci 2013;25:1044–53. doi:10.1016/S1001-0742(12)60144-2.

[60] Wang XJ, Wang Y, Wang X, Liu M, Xia SQ, Yin DQ, et al. Microwave-assisted preparation of bamboo charcoal-based iron-containing adsorbents for Cr(VI) removal. Chem Eng J 2011;174:326–32. doi:10.1016/J.CEJ.2011.09.044.

[61] Wang Y, Wang XJ, Liu M, Wang X, Wu Z, Yang LZ, et al. Cr(VI) removal from water using cobalt-coated bamboo charcoal prepared with microwave heating. Ind Crops Prod 2012;39:81–8. doi:10.1016/J.INDCROP.2012.02.015.

[62] Saravanan P, Vinod VTP, Sreedhar B, Sashidhar RB. Gum kondagogu modified magnetic nano-adsorbent: An efficient protocol for removal of various toxic metal ions. Mater Sci Eng C 2012;32:581–6. doi:10.1016/J.MSEC.2011.12.015.

[63] Jiang Y, Gong J-L, Zeng G-M, Ou X-M, Chang Y-N, Deng C-H, et al. Magnetic chitosan–graphene oxide composite for anti-microbial and dye removal applications. Int J Biol Macromol 2016;82:702–10. doi:10.1016/J.IJBIOMAC.2015.11.021.

[64] Yu J-X, Wang L-Y, Chi R-A, Zhang Y-F, Xu Z-G, Guo J. Competitive adsorption of Pb2+ and Cd2+ on magnetic modified sugarcane bagasse prepared by two simple steps. Appl Surf Sci 2013;268:163–70. doi:10.1016/J.APSUSC.2012.12.047.

[65] Devi P, Saroha AK. Synthesis of the magnetic biochar composites for use as an adsorbent for the removal of pentachlorophenol from the effluent. Bioresour Technol 2014;169:525–31. doi:10.1016/j.biortech.2014.07.062.

[66] Yuwei C, Jianlong W. Preparation and characterization of magnetic chitosan nanoparticles and its application for Cu(II) removal. Chem Eng J 2011;168:286–92. doi:10.1016/j.cej.2011.01.006.

[67] Harikishore Kumar Reddy D, Lee S-M. Magnetic biochar composite: Facile synthesis, characterization, and application for heavy metal removal. Colloids Surfaces A Physicochem Eng Asp 2014;454:96–103. doi:10.1016/J.COLSURFA.2014.03.105.

[68] Noraini MN, Abdullah EC, Othman R, Mubarak NM. Single-route synthesis of magnetic biochar from sugarcane bagasse by microwave-assisted pyrolysis. Mater Lett 2016;184:315–9. doi:10.1016/J.MATLET.2016.08.064.

[69] Zhou Y, Gao B, Zimmerman AR, Chen H, Zhang M, Cao X. Biochar-supported zerovalent iron for removal of various contaminants from aqueous solutions. Bioresour Technol 2014;152:538–42. doi:10.1016/J.BIORTECH.2013.11.021.

[70] Song Z, Lian F, Yu Z, Zhu L, Xing B, Qiu W. Synthesis and characterization of a novel MnOx-loaded biochar and its adsorption properties for Cu2+ in aqueous solution. Chem Eng J 2014;242:36–42. doi:10.1016/J.CEJ.2013.12.061.

[71] Li Y, Xiao H, Chen M, Wang X. Solvent-free synthesis of the cellulose-based hybrid beads for adsorption of lead ions in aqueous solutions Hybrid beads for adsorption of lead ions in aqueous solutions. RSC Advances 2017:53899–906. doi:10.1039/c7ra09592a.

[72] Li B, Pan Y, Zhang Q, Huang Z, Liu J, Xiao H. Porous cellulose beads reconstituted from ionic liquid for adsorption of heavy metal ions from aqueous solutions. Cellulose 2019;26:9163–78. doi:10.1007/s10570-019-02687-4.

[73] Wang F, Pan Y, Cai P, Guo T, Xiao H. Single and binary adsorption of heavy metal ions from aqueous solutions using sugarcane cellulose-based adsorbent. Bioresour Technol 2017;241:482–90. doi:10.1016/j.biortech.2017.05.162.

Chapter 3 Adsorption of Pb (II) ions onto magnetically modified hemp biochar prepared by microwave-assisted pyrolysis

Abstract

Biochars were made by microwave-assisted pyrolysis process using hemp stalks biomass as the feed. This biochar was made magnetic by two simple step process. The magnetic char was examined for its potential application as a renewable adsorbent for the removal of lead ions from aqueous solution via a batch-mode experiment. The 200 – 300 µm size biochar powder obtained from microwave pyrolysis of 1.5 kg hemp stalks biomass at an average temperature of 600 ˚C were first impregnated with H_2O_2 (30%) solution and then magnetized by mixing a solution of Fe^{3+}/Fe^{2+} with biochars suspension and then treated with NaOH. The synthesized magnetic adsorbent characterizations were performed with SEM, FT-IR, vibrating sample magnetometry (VSM), energy-dispersive X-ray spectroscopy (EDS) as well as BET surface area (S_{BET}). The S_{BET} of the magnetic hemp biochar was 84 m^2 g^{-1}.

The impacts of operating temperature, pH, time of adsorption and initial concentration of Pb (II) ions solution on the ion's removal process were examined. Results showed that the magnetic biochar performed well in remediating lead ions-contaminated water with a Langmuir sorption ability, q_{max} of 61 mg g^{-1}. Modelling the kinetics of adsorption showed that the pseudo-second order kinetics model fits experimental data better. Results from isotherm models showed that Freundlich isotherm characterized the adsorption of Pb (II) ions by the magnetic hemp biochar better than other models. The adsorption performance of biochar after 5 regeneration cycles was over 70%. The

adsorbent in solution was easily captured with a low magnetic field, thereby enhancing the ease of recovery of spent adsorbents from solution. The as-prepared magnetic biochar adsorbents demonstrated as potential adsorbents in remediating heavy metal ions-contaminated water.

Keywords: Magnetic biochar; hemp; adsorbent; microwave-pyrolysis, water treatment; heavy metal ions.

3.1. Introduction

Wastewater containing heavy metal ions from various industries such as electroplating, mining, glass, ceramics, textiles, storage batteries and metal finishing are discharged to the environment. The rising concerns about water polluted by heavy metal ions discharged from industrial wastes have increased recently because of their accumulation in biota and toxic effects on organisms [1]. Among various heavy metal ions, much attention has been paid to lead ions due to it long residence times and high toxicity. These pollutants in water bodies accumulates in the food chains and endangers aquatic lives and human beings [2]. Lead poisons have been confirmed to decrease kidney functions and activities of enzymes as well as cause neuromuscular difficulties [3]. Hence, there is an urgent call for the remediation and recycling of metal ions-contaminated water to protect the food chains and secure alternative sources of water [4].

Different methods have been applied to capture these ions from solution including reverse osmosis, chemical precipitation, adsorption, membrane technologies, ion exchange and electrochemical treatment [5]. Amongst these methods, adsorption is the most convenient, universal and fast technology to remediate metal ions-contaminated water efficiently at a relatively low cost [6,7]. The merits of adsorption technology are

the potential to easily regenerate the spent adsorbent and its low residue generation [8]. Furthermore, bio-sorbents are environmentally friendly and readily available in large quantities. Different types of adsorbents, natural and manufactured products have evolved [9]. Activated carbon has been demonstrated as a very effective carbon-based adsorbent in the sorption of organic and inorganic toxic wastes from water [4]. Although, activated carbon successfully adsorbs metal ions from polluted water, it cost of preparation is high and has a very low selectivity which limits its application, whereas "sustainable" biochar can be manufactured at a relatively lower cost. In recent years, biochars have been considered as a lower cost bio-sorbent with various promising potential environmental applications including carbon sequestration, water treatment and soil improvement [10]. Researchers have demonstrated that biochar has been an effective adsorbent to adsorb pollutants from water and as a substance to immobilize metal ions in metal-polluted soil [11–13].

Biochar is a highly porous material that is very rich in carbon. It is a fine carbon material manufactured by the thermal degradation of biomass in a system with limited oxygen. Biochars have been utilized as efficient sorbents to eliminate various inorganic and organic pollutants from water. Their high adsorption capacities may be due to their high porosity structure and functional groups on their large surface area (e.g. phenolic groups, hydroxyl, ketone, aldehyde, carboxyl) thus, they have a very strong attraction towards cations [14–16].

Biochars are manufactured by gasification, fast and slow pyrolysis of different biomasses [17,18]. The moisture contents of biomass required for fast pyrolysis needs to be <10% and enough energy is required to run the process. The different biomasses are converted to bio-oil and biochars by fast pyrolysis [19]. About 10–25% of

feedstock is converted to recoverable gas used to provide heat for the processes. Researchers have produced biochars from sludge [20], diary manure [12,15], algal biochar [21,22], crop residues [23], corn cobs and stover [18], etc. Oak bark and wood chars have been produced by fast pyrolysis for the adsorption of lead [14]. To the best of our knowledge, there has not been a study on the adsorption performance of biochars produced from hemp stalks using microwave-assisted pyrolysis.

Until recently, the widely used and traditional carbon-based adsorbent to treat metal ions-polluted water has been activated carbon. Hence, for biochars to favorably compete for industrial applications, researchers must ensure that biochars are the most efficient bio-sorbents with a targeted chemical property. Therefore, current researches on biochars are centered around their characterizations and modification to meet industrial applications [24].

Because biochars are carbonaceous materials composed of surface functional groups fastened to ‘fused’ aromatic rings, it is strongly believed that biochar will have similar chemical properties to those of aromatic hydrocarbon [25]. Hence, the chemical reactions of aromatic hydrocarbons may be applicable to biochars. The existence of these functional surface groups on the biochars thus means they modifiable via chemical and physical methods to make adsorbents that are targeted towards a specific function.

Extensive research has been carried out on how to remove heavy metal cations from water using unmodified biochar, capitalizing on their fast sorption kinetics, large surface area and micro or meso-pores structure of biochar materials [26].

One of the major challenges with practical wastewater treatment is the challenge of regenerating the adsorbent from solutions by the conventional methods: centrifugation

and filtration. Separation using a magnetic field has been shown as a potential method to separate solid from liquid phase [27]. Using an external or internal field to isolate magnetic bio-sorbents from the aqueous solution is convenient. However, magnetic modification of adsorbents for wastewater and water purification is somewhat new research area [28,29]. Only very few studies have examined magnetic bio-sorbents. These includes magnetic sugarcane bagasse [30], magnetic Saccharomyces cerevisiae [31], magnetic biochar from slow pyrolysis [32], magnetic oak bark and wood via fast pyrolysis [33], magnetically modified spent coffee grounds [34] and reviews on magnetic materials for water purifications [35,36].

The few available studies on the application of modified or unmodified biochar to wastewater treatment have all employed the biochar prepared by conventional pyrolysis of different biomasses. Therefore, it is of more interest to study the adsorption performance of magnetically modified hemp biochar prepared by microwave-assisted pyrolysis. Microwave-assisted pyrolysis is energy efficient, easier to control, ensures rapid heating and reduces residence time. Low strength internal or external magnetic fields can easily manipulate magnetic bio-sorbents, allowing easy recovery of metal ion-loaded adsorbent from contaminated water which might contain oil, grease and suspended solids to some extent. With the conventional filtration, these impurities may lead to frequent separation and regeneration due to carbon fouling. Magnetic separation permits easy isolation of adsorbents and washing before redispersion [29].

In this work, we aimed at the magnetization of a microwave-assisted pyrolyzed hemp biochar (BC) to overcome clogging of the filter bed during adsorbent filtration. The hemp stalks biomass (1.5kg) was pyrolyzed in a microwave batch reactor at about 600

˚C average temperature within 1.5 h residence time. The hemp BC was then modified chemically for the magnetization in two simple steps: (1) oxidation of the BC using H_2O_2 to improve its affinity towards heavy metal ions. (2) magnetization of BC via the co-precipitation of magnetic particles onto the matrix of the oxidized BC to aid the separation of the spent biochars from aqueous solution. Adsorption isotherm, pH dependence, adsorption kinetics of Pb (II) ions by magnetic modified hemp biochar from solution were examined. The isotherms of adsorption were modelled by Freundlich, Temkin, Langmuir and Dubinin-Redushkevich models. The kinetics data were examined using pseudo-first-order (PFO), pseudo-second-order (PSO) and intraparticle kinetic models. The effects of multiple regenerations on biochar adsorption capacity and magnetic properties were also identified.

3.2. Experimental

3.2.1. Materials

The hemp stalks biomass was purchased in bags from Plains hemp, Manitoba, Canada. All chemicals were reagent grades. Ferrous Sulfate (98%), ferric sulfate (>96%), Sodium Nitrate and EDTA-2Na were purchased from Alfa Aesar, USA. Granular NaOH, HNO_3 and H_2O_2 (30%) solutions were from Fisher Scientific. The standard solution of Pb^{2+} (1.000 g L^{-1}) was made in the lab by mixing the right mass of $Pb(NO_3)_2$ salt in distilled water. All reagents were utilized without further purification.

3.2.2. Pyrolysis of Hemp Biochar

Hemp biochar was produced by pyrolyzing 1.5 kg of shredded hemp stalk as received in a custom-built SS 309 reactor at an average temperature of 600 ˚C, 2.7 kW microwave power and reaction time of 1.5 h [37]. The moisture of the hemp stalks biomass as received was between 9 – 11%.

3.2.3. Preparation of H_2O_2 Modified Biochar

3.2.3.1. Biochar Pre-treatment

The hemp biochar samples from microwave-assisted pyrolysis were milled to 200 - 300 µm size, washed exhaustively in distilled water before drying in air oven overnight at 105 ˚C prior to the chemical modification of the biochar.

3.2.3.2. H_2O_2 Impregnation of Hemp Biochar

Some amount (55 g) of the pre-treated hemp BC samples was soaked in 350 mL H_2O_2 (30%) and stirred for 6h with a magnetic stirrer at 300 rpm under room temperature (24±1 ˚C). After impregnation with H_2O_2, the biochars were filtered under vacuum, washed repeatedly in distilled water, followed by ethanol and then air-dried at 60 ˚C in the oven for 24 h.

3.2.4. Preparation of Magnetic Hemp Biochar

The magnetically modified hemp BC was made as detailed by Nakahira et al [38]. All water used in the process was distilled water. Briefly summarized, the H_2O_2 impregnated hemp biochars [15g, 200 - 300 µm] were soaked in water (150 mL). A fresh solution of ferric sulfate was made by dissolving 5.55g of $Fe_2(SO4)_3nH_2O$; (n = 6 - 9) in water (390 mL). Similarly, another solution of ferrous sulfate was also made from the dissolution of 6.00 g $FeSO_4.7H_2O$ in water (45 mL). These Fe solutions were mixed and actively stirred at 25 – 30 ˚C. The output $Fe^{2+}/Fe^{3+}SO4^{2-}$ solution was mixed with the aqueous suspension of H_2O_2 impregnated biochars (15 g) at room temperature and stirred slowly for 30 minutes. At this point, 10 M-NaOH (aqueous) was added in drops to the BC/ Fe^{2+}/Fe^{3+} system to raise its pH to approximately 10 – 11. At this point, these suspensions were agitated for 60 minutes and then kept for 24h at ambient condition. The resulting suspensions were filtered, and the residues were

washed repeatedly in distilled water followed by ethanol before drying overnight at 50 ˚C. The mass ratio of $FeSO_4.7H_2O$ to $Fe_2(SO4)_3nH_2O$ in solutions was fixed at 1.1:1, mass of adsorbent and volume of distilled water were all kept constant. The weight percent of the sum of ferric and ferrous sulphate in solutions used for modification was varied from 1% to 4% as shown in Table A3.1 of Appendix A. The prepared magnetic hemp biochars were labelled as MHBC-1, MHBC-2, MHBC-3 and MHBC-4, respectively, according to the weight percent of the iron sulphates in the solution containing the biochar samples. A general schematic of the biochar modification is shown in **Figure 3-1**

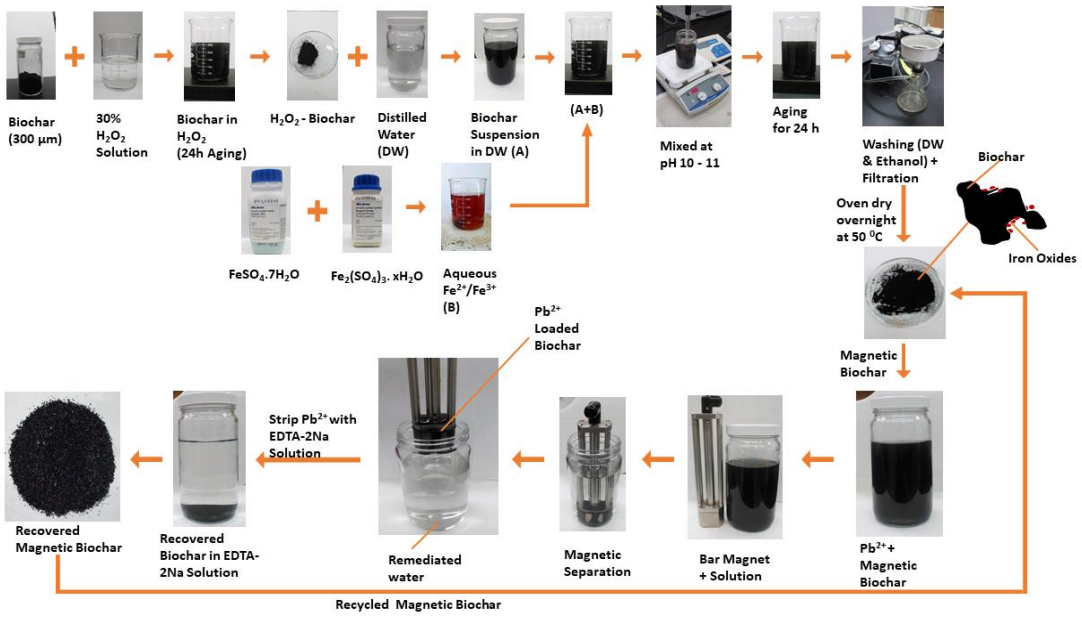

Figure 3-1 *General scheme for the preparation of magnetic hemp biochar*

3.2.5. Characterization of Hemp Biochar

The biochar surface functional groups were identified with FT-IR before and after the modification and Pb (II) ions uptake. A NEXUS 470 spectrophotometer (Nicolet Thermo Instruments, Canada) was used to record the FT-IR spectra after the hemp

biochars were grinded with KBr. The BET was performed with an Autosorb instrument from Belsorp-Max BEL Inc, Osaka, Japan. The structure of biochar surface before and after the adsorption of Pb^{2+} ions including the chemical composition of the biochar were determined with SEM and EDS respectively. The Scanning Electron Microscope (JEOL JSM-6400) was outfitted with an EDS (EDAX Genesis 4000 Energy Dispersive X-ray) analyser.

Hysteresis measurement was performed using a Lake Shore 7304 Vibrating Sample Magnetometer (VSM). The graph of magnetization (M) versus field strengths (H) which gives the hysteresis loop represents the magnetic properties of the biochar adsorbent. The adsorbent saturation magnetization was determined from this loop.

3.2.6. Batch Adsorption Experiments

Pb (II) ion was used for the study to determine if the magnetic hemp biochars were suitable for treating heavy metal ion-contaminated water. A stock solution of Pb (II) was diluted to prepare the different adsorbate solution at varying concentrations. The desired pH was maintained by adding drops of 0.01 M NaOH or 0.01 M HNO_3 into the solution. This study was performed with a 40 mL adsorbate solution at 20 mg L^{-1} concentration and beginning pH of 5.0, dosage of 0.02 g of adsorbent per 40 mL solution in a temperature-regulated shaker (SWB25) from a German Thermo Electron Corp. The system was agitated at a 130 rpm speed. The effects of contact time, temperature, pH, initial concentration of Pb^{2+} solution on the adsorption process were investigated. Residual Pb^{2+} concentration in the filtrate after sorption was evaluated with ICP-OES (VISTA-MPX Axial, Varian Inc, USA). The percent metal ion removal R (%) was computed with **equation 3.1**.

$$R = \frac{(C_i - C_e)}{C_i} \times 100$$ *Equation 3.1*

where C_i(mg L^{-1}) and C_e(mg L^{-1}) are the concentrations of the Pb (II) solution at the beginning and at equilibrium respectively. The metal ion loading capacity (Q) was determined using **equation 3.2**.

$$Q = \frac{(C_i - C_e)}{m} \times V$$ *Equation 3.2*

where Q (mg g^{-1}) is the quantity of Pb (II) ions removed from solution per gram of the biochar absorbent, m (g) is the absorbent mass, V (L) is the metal ion solution volume.

3.2.6.1. Adsorption Kinetic Models

When removing cations from solution via batch mode experiment, the process kinetics helps to identify the mechanisms governing the process of metal uptake. The kinetics data - also identify the potential rate-limiting step during adsorption process. Two adsorption reaction kinetics models and one adsorption diffusion model were employed to investigate the kinetics of Pb (II) ion adsorption onto magnetic hemp biochar. These are pseudo-first order (PFO), pseudo-second order (PSO) kinetics model and intraparticle diffusion model respectively.

The non-linear forms of the PFO and PSO kinetics are presented in **equations 3.3 and 3.4** respectively [39].

$$q_t = q_e(1 - e^{-K_1 t})$$ *Equation 3.3*

$$q_t = \frac{K_2 q_e^2 t}{1 + K_2 q_e t}$$ *Equation 3.4*

where q_e and q_t are the sorption capabilities at equilibrium and a given time, t during the process respectively in (mg g^{-1}), K_1 (min^{-1}) and K_2 (g mg^{-1} min^{-1}) are the rate constants for PFO and PSO models respectively.

The model for intraparticle diffusion is given by **equation 3.5**.

$$q_t = K_{id} t^{1/2} + C$$ *Equation 3.5*

where q_t (mg g^{-1}) is the quantity of adsorbate removed from solution in a given time t (min), K_{id} is a constant of intraparticle diffusion (mg g^{-1} $min^{-1/2}$) and C is a constant that is related to the thickness of the boundary layer [40]. When a graph of q_t against $t^{1/2}$ is linear, it implies that intraparticle diffusion is the rate controlling step during the adsorption process.

3.2.6.2. Adsorption Isotherm Models

The isotherms were determined by agitating the MHBC-3 (0.02 g) with 40 mL of Pb (II) solution at varying initial concentrations. The adsorption isotherms for lead ions were characterized by fitting the experimental data to the Langmuir, Freundlich, Temkin and Dubinin-Redushkevich models. The detail descriptions of these models are given in Appendix A.

3.2.6.3. Separation Experiments

The isolation of MHBC-3 from solution was investigated in a batch-mode experiment. 250 mL of distilled water was measured into 500 mL glass vial (dia. = 6.5 cm). Then 125 mg of MHBC-3 was placed in the vial. After agitating this suspension for 5 minutes with a mixer (Barnant mixer series 20) at a speed of 100 rpm, the vial was then placed on the table and a magnet jig from Industrial Magnetics, Inc (ON/OFF Magnetic Jig, JP155R) was inserted in the suspension (internal magnetic field separation). The depth of the suspension with the inserted magnet jig at the center of the vial was 8.0 cm. Another trial was also performed using an external magnetic field whereby the glass vial was placed on the jig instead of inserting the jig into the suspension. After completing the isolation, 20 mL of the distilled water aliquot was collected at intervals from a fixed point in the vial (6.0 cm from the bottom of vial)

through a needle and syringe to measure the turbidity with a turbid meter (Hach 2100Q Portable Turbidimeter).

3.2.6.4. Adsorbent Regeneration

For adsorption-desorption study, Pb (II) ions were loaded onto the MHBC-3 under the following operating conditions: initial concentration of Pb (II) solution – 20 mg L^{-1}, pH - 5, fixed adsorbent dose – 1.0 g L^{-1}, temperature - 25 ˚C and contact time 2 h. . The Pb-loaded MHBC-3 was filtered under vacuum, washed in distilled water before drying overnight at 60 ˚C in temperature-controlled oven.

Batch desorption study was performed by using a fixed dose of Pb-loaded MHBC-3 (1.0 g L^{-1}) in EDTA-2Na (0.1 mol L^{-1}) solution at 25 ˚C and in 2 hours in a glass vial. After mixing at 100 rpm and 25 ˚C using Barnant mixer series 20, the vial was withdrawn, and the suspension was filtered using filter paper under vacuum. The cake was obtained, washed thoroughlyin distilled water to approximately 7.0 pH and dried overnight at 60 ˚C for the next cycle of adsorption–desorption. The filtrates (EDTA-2Na) sample were analyzed using ICP-OES to quantify the concentration of Pb (II) ions desorbed and amount of Fe leached during regeneration.

3.3. Results and Discussion

3.3.1. Characterization of Magnetic Hemp Biochar

To know the properties such as pH and pH_{pzc}, surface structure, moisture and ash content, chemical composition, porosity and surface area as well as surface functional groups, the magnetic hemp biochar (MHBC-3) was characterised. The characterization results are shown in **Table 3.1**.

3.3.1.1. BET and Elemental Analysis

The magnetic modification of hemp biochar adsorbent decreased its BET from 142.50 $m^2\ g^{-1}$ to 83.76 $m^2\ g^{-1}$ as given in **Table 3.1**. This observation shows that the magnetic biochar has relatively greater surface area of 83.76 $m^2\ g^{-1}$ in comparison with other magnetic biochars. Mohan et. al, reported much less BET surface areas for both magnetic oak wood (6.1 $m^2\ g^{-1}$) and magnetic oak bark (8.8 $m^2\ g^{-1}$) biochars respectively [33]. The rise in percent iron content of the MHBC-3 adsorbent from 0.01 to 13.66% confirms that the magnetic modification was successful. As one would expect, modification caused a decrease in surface area of MHBC-3. The observation may be due to the obstruction of the small pores or coverage of the surface of adsorbent by the iron oxide particles embedded in the biochar. Nonetheless, the adsorption performance of MHBC-3 for Pb (II) is much higher than that of unmodified hemp biochar, thereby demonstrating the effectiveness of the magnetic modification in enhancing adsorption towards Pb (II) ions. This is elaborated further in later sections of this article. Average pore diameter of MHBC-3 from analysis was 6.68 nm, suggesting the presence of mesoporous structure in MHBC-3 adsorbent.

The removal of organic matter, ash content, from the biochar due to modification (from 48.37 wt% to 44.97 wt%) correlates with the higher carbon contents for MHBC-3. The

carbon content was increased from 45.69 wt% to 58.94 wt%. Additionally, the meso-porosity developed in the modified biochar, MHBC-3, which is different from the microporous unmodified hemp biochar, may partly be due to the removal of ash from the biochars when forming the biochar hybrid particles and iron oxides.

When treating the biochar samples with Fe^{2+}/Fe^{3+}/NaOH, the porous surfaces of the biochar may assist in nucleating iron oxide precipitates. The carboxyl (-COOH) and hydroxyl (-OH) surface functional groups on biochar tend to associate or complex with the iron hydroxide/oxide particles present in the solution, thus promoting their linkage with biochar. This could be shown as biochar-O-Fe_xO_y (Fe_3O_4/Fe_2O_3) to representing the potential chemical bonding between the particles of iron oxide and biochar. This chemical interaction could be supplemented with some form of mechanical interlocks between H-bonding and phases, e.g. the hydrogen bonding between C–OH on biochar surfaces and Fe–OH at the surface of metal oxides. Some columbic interactions may also exist. The magnetic iron particles tightly bonded to the biochar particles could be attributed to these interactions.

The results from point of zero charge (pH_{pzc}) and the pH analysis of MHBC-3, shown in **Table 3.1** imply that the adsorbent has some basic tendency.

Table 3.1 *Characteristics of unmodified and magnetic hemp biochar (MHBC-3)*

Parameter	*Units*	*Values*	
		Unmodified hemp biochar	**Magnetic hemp biochar**
BET surface area	$m^2\ g^{-1}$	142.50	83.76
Total pore volume	$cm^3\ g^{-1}$	0.12	0.14
Zeta Potential	mV	- 49.49	- 45.30
pH_{pzc}		7.07	6.61
pH		8.89	9.05
Ash content	%	48.37	44.97
Moisture Content	%	2.59	3.13
C	%	45.69	58.94
Fe	%	0.01	13.66

3.3.1.2. Morphology and Chemical Composition of Biochar Adsorbent

The structure of this biochar adsorbents before modification, before and after metal adsorption was observed using SEM at different magnifications. The SEM images shown in **Figure 3-2** indicate that the biochar surface is heterogenous and uneven which may affect the Pb (II) adsorption process [41]. The surface of magnetic-modified biochar adsorbent (see **Figure 3-2 (c and d)**) is coarse and hairy with crevices that are irregular with varying dimensions. These observations may signify the presence of openings acting as active sites for ions transfer and adsorption. The hairy-like particles on the magnetic hemp biochar surface may be due to iron oxide particles that are bonded to the biochar surface.

The SEM images after Pb (II) ion sorption also shows some crevice on the spent biochars. Comparing the SEM images in **Figure 3-2**, the biochar surface after Pb (II) adsorption, **Figure 3-2 (e and f)**, were more disaggregated and the surface roughness increased. These changes in the char surface in the scan of the Pb-loaded biochar may

be ascribed to the effects of adsorption process on the biochar when Pb (II) solution interfaces with the biochar particles.

During batch mode adsorption at the same agitation, It may be possible for the pores on the surface of MHBC-3 biochar may have served as the channels for the adsorbate ions in the solution, thus granting the ions access to the meso-pores where chemical interactions and surface adsorption take place with the reacting groups on the active sites of biochar [42].

Bright spots in the micrographs **Figure 3-2 (c-f)** also indicate that some degree of conductivity due to the presence of metals exist. When iron oxide forms, most biochar cavities are obstructed by iron oxide crystals developed in the biochar [43]. This is proven from the decreased BET surface area.

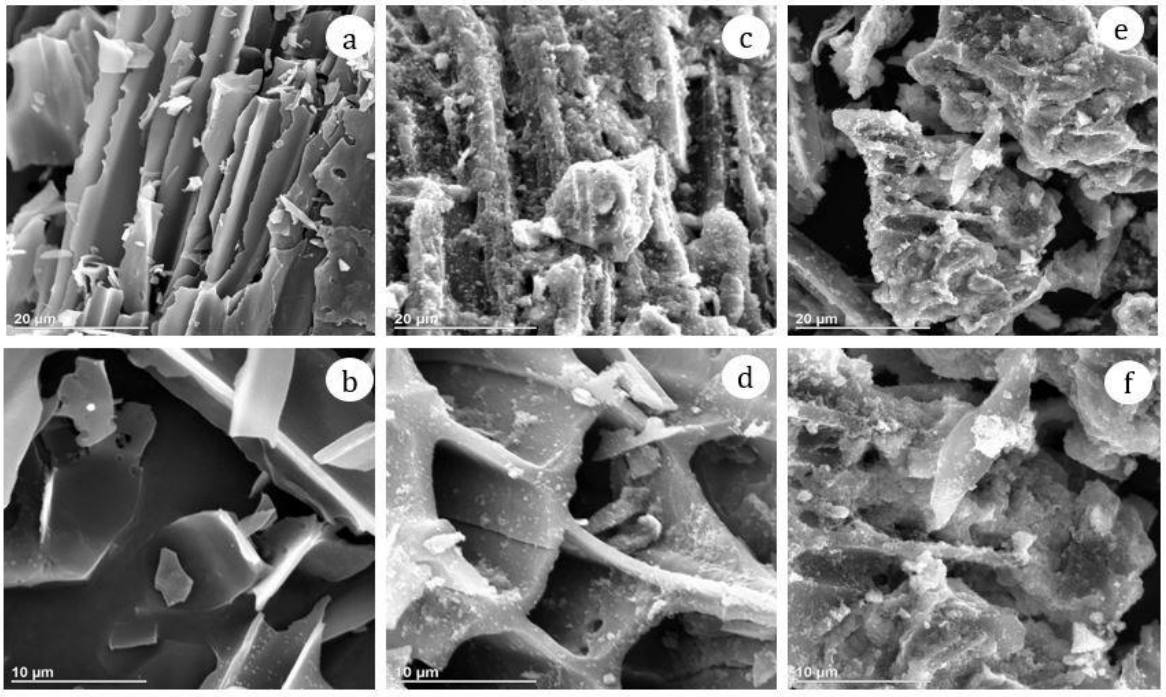

Figure 3-2 *SEM micrograph of hemp biochars (a) unmodified hemp x1500 (b) unmodified hemp x3000 (c) magnetic hemp (MHBC-3) x1500 (d) magnetic hemp (MHBC-3) x3000 (e) and (f) are lead-loaded magnetic biochars at x1500 and x3000 respectively.*

EDS analysis of the chemical composition for MHBC-3 biochar was performed and the spectra are shown in **Figure 3-3**. The analysis showed that the biochar possessed high carbon content (74.5%), iron content (12.4%), oxygen content (11.9%) and small amounts of other elements like calcium, silicon, potassium and sodium. The sudden rise in iron content from nearly 0% to 12.4% (EDS results, see **Figure 3-3**) after magnetization further confirms the data from elemental analysis shown in **Table 3.1** and gives credence to the fact that magnetization was successful.

The MHBC-3 EDS spectra after adsorption are also given in **Figure 3-3** for Pb (II) sorption. As can be seen from **Figure 3-3**, the peaks of Pb (II) are obvious, confirming its existence on the surface of the magnetic biochar after adsorption. It is equally important to notice that the carbon and iron content of the spent MHBC-3 biochar is lower than that of unused MHBC-3 adsorbent. The observation from the EDS of MHBC-3 before and after Pb (II) ions removal shows that the MHBC-3 adsorbent effectively removed Pb (II) ions from its solution.

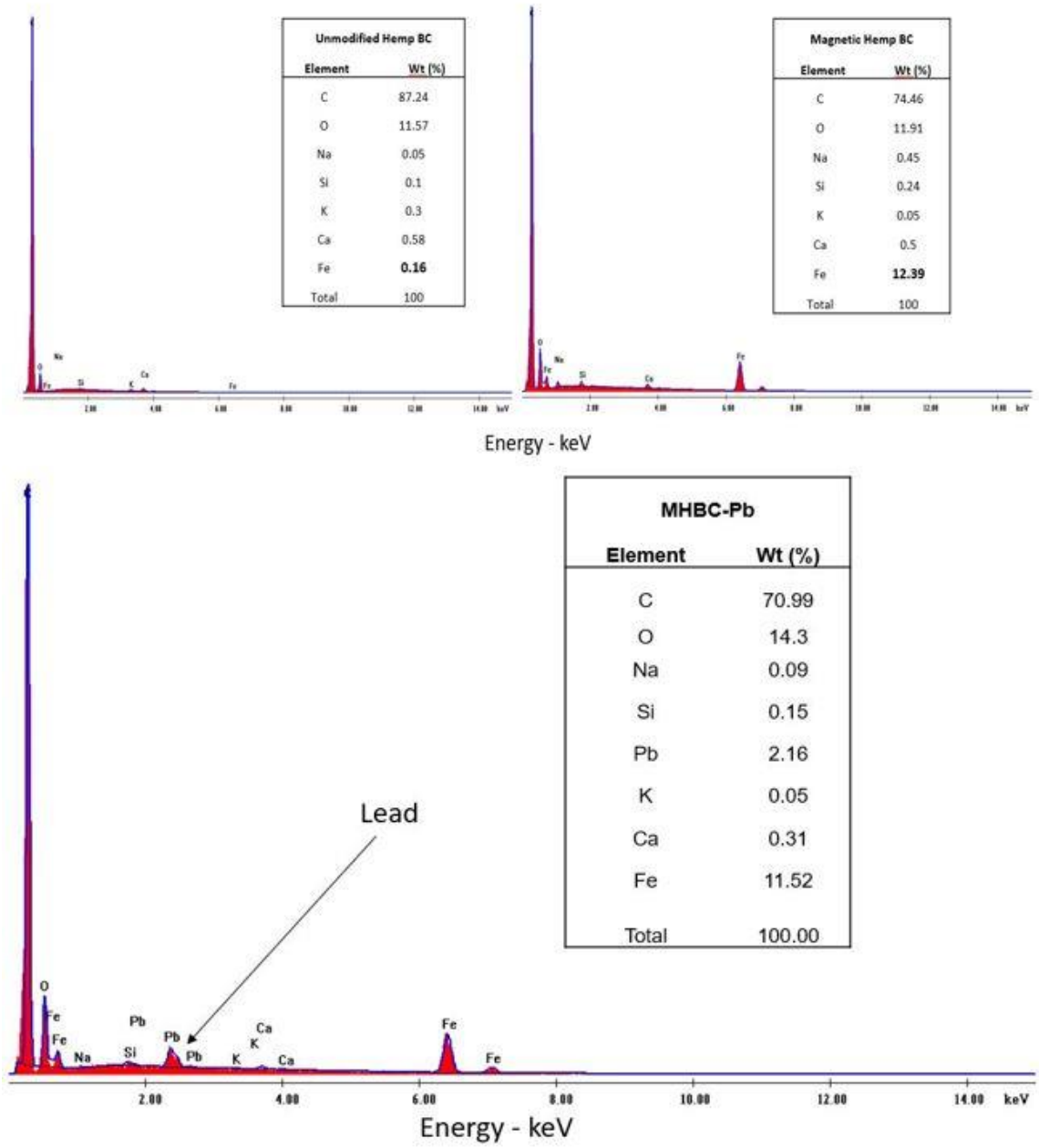

Figure 3-3 *EDS Spectra of hemp biochars before modification, after magnetic modification and after loading with Pb (II) ions.*

3.3.1.3. FT-IR Spectroscopic Characterization

The spectra of the hemp biochars in the region of (4000 – 500 cm^{-1}) before and after modification are given in **Figure 3-4**. The peaks between 1800 - 1685 cm^{-1} may be assign to C=O stretching vibrations from anhydrides carboxylic acids, ketones and esters. The band at 1600 cm^{-1} is assigned to C=C [44]. Similar results have been reported when saligna wood chips was used as the biomass for producing biochars

[45]. The presence of C-H indicates that the cellulose of the hemp biomass was not carbonized entirely during micro-wave pyrolysis process. The C=C bond is assigned to lignin's aromatic rings. The peaks at 650 cm^{-1} and 1470 cm^{-1} are assigned to Fe-O and N-O respectively [46].

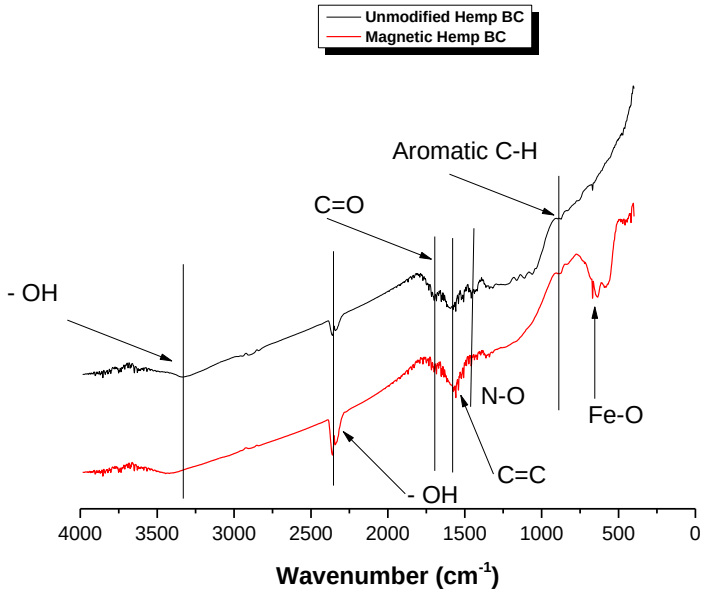

Figure 3-4 *FTIR spectra of hemp biochars before and after modification*

3.3.1.4. Vibrating Sample Magnetometry

The characteristics of a ferromagnetic material determines their suitability for application. This characteristic is given by its hysteresis loop derived from the plot of material's magnetization (M) against a field strength. Magnetization characteristic was performed at 27 ˚C by vibrating sample magnetometry (VSM) as shown in **Figure 3-5**. The value of the saturation magnetization was 10.68 emu g^{-1} for MHBC-3. This high value may be associated to the high content of iron oxides present in the biochar hybrid particles. The type and nature of the biochar determines the steps in the magnetization process.

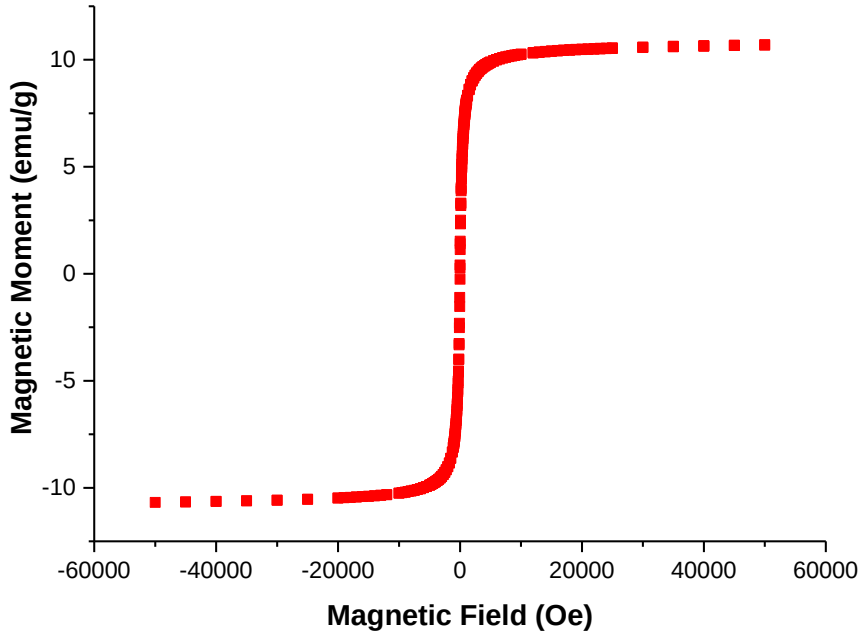

Figure 3-5 *Magnetic moment of hemp biochar (MHBC-3) at 27 ˚C*

The biochar surface is rich in various oxygen-containing functional groups including carboxylic acid, hydroxy, quinone, anhydride, ketone, alcohol, and other groups [47]. At the time of microwave pyrolysis of the hemp stalks biomass, varying amounts of oxygen (11.6 wt.%) were left in the biochar as shown in **Figure 3-3** depending on the pyrolysis temperature and time. Biochars consists of hydrophobic, hydrophilic, basic and acidic sites that are found throughout the subsurface volume and on the pore surfaces. The type of feedstock and the pyrolysis condition affects contributions of these functional groups and their properties. These operating variables include pyrolysis time, operating power which affects rate of heat transfer, temperature, reactor configuration and biomass particle size distribution [47]. Apart from carboxylic acid and phenolic hydroxyls, other functional groups such as lactones, anhydrides, ethers and quinines contain lone pairs of electrons which can act as Lewis bases, thus forming

coordinate bonds with metal cations. Because some hydrophilic functional groups that contain oxygen are present throughout the biochar, water molecules can travel into the solid regions thereby causing swellings [43]. Hence, heavy metal cations bind with adsorption sites on the biochar surface and, maybe, throughout some parts of the hemp biochar solid regions [43,47].

3.3.2. Adsorption Behavior

3.3.2.1. Biochar Adsorbents Comparative Test

The sorption efficiencies of Pb (II) ions induced by different absorbents, including raw biochar, H_2O_2 impregnated biochar and magnetically modified biochars (MHBC) are given in **Figure 3-6**. The adsorption efficiency of Pb (II) from solution by raw biochar was very low, under 40%. As expected, the modification of biochars improved their adsorption towards Pb (II). Furthermore, the adsorption efficiency of biochars was greatly increased after the magnetic modification. These results show that magnetic hemp biochars are excellent adsorbents or carriers of Pb (II) ions in aqueous solution. The study was done within 2 h contact time at 25 ˚C, using an adsorbent dose of 0.5 g/L at pH 5.0 and the initial concentration of Pb (II) solution was 20 mg/L.

The effects of weight percent of iron salts (Ferrous and Ferric sulphate) in solutions used for the magnetic modification on Pb (II) removal could also be identified from the results shown **Figure 3-6 (samples 3 - 6).** The adsorption efficiency of the magnetic chars increased with the wt.% of iron salts (Fe^{2+}/Fe^{3+}) from 0% to 3% significantly. This increase in adsorption efficiency was however negatively affected when the concentration of iron salts was slightly increased to 4%. It could be inferred that the iron oxide particles at an over-dosage can induce the blockage or collapse of

the biochar pores. Therefore, the optimal concentration of $FeSO_4.7H_2O$ and $Fe_2(SO4)_3.nH_2O$ in the solution used to modify the biochar was found at 3.0 wt.%.

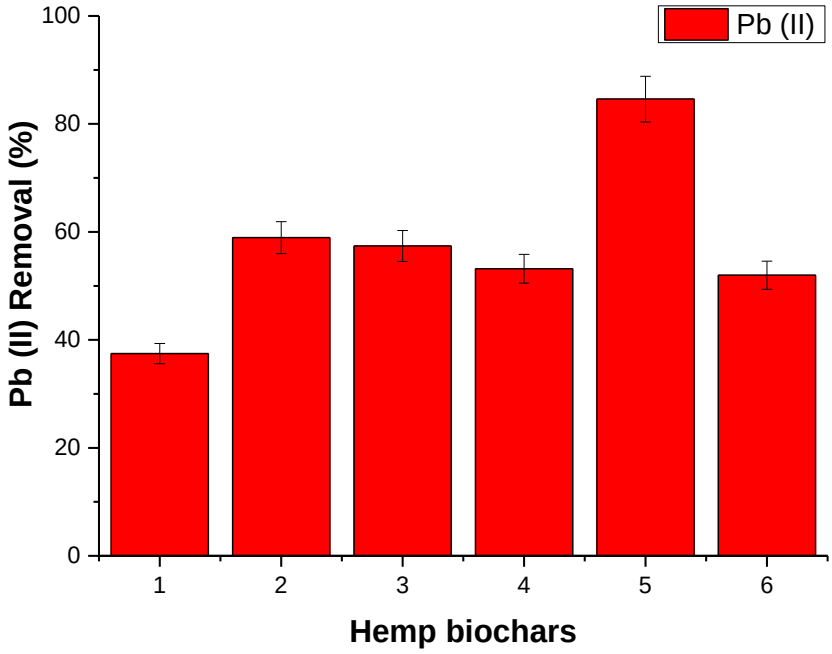

Figure 3-6 *Lead removal efficiency by different biochars; (1) Unmodified hemp (2) H_2O_2 impregnated Hemp (3) MHBC-1 (4) MHBC-2 (5) MHBC-3 (6) MHBC-4*

3.3.2.2. Effects of pH

Pb (II) ions adsorption in solutions is largely dependent on the aqueous solution pH which influence the ionization of cations as well as the concentration of competing H^+ or H_3O^+ ions in solution. To reveal the pH effects on Pb (II) sorption, the pH of a 20 mg/L solution was adjusted from 2 to 7. The results are presented in **Figure 3-7**. As expected, the highest Pb (II) sorption occurred at a high pH values or close to neutral conditions. It is worth noting that the current study was performed at pH values in which the metal ions would not hydrolyzed and precipitate from solution. This pH is estimated to be 7.7 for $Pb(OH)_2$ [33]. The optimal pH for the sorption of Pb (II) from

solution by MHBCs was 7.0, which facilitates the practical application and allows the adsorption efficiency of MHBC-3 to be as high as 98.7%.

In aqueous solutions, Pb^{2+} species is pre-dominant at pH between 2–7. When the pH is high, $PbOH^{+}$ can exist [14]. The removal efficiency of Pb (II) by the adsorbents was very low at a pH below 3. At a lower pH, the hydronium ions (H_3O^{+}) concentration is higher. Hence, there are more protons contending with Pb^{2+} for the active sites of biochar. Although the surface of biochar adsorbent has a net negative charge, it becomes challenging to adsorb cations which are positively charged due to repulsion between adsorbates on biochar [48,49]. Higher pH (pH > 3) values are favourable to the deprotonation of the adsorbent's carboxylic acid, phenolic, hydroxyl and other acidic functional groups, thereby making adsorbent's surface negatively charged. These negative active sites are formed on both ferric oxide/Fe_3O_4 and biochar surfaces. Thus, there is an increased electrostatic attraction between the Pb^{2+} ions in solution and adsorbent surface. This improves the Pb^{2+}ions sorption. To correlate ions uptake efficiency with the adsorption process, the kinetic and equilibrium studies of Pb (II) were further conducted at an initial solution pH 5.0.

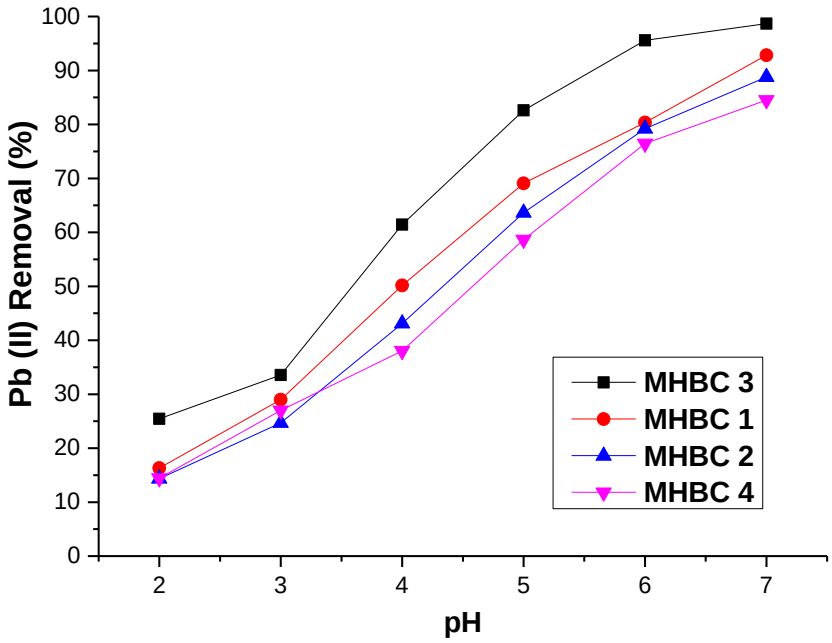

Figure 3-7 *Effects of pH on adsorption of Pb (II) ions from aqueous solution at 25 ˚C by various magnetic hemp biochars*

3.3.2.3. Effects of Temperature

The effects of operating temperature on the sorption of Pb (II) ions from a 20 mg/L solution was studied by varying the solution temperature between 25 and 65 ˚C at a pH of 5.0 in 2 h using adsorbent dose of 0.5 g/L. The experimental results are shown in **Figure 3-8.** Adsorption of Pb (II) ions from aqueous increased tremendously as the temperature was raised from 25 to 35 ˚C. This observation shows that adsorption mechanism on MHBCs is an endothermic process. Above 35 ˚C, the sorption efficiency did not change distinctively. Therefore, an optimum temperature of 35 ˚C was chosen for Pb (II) ions adsorption onto MHBCs.

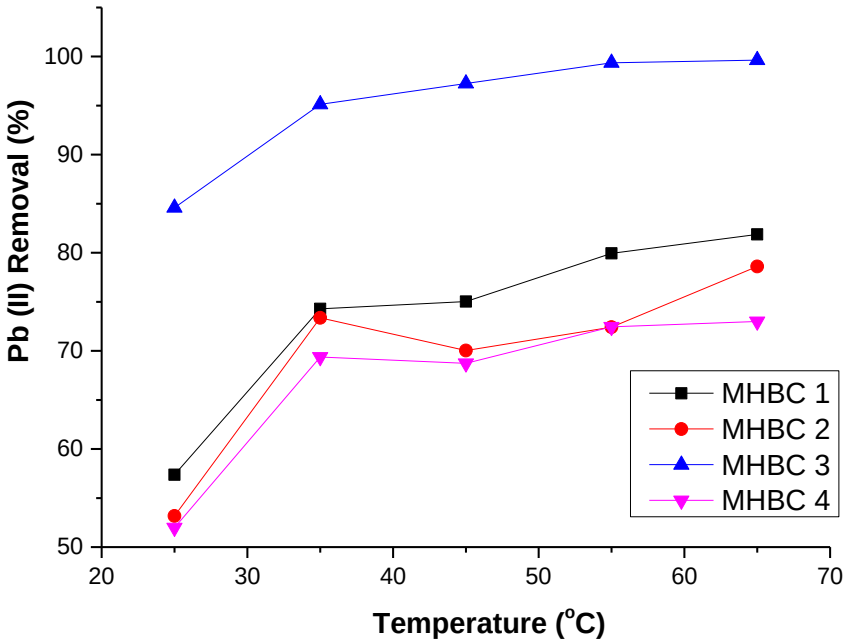

Figure 3-8 *Effects of temperature on the adsorption of Pb (II) ions by various magnetic hemp biochars*

3.3.3. Adsorption Kinetics and Isotherms

3.3.3.1. Adsorption kinetics

The impacts of exposure time on the sorption efficiency of MHBC-3 for Pb (II) ions in solution was examined and results are presented in **Figure 3-9**. The study was conducted at various temperatures (25, 35 and 45 ˚C) and pH 5.0. Initially, the adsorption proceeded very fast (within the first 10 minutes, more than 70% was adsorbed). This could be associated to the vacancy of numerous active sites on the MHBC-3 surface. However, as more Pb (II) ions adsorbed on MHBC-3, the available active sites becomes limited, thus lowering the rate of adsorption. The slower rate of adsorption may be due to different factors including electrostatic repulsion between the captured absorbates and the incoming ions and the decreased in the number of active-sites available to be filled. As expected, the occupation of the remaining

available active sites occurred in a much slower pace than the beginning when there were large number of sites for adsorption. Several studies have reported a two-phase pattern in adsorption kinetics [50-54].

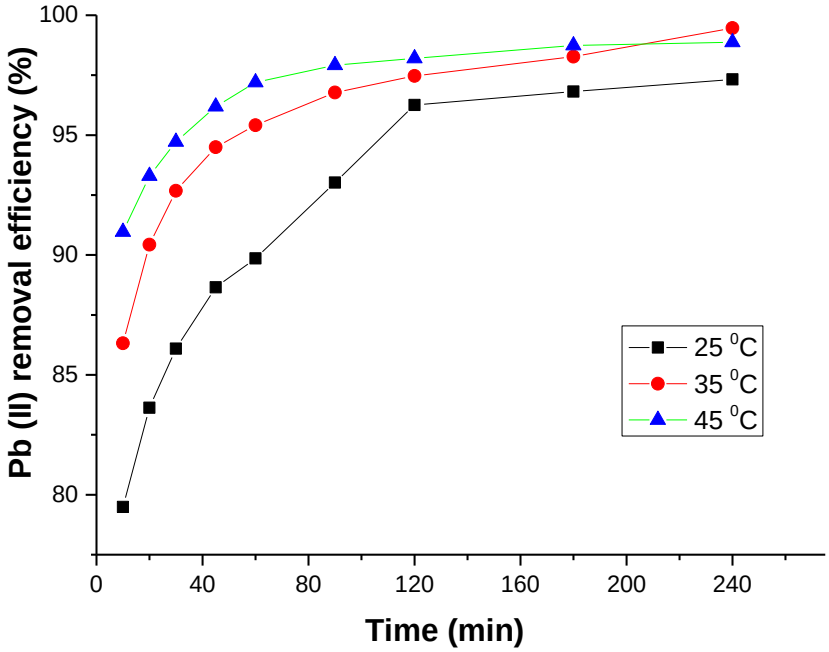

Figure 3-9 *Effects of contact time on adsorption of Pb (II) from aqueous solution by MHBC-3*

The loading of Pb (II) onto MHBC-3 t was modelled with two kinetics models. These are pseudo-first-order (PFO) and pseudo-second-order (PSO) models. A non-linear approach, trial and error method were used to evaluate these models. This approach determines the parameters of model by decreasing the determination coefficient between the models and experimental data with solver add-in in excel [55,56].

To use non-linear regression to examine the goodness of fit of these models to values obtained from experiment, the optimization method needs the error functions to be specified in order to fit the model parameters with the data from experiment. Here in, the adjusted coefficient of determination (adj. R^2), root mean square error (RMSE) and

reduced Chi square test (ε^2) were employed as error parameters for the models and these were calculated according to equations A3.6 and A3.7 in Appendix A.

3.3.3.1.1. Pseudo First and Second Order Kinetic Modelling

The graphs of **Figure 3-10** show PFO and PSO kinetics for Pb (II) ion adsorption by MHBC-3 biochar. The parameters of these kinetic models with their corresponding error functions are shown in **Table 3.2**. An analysis of **Figure 3-10** shows that the kinetics of Pb (II) ion adsorption could be better characterized by PSO kinetic model. Furthermore, PSO estimated parameter ($q_{e,model}$) is much closer to the data derived from the analysis of the experimental results of Pb(II) ion adsorption by MHBC-3.

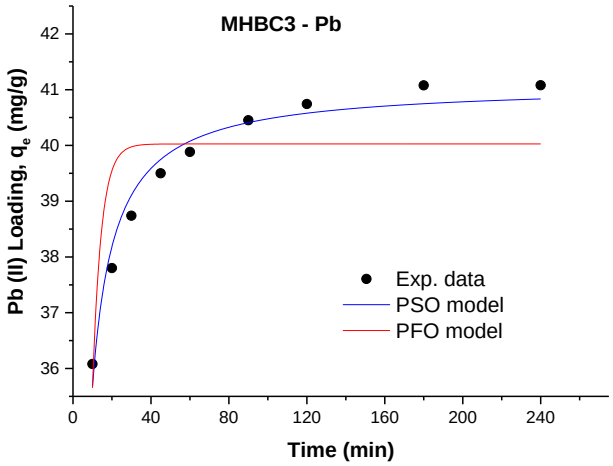

Figure 3-10 *Effect of contact time on Pb (II) ions loading onto MHBC-3 at 35 ˚C*

For PSO from **Table 3.2**, predicted adsorption ($q_{e,cal}$) was 40.83 mg/g while the experimental value was 41.08 mg/g at this operating condition. Furthermore, the adjusted R^2 is high, 0.962, while the reduced root mean square and reduced chi-square are lower values, 0.289 and 0.107 respectively, further demonstrates that PSO model better fits the data from experiment than PFO model. These results suggest that the rate-limiting step during the uptake of Pb (II) ions onto MHBC-3 biochar has the

chemisorption rate-limiting mechanism [57]. This involves the transfer of electron(s) or sharing of pairs of electrons between the adsorbate (Pb^{2+}) and MHBC-3 adsorbent.

Table 3.2 *PFO and PSO Kinetic parameters for Pb (II) adsorption onto MHBC-3*

Kinetic Models	***Parameters***	***Adsorbent***
Pseudo First Order (PFO)		MHBC3 - Pb
	$q_{e,\ cal}$ (mg g^{-1})	40.02
	K_1 (min^{-1})	0.221
	adj. R^2	0.599
	ε^2	1.138
	RMSE	0.94
Pseudo Second Order (PSO)		
	$q_{e,\ cal}$ (mg g^{-1})	40.83
	K_2 (g mg^{-1} min^{-1})	0.016
	adj. R^2	0.962
	ε^2	0.107
	RMSE	0.289

3.3.3.1.2. Intraparticle Diffusion Kinetic Modelling

The Pb (II) adsorption kinetics by MHBC-3 biochar was also described by the intraparticle diffusion model. The model assumes that intra-particle diffusion is the singular rate-controlling step if a plot of q_t against $t^{1/2}$ gives a linear graph that pass through the origin [58,59]. However, because other processes like equilibrium adsorption and/or surface diffusion could likewise be a rate-controlling step for the different phases of the model profile, the assumption is not always the case. Thus, the plot of intraparticle diffusion model has multiple linear regions [60,61]. The model

plot for the uptake of Pb (II) ions from solution by MHBC-3 biochar is presented in **Figure 3-11**. The model parameters derived from the plot are shown in **Table 3.3**.

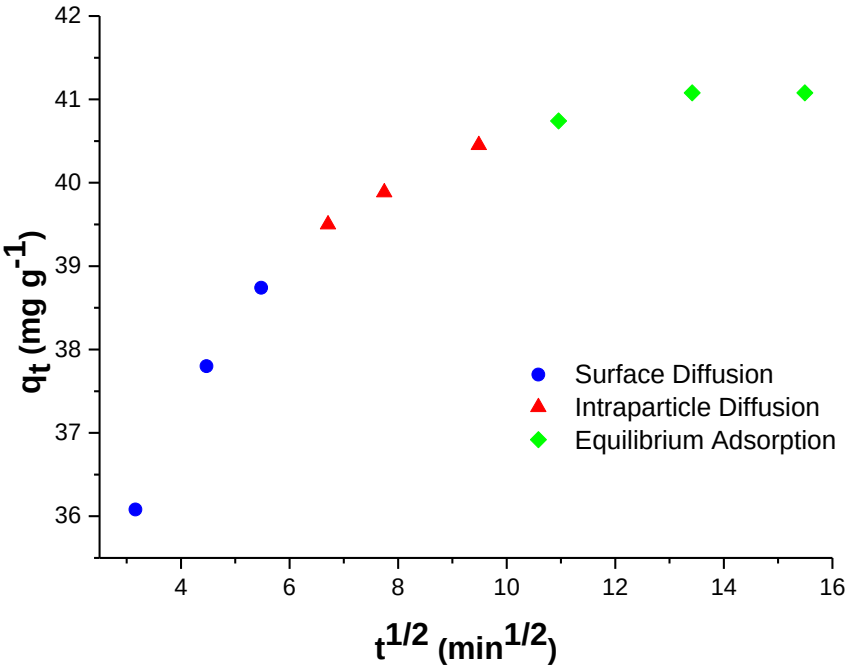

Figure 3-11 *Kinetic stages in intraparticle diffusion plot of Pb (II) ions adsorption on MHBC-3*

As shown in **Figure 3-11** and **Table 3.3**, there are multiple straight-line regions in the plot of intraparticle diffusion model. This implies that the loading of Pb (II) ions to MHBC-3 biochar happened through three phases: Phase 1 is the zone where surface diffusion takes place instantaneously in the system. In this region, the kinetics of Pb (II) ions adsorption may be pre-dominated by film diffusion as a result of the transport of the lead cations from solution through the boundary layer to the biochar surface. Diffusion rate is maximum in this region because there are enough adsorption sites and surface area [58]. Phase 2 describes the slow adsorption of Pb (II) ions by MHBC-3 adsorbent pore structures from the mesopores to micropores. Within this region, there is a layer on the biochar surface because of the attraction between ions and molecular association that exist between the MHBC-3 adsorbent active sites and metal

ions [58]. Here, the diffusion rate in the adsorbent pores may decrease in comparison to the first phase as a result of these thick layers. Phase 3 is final phase of the process when equilibrium is attained during the adsorption process. In this region, the decreased in concentration of the adsorbate in solution, the increased repulsive interactions existing on the adsorbent's surface and because the active sites left on the MHBC-3 adsorbent is now very small, the uptake or adsorption is slowed [62,63]. The diffusion rate in this phase was the lowest (smallest K_{id}) amongst the three phases. This shows that the adsorption process is driving towards completion.

Table 3.3 *Intraparticle diffusion parameters for MHBC-3 adsorption of Pb (II) ions*

Kinetic Models	***Parameters***	***MHBC3 - Pb***
Surface diffusion stage	K_{id} (mg g^{-1} $min^{-0.5}$)	1.16
	C	32.48
	adj. R^2	0.98
Intraparticle diffusion stage	K_{id} (mg g^{-1} $min^{-0.5}$)	0.341
	C	37.22
	adj. R^2	0.99
Equilibrium adsorption stage	K_{id} (mg g^{-1} $min^{-0.5}$)	0.08
	C	39.95
	adj. R^2	0.59

From the intraparticle diffusion plot in **Figure 3-11** and observations in **Table 3.3**, multiple steps exist in the rate of Pb (II) ions adsorption by magnetic hemp biochar. Moreover, the intraparticle diffusion profile did not go through the origin. Therefore, not only the intraparticle diffusion step controlled the ion removal process, but also other process did as describe above. If the constant C has a zero value, this will indicate that the intraparticle diffusion mechanism is the sole rate-controlling step of the

adsorption. However, the high value of C shows that surface adsorption contributed greatly to the rate-limiting step of the Pb (II) adsorption by MHBC-3. Furthermore, higher C values indicates a greater effect of boundary layer on Pb (II) ions diffusion through the surface of the biochar [64,65].

3.3.3.2. Adsorption Isotherms

Equilibrium experiments were undertaken for the loading of Pb (II) ions onto magnetic hemp biochar (MHBC-3). The initial solution concentration was between 5 mg L^{-1} to 500 mg L^{-1}. The biochar dose used was 0.5 g L^{-1} at 35 ˚C and a pH 5.0. From the experiment, metal ions uptake by the biochar was determined. The Freundlich, Temkin Langmuir, and Dubinin-Redushkevich models were employed to characterise the ions loading process. The detailed description of these models can be found in the supplementary file. The non-linear method which uses trial and error approach was used to evaluate the isotherm models. As mentioned earlier, this method obtains isotherm model parameters by ensuring that determination coefficient between isotherm models and experimental data is minimum. This is achieved using an add-in in Microsoft excel called solver [55,56].

The isotherms obtained for the uptake of Pb (II) ions by magnetic hemp biochar are presented in **Figure 3-12**. From the plots of the isotherms based on different models, their respective parameters were obtained as shown in **Table 3.4**.

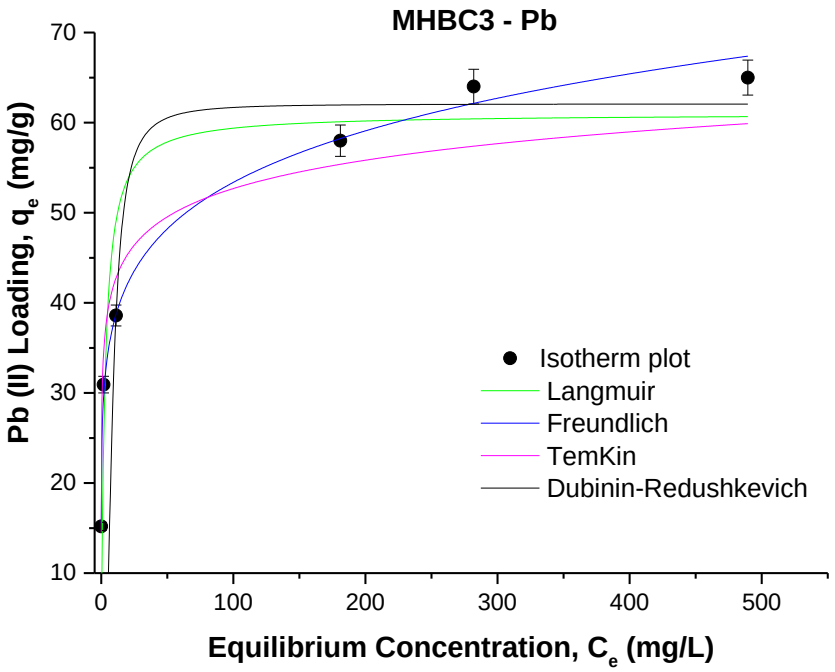

Figure 3-12 *Langmuir, Freundlich, Temkin and Dubinin-Redushkevich adsorption isotherms for Pb (II) ions on MHBC-3*

With the parameters from the three isotherm models, it was possible to decide the model that best fit the data from the experiment. Here in, the adjusted coefficient of determination (adj. R^2), reduced chi-square test (ε^2) and the root mean square error (RMSE) are shown in **Table 3.4**. In **Table 3.4**, the Freundlich model describes the sorption of Pb (II) from aqueous solution onto MHBC-3 better than other models (see the isotherm section of Appendix A).

Table 3.4 *Isotherm parameters for adsorption of Pb (II) ions on MHBC-3*

Isotherm Models	*Parameters*	*MHBC3 - Pb*
Langmuir	q_{max} (mg g^{-1})	61.00
	K_L (L mg^{-1})	0.38
	adj. R^2	0.76
	ε^2	100.20
	RMSE	8.17
Freundlich	K_F (mg g^{-1})(L mg^{-1})$^{1/n}$	27.15
	n	6.81
	adj. R^2	0.99
	ε^2	1.15
	RMSE	0.88
Temkim	A_T (L mg^{-1})	1110.60
	b_T	565.01
	adj. R^2	0.96
	ε^2	12.97
	RMSE	2.94

The Langmuir parameter, q_{max} calculated in this research was compared with other published study on the adsorption of Pb (II) ions by magnetic biochars and activated carbon from aqueous solution. These finding are shown in **Tables 3.5**. In this work, the R_L parameter is between 0 and 1, because $K_L > 0$, thus demonstrating that the Pb(II) loading process was favourable (calculated from **equation A3.2**). From **Tables 3.5**, the highest loading obtained using the MHBC-3 biochar for the uptake of Pb (II) ions is in the range of values reported from previous studies on magnetic biochars and commercial activated carbon adsorbents. Therefore, the magnetic hemp biochar, MHBC-3 utilized in this research was excellent in removing Pb (II) ions from lead-contaminated aqueous solution. The adsorption parameters and characteristics are in the scope of published work for activated carbon and magnetic biochar adsorbents.

Table 3.5 *Comparison of Langmuir adsorption capacities of magnetic hemp biochar versus other biochars/activated carbon for Pb (II) ions removal from solution*

Adsorbents	***Medium***	***pH***	***Temp. (˚C)***	***Conc. range (mg/L)***	***Surface area (m^2/g)***	***Pb (II) Loading, q_{max} (mg/g)***	***Ref.***
Magnetic microwave pyrolyzed hemp biochar	Aqueous solution	***5.0***	***35***	***5-500***	***83.8***	***61.00***	This study[1]
Unmodified hemp biochar	Aqueous solution	***5.0***	***35***	***5-500***	***142.5***	***27.02***	This study[1]
Magnetic oak bark char	Aqueous solution	5.0	35	1-100	8.8	37.24	[33]
Pine bark char	Aqueous solution	5.0	25	1-100	1.88	3.00	[14]
Oak bark char	Aqueous solution	5.0	40	1-100	25.4	22.61	
Pinewood biochar	Synthetic	5.0	35	5.0 - 40	Not available	4.03	[66]
Raw sugarcane bagasse biochar	Aqueous solution	-	22	5-200	17.7	6.48	[67]
DWSBC (digested whole sugar beet biochar)	Aqueous solution	5.0	22	5-600	128.5	40.82	
Commercial activated carbon (AC)	Aqueous solution	5.0	35	2.0-10	1000	21.80	[68]
Commercial granular activated carbon	Aqueous solution	5.0	40	1-150	1058	43.10	[69]
Commercial activated carbon (CGAC)	Aqueous solution	7.0	25	50-500	4273	20.30	[39]

[1]The values in bold and italics are results obtained in this study

3.3.4. Regeneration of Magnetic Hemp Biochar

3.3.4.1. Recyclability of MHBC-3 for Pb (II) Sorption

Multiple regeneration experiments were performed via adsorption-desorption cycles at 25 ˚C. In the adsorption step, Pb-loaded MHBC-3 was prepared with a dose of 1.0 g L^{-1}, Pb (II) solution concentration of 20 mg L^{-1} at pH 5.0 and contact time of 2 h. For the desorption stage, the prepared Pb-loaded MHBC-3 adsorbents were desorbed using 0.1 mol L^{-1} EDTA-2Na during a contact time of 2 h with a solid concentration at10 g L^{-1}.

This method is required to maintain the adsorption performance of the biochar and ensure the recovery of valuable metals from wastewater streams. The biochar was reused five times at the above stated operating conditions. The adsorption efficiency for the five cycles were 99.9, 92.85, 88.15, 73.15, 71.35 % respectively as shown in **Figure 3-13**. This progressive decline in adsorption performance of MHBC-3 as the number of cycles increase may be because of the prior regeneration process which may have altered the porous structures of MHBC-3 and subsequently resulted in blockage or loss of adsorption sites [70]. The adsorption performance of MHBC-3 after five cycles was still satisfactory; over 70% removal efficiency for Pb (II) ions. This demonstrates that magnetic hemp biochar (MHBC-3) is a renewable absorbent for treatment of lead ions-contaminated water.

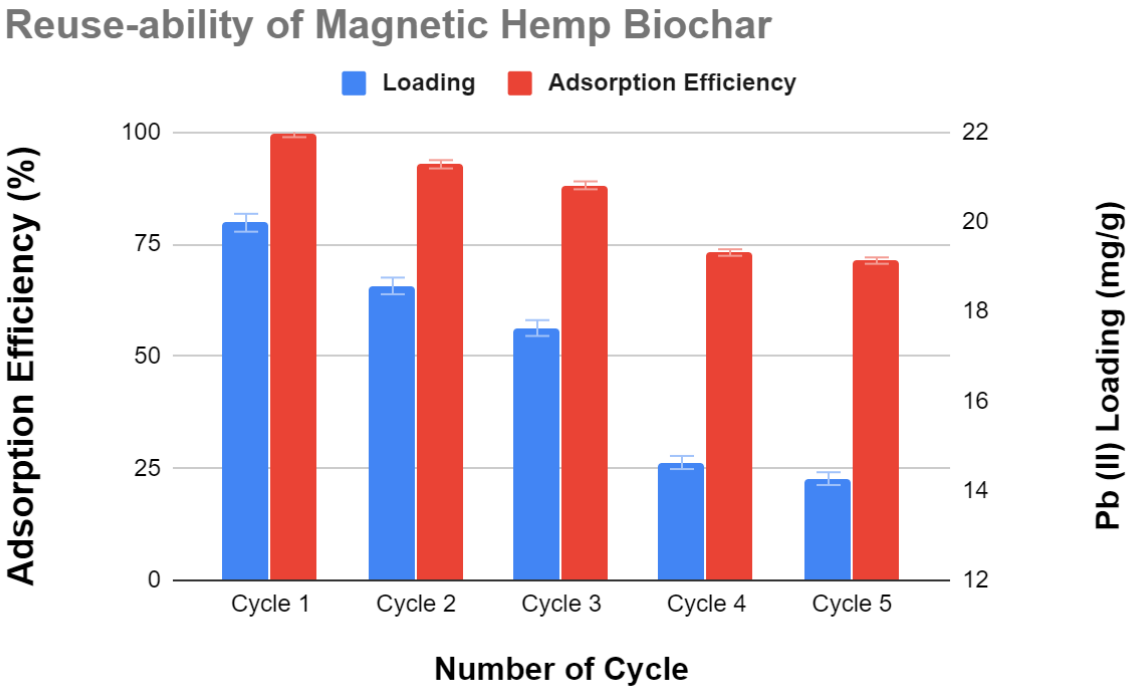

Figure 3-13 *Pb (II) ions removal efficiency by regenerated MHBC-3*

Additionally, the desorption efficiency of Pb (II) by the eluent (EDTA-2Na) and loss of iron oxides from biochar surface due to leaching was determined; and these results are given in **Figure 3-14**. During the adsorption/desorption cycle, it was assumed that iron particles leaching is negligible since the adsorption occurred in aqueous solution and the iron particles are tightly bonded to the char surface as demonstrated earlier. For the first desorption cycle with 18.2 mg/g of Pb (II) ions desorbed (91.1% desorption efficiency), the loss of iron particles was 2.4 mg/g. The loss of iron particles was significantly lower in subsequent regeneration cycles. This indicates that the loss of magnetism by the MHBC-3 due to regeneration was not an issue. Furthermore, the FT-IR spectra of the magnetic hemp biochar and regenerated biochar as shown in **Figure A3-1** showed that all active functional groups including the peak at 650 cm^{-1} assigned to Fe-O were intact; thus, the regeneration process did not have significant impact on the magnetic properties of the adsorbent.

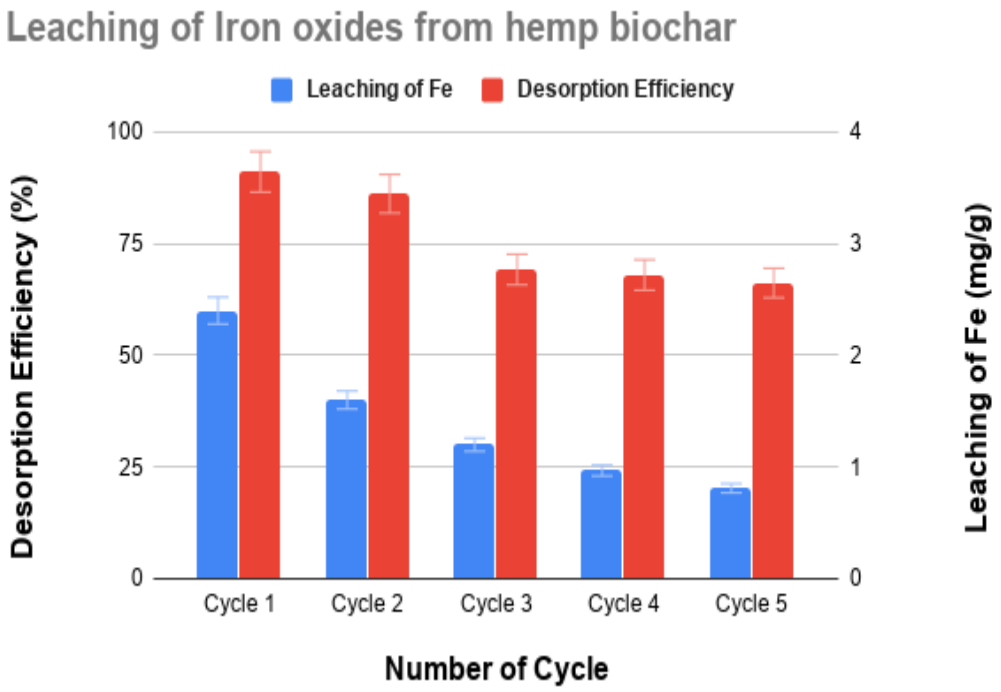

Figure 3-14 *Dissociation performance of EDTA-2Na for Pb-loaded MHBC-3*

3.3.4.2. Separation of adsorbent from solution

The magnetic separation studies were undertaken with - MHBC-3 dose of 0.5 g/L and at various separation time (1, 5, 10, 20 and 30 min) as shown in **Figure 3-15**. This study considered separation by both internal and external magnetic field. An external magnetic field is generated by placing the biochar suspension on the magnetic jig while the internal magnetic field occurs when the magnetic jig is inserted into the biochar suspension. From **Figure 3-15**, the magnetic hemp biochar suspension had an initial turbidity of 456 NTU. Within the first 1 minute of exposing the biochar suspension to a magnetic field, the turbidity decreased sharply to 154 NTU and 111 NTU for the external and internal magnetic fields respectively. After 30 minutes of exposure, the turbidity of the suspensions was lowered to 19.9 NTU and 8.79 NTU for the external and internal field respectively. This demonstrates that the Pb-loaded MHBC-3 could be recovered from solution within few minutes using a magnetic field strength. As

expected, internal separation was a more effective method of recovering the spent MHBC-3 because of the proximity of the biochar magnetic particles to the magnetizing jig. In conclusion, the small quantity of leached iron particles did not significantly impact on the magnetic separation of the recycled MHBC-3.

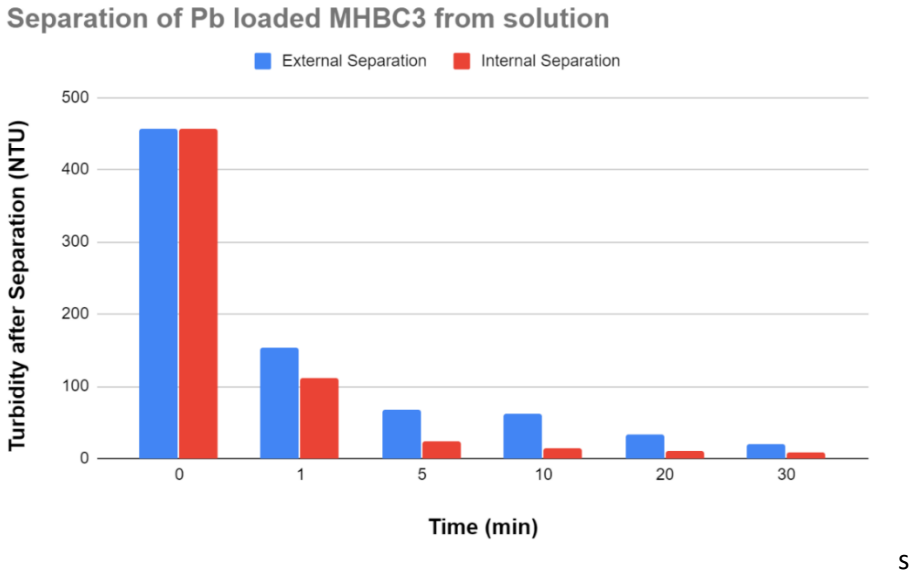

s

Figure 3-15 *Magnetic separation performance of magnetic hemp biochar (MHBC-3)*

Magnetic hemp biochars were manipulated effortlessly with a weak strength magnetic field, allowing for an easy recovery of the used biochar from aqueous solution. Magnetic hemp biochars could be used to remediate lead polluted water with high content of oil, grease and suspended solids. This will be particularly applicable where impurities are more likely to result in carbon fouling, hence requiring constant separation/regeneration treatments. Easy separation with a low magnetic field strength can permit separation and washing of the spent biochar before redispersion.

3.4. Conclusions

Hemp biochar was produced by microwave-assisted pyrolysis of hemp stalks biomass. This was converted to magnetic hemp biochar via hydrogen peroxide oxidation followed by chemical co-precipitation of iron oxides onto the biochar. The modification reduced the BET of the char from 142.5 to 83.8 m^2 g^{-1} due to the iron oxides formation with a saturation magnetization of 10.7 emu g^{-1}. The magnetic biochar effectively adsorbed Pb (II) ions from aqueous solution. The correlation coefficients indicate that the adsorption process of Pb (II) onto the magnetic char follows a pseudo-second-order (PSO) kinetics and the equilibrium data was well characterized by the Freundlich isotherm. A Langmuir maximum adsorption capacity of the adsorbent was 61.0 mg g^{-1} for an initial solution concentration of range of 5 - 500 mg L^{-1} at pH 5.0 and a temperature of 35 ˚C using adsorbent dose of 0.5 g L^{-1}. The adsorption efficiency of the adsorbent in removing Pb (II) ions from aqueous solution and its magnetic separation performance were still very satisfactory after 5 regeneration cycles. Magnetic hemp biochar was manipulated easily by a low magnetic field strength, ensuring an easy recovery of the spent adsorbents from aqueous system. The magnetic hemp biochar is a green-based, renewable and cost-effective absorbent with a potential to remediate lead ions-contaminated water.

.

3.5. References

[1] Godwin P, Pan Y, Xiao H, Afzal MT. Progress in the preparation and application of modified biochar for improving heavy metal ion removal from wastewater. J Bioresour Bioprod 2019;4:31–42. doi:10.21967/JBB.V4I1.180.

[2] Wang N-X, Zhang X-Y, Wu J, Xiao L, Yin Y, Miao A-J, et al. Effects of microcystin-LR on the metal bioaccumulation and toxicity in Chlamydomonas reinhardtii. Water Res 2012;46:369–77. doi:10.1016/J.WATRES.2011.10.035.

[3] Seiler HG, Sigel H, Sigel A. Handbook on toxicity of inorganic compounds 1988.

[4] Ali I. The Quest for Active Carbon Adsorbent Substitutes: Inexpensive Adsorbents for Toxic Metal Ions Removal from Wastewater. Sep Purif Rev 2010;39:95–171. doi:10.1080/15422119.2010.527802.

[5] Demirbas A. Heavy metal adsorption onto agro-based waste materials: A review. J Hazard Mater 2008;157:220–9. doi:10.1016/J.JHAZMAT.2008.01.024.

[6] Bailey SE, Olin TJ, Bricka RM, Adrian DD. A review of potentially low-cost sorbents for heavy metals. Water Res 1999;33:2469–79. doi:10.1016/S0043-1354(98)00475-8.

[7] Dupont L, Guillon E. Removal of hexavalent chromium with a lignocellulosic substrate extracted from wheat bran. Environ Sci Technol 2003;37:4235–41. doi:10.1021/es0342345.

[8] Yu J-X, Wang L-Y, Chi R-A, Zhang Y-F, Xu Z-G, Guo J. Competitive adsorption of Pb2+ and Cd2+ on magnetic modified sugarcane bagasse prepared by two simple steps. Appl Surf Sci 2013;268:163–70. doi:10.1016/J.APSUSC.2012.12.047.

[9] Gupta VK, Al Khayat M, Singh AK, Pal MK. Nano level detection of Cd(II) using poly(vinyl chloride) based membranes of Schiff bases. Anal Chim Acta 2009;634:36–43. doi:10.1016/J.ACA.2008.11.065.

[10] Xue Y, Gao B, Yao Y, Inyang M, Zhang M, Zimmerman AR, et al. Hydrogen peroxide modification enhances the ability of biochar (hydrochar) produced from hydrothermal carbonization of peanut hull to remove aqueous heavy metals: Batch and column tests. Chem Eng J 2012;200–202:673–80. doi:10.1016/j.cej.2012.06.116.

[11] Chen X, Chen G, Chen L, Chen Y, Lehmann J, McBride MB, et al. Adsorption of copper and zinc by biochars produced from pyrolysis of hardwood and corn straw in aqueous solution. Bioresour Technol 2011;102:8877–84. doi:10.1016/J.BIORTECH.2011.06.078.

[12] Xu X, Cao X, Zhao L, Wang H, Yu H, Gao B. Removal of Cu, Zn, and Cd from aqueous solutions by the dairy manure-derived biochar. Environ Sci Pollut Res 2013;20:358–68. doi:10.1007/s11356-012-0873-5.

[13] Inyang M, Gao B, Yao Y, Xue Y, Zimmerman AR, Pullammanappallil P, et al. Removal of heavy metals from aqueous solution by biochars derived from anaerobically digested biomass. Bioresour Technol 2012;110:50–6. doi:10.1016/J.BIORTECH.2012.01.072.

[14] Mohan D, Pittman CU, Bricka M, Smith F, Yancey B, Mohammad J, et al. Sorption of arsenic, cadmium, and lead by chars produced from fast pyrolysis of wood and bark during bio-oil production. J Colloid Interface Sci 2007;310:57–73. doi:10.1016/J.JCIS.2007.01.020.

[15] Cao X, Ma L, Gao B, Harris W. Dairy-Manure Derived Biochar Effectively Sorbs Lead and Atrazine. Environ Sci Technol 2009;43:3285–91. doi:10.1021/es803092k.

[16] Park JH, Choppala GK, Bolan NS, Chung JW, Chuasavathi T. Biochar reduces the bioavailability and phytotoxicity of heavy metals. Plant Soil 2011;348:439–51. doi:10.1007/s11104-011-0948-y.

[17] Brewer CE, Schmidt-Rohr K, Satrio JA, Brown RC. Characterization of biochar from fast pyrolysis and gasification systems. Environ Prog Sustain Energy 2009;28:386–96. doi:10.1002/ep.10378.

[18] Mullen CA, Boateng AA, Goldberg NM, Lima IM, Laird DA, Hicks KB. Bio-oil and bio-char production from corn cobs and stover by fast pyrolysis. Biomass and Bioenergy 2010;34:67–74. doi:10.1016/J.BIOMBIOE.2009.09.012.

[19] Dinesh Mohan * , † , ‡, and CUPJ†, § PHS. Pyrolysis of Wood/Biomass for Bio-oil: A Critical Review 2006. doi:10.1021/EF0502397.

[20] Lu H, Zhang W, Yang Y, Huang X, Wang S, Qiu R. Relative distribution of Pb2+ sorption mechanisms by sludge-derived biochar. Water Res 2012;46:854–62. doi:10.1016/J.WATRES.2011.11.058.

[21] BIRD MI, WURSTER CM, DE PAULA SILVA PH, PAUL NA, DE NYS R. Algal biochar: effects and applications. GCB Bioenergy 2012;4:61–9. doi:10.1111/j.1757-1707.2011.01109.x.

[22] Bird MI, Wurster CM, de Paula Silva PH, Bass AM, de Nys R. Algal biochar – production and properties. Bioresour Technol 2011;102:1886–91. doi:10.1016/J.BIORTECH.2010.07.106.

[23] Xu R, Xiao S, Yuan J, Zhao A. Adsorption of methyl violet from aqueous solutions by the biochars derived from crop residues. Bioresour Technol 2011;102:10293–8. doi:10.1016/J.BIORTECH.2011.08.089.

[24] Chingombe P, Saha B, Wakeman RJ. Surface modification and characterisation of a coal-based activated carbon. Carbon N Y 2005;43:3132–43. doi:10.1016/J.CARBON.2005.06.021.

[25] Abe M, Kawashima K, Kozawa K, Sakai H, Kaneko K. Amination of activated carbon and adsorption characteristics of its aminated surface. Langmuir 2000;16:5059–63. doi:10.1021/la990976t.

[26] Chaukura N, Gwenzi W, Mupatsi N, Ruziwa DT, Chimuka C. Comparative Adsorption of Zn2+from Aqueous Solution Using Hydroxylated and Sulphonated Biochars Derived from Pulp and Paper Sludge. Water Air Soil Pollut 2017;228. doi:10.1007/s11270-016-3191-6.

[27] Chang YC, Chang SW, Chen DH. Magnetic chitosan nanoparticles: Studies on chitosan binding and adsorption of Co(II) ions. React Funct Polym 2006;66:335–41. doi:10.1016/j.reactfunctpolym.2005.08.006.

[28] Faulconer EK, von Reitzenstein NVH, Mazyck DW. Optimization of magnetic powdered activated carbon for aqueous Hg(II) removal and magnetic recovery. J Hazard Mater 2012;199–200:9–14. doi:10.1016/J.JHAZMAT.2011.10.023.

[29] Mohan D, Sarswat A, Singh VK, Alexandre-Franco M, Pittman CU. Development of magnetic activated carbon from almond shells for trinitrophenol removal from water. Chem Eng J 2011;172:1111–25. doi:10.1016/J.CEJ.2011.06.054.

[30] Yamamura APG, Yamaura M, Costa CH. Magnetic biosorbent for removal of uranyl ions. Int J Nucl Energy Sci Technol 2011;6:8. doi:10.1504/IJNEST.2011.039243.

[31] Patzak M, Dostalek P, Fogarty R V., Safarik I, Tobin JM. Development of magnetic biosorbents for metal uptake. Biotechnol Tech 1997;11:483–7. doi:10.1023/A:1018453814472.

[32] Zhang M, Gao B, Varnoosfaderani S, Hebard A, Yao Y, Inyang M. Preparation and characterization of a novel magnetic biochar for arsenic removal. Bioresour Technol 2013;130:457–62. doi:10.1016/j.biortech.2012.11.132.

[33] Mohan D, Kumar H, Sarswat A, Alexandre-Franco M, Pittman CU. Cadmium and lead remediation using magnetic oak wood and oak bark fast pyrolysis bio-chars. Chem Eng J 2014;236:513–28. doi:10.1016/J.CEJ.2013.09.057.

[34] Safarik I, Horska K, Svobodova B, Safarikova M. Magnetically modified spent coffee grounds for dyes removal. Eur Food Res Technol 2012;234:345–50. doi:10.1007/s00217-011-1641-3.

[35] Ambashta RD, Sillanpää M. Water purification using magnetic assistance: A review. J Hazard Mater 2010;180:38–49. doi:10.1016/J.JHAZMAT.2010.04.105.

[36] Safarik I, Horska K, Pospiskova K, Safarikova M. Magnetically Responsive Activated Carbons for Bio - and Environmental Applications. Int Rev Chem Eng 2012;4:346–52.

[37] Salema AA, Afzal MT, Bennamoun L. Pyrolysis of corn stalk biomass briquettes in a scaled-up microwave technology. Bioresour Technol 2017;233:353–62. doi:10.1016/j.biortech.2017.02.113.

[38] NAKAHIRA A, NISHIDA S, FUKUNISHI K. Synthesis of Magnetic Activated Carbons for Removal of Environmental Endocrine Disrupter Using Magnetic Vector. J Ceram Soc Japan 2006;114:135–7. doi:10.2109/jcersj.114.135.

[39] Asuquo E, Martin A, Nzerem P, Siperstein F, Fan X. Adsorption of Cd(II) and Pb(II) ions from aqueous solutions using mesoporous activated carbon adsorbent: Equilibrium, kinetics and characterisation studies. J Environ Chem Eng 2017;5:679–98. doi:10.1016/j.jece.2016.12.043.

[40] Ho YS, McKay G. The kinetics of sorption of divalent metal ions onto sphagnum moss peat. Water Res 2000;34:735–42. doi:10.1016/S0043-1354(99)00232-8.

[41] Ge X, Wu Z, Wu Z, Yan Y, Cravotto G, Ye BC. Microwave-assisted modification of activated carbon with ammonia for efficient pyrene adsorption. J Ind Eng Chem 2016;39:27–36. doi:10.1016/j.jiec.2016.05.003.

[42] Pezoti O, Cazetta AL, Bedin KC, Souza LS, Martins AC, Silva TL, et al. NaOH-activated carbon of high surface area produced from guava seeds as a high-efficiency adsorbent for amoxicillin removal: Kinetic, isotherm and thermodynamic studies. Chem Eng J 2016;288:778–88. doi:10.1016/j.cej.2015.12.042.

[43] Mohan D, Rajput S, Singh VK, Steele PH, Pittman CU. Modeling and evaluation of chromium remediation from water using low cost bio-char, a green adsorbent. J Hazard Mater 2011;188:319–33. doi:10.1016/j.jhazmat.2011.01.127.

[44] Coates J. Interpretation of Infrared Spectra, A Practical Approach. Encycl Anal Chem 2006:10815–37. doi:10.1002/9780470027318.a5606.

[45] Chia CH, Gong B, Joseph SD, Marjo CE, Munroe P, Rich AM. Imaging of mineral-enriched biochar by FTIR, Raman and SEM-EDX. Vib Spectrosc 2012;62:248–57. doi:10.1016/j.vibspec.2012.06.006.

[46] Wang C, Wang H. Pb(II) sorption from aqueous solution by novel biochar loaded with nano-particles. Chemosphere 2018;192:1–4. doi:10.1016/j.chemosphere.2017.10.125.

[47] Mohan D, Sharma R, Singh VK, Steele P, Pittman CU. Fluoride Removal from Water using Bio-Char, a Green Waste, Low-Cost Adsorbent: Equilibrium Uptake and Sorption Dynamics Modeling. Ind Eng Chem Res 2012;51:900–14. doi:10.1021/ie202189v.

[48] Wang ZX, Li G, Yang F, Chen YL, Gao P. Electro-Fenton degradation of cellulose using graphite/PTFE electrodes modified by 2-ethylanthraquinone. Carbohydr Polym 2011;86:1807–13. doi:10.1016/j.carbpol.2011.07.021.

[49] Iqbal M, Saeed A, Kalim I. Characterization of adsorptive capacity and investigation of mechanism of Cu2+, Ni2+ and Zn2+ adsorption on mango peel waste from constituted metal solution and genuine electroplating effluent. Sep Sci Technol 2009;44:3770–91. doi:10.1080/01496390903182305.

[50] Li Y, Chen MD, Wan X, Zhang L, Wang X, Xiao H. Solvent-free synthesis of the cellulose-based hybrid beads for adsorption of lead ions in aqueous solutions. RSC Adv 2017;7:53899–906. doi:10.1039/c7ra09592a.

[51] El-Ashtoukhy ESZ, Amin NK, Abdelwahab O. Removal of lead (II) and copper (II) from aqueous solution using pomegranate peel as a new adsorbent. Desalination 2008;223:162–73. doi:10.1016/j.desal.2007.01.206.

[52] Ibrahim MNM, Ngah WSW, Norliyana MS, Daud WRW, Rafatullah M, Sulaiman O, et al. A novel agricultural waste adsorbent for the removal of lead (II) ions from aqueous solutions. J Hazard Mater 2010;182:377–85. doi:10.1016/j.jhazmat.2010.06.044.

[53] Feng N, Guo X, Liang S. Adsorption study of copper (II) by chemically modified orange peel. J Hazard Mater 2009;164:1286–92. doi:10.1016/j.jhazmat.2008.09.096.

[54] Iqbal M, Schiewer S, Cameron R. Mechanistic elucidation and evaluation of biosorption of metal ions by grapefruit peel using FTIR spectroscopy, kinetics and isotherms modeling, cations displacement and EDX analysis. J Chem Technol Biotechnol 2009;84:1516–26. doi:10.1002/jctb.2212.

[55] Wong YC, Szeto YS, Cheung WH, McKay G. Adsorption of acid dyes on chitosan - Equilibrium isotherm analyses. Process Biochem 2004;39:695–704. doi:10.1016/S0032-9592(03)00152-3.

[56] Brown AM. A step-by-step guide to non-linear regression analysis of experimental data using a Microsoft Excel spreadsheet. Comput Methods Programs Biomed 2001;65:191–200. doi:10.1016/S0169-2607(00)00124-3.

[57] Kumar PS, Ramakrishnan K, Kirupha SD, Sivanesan S. Thermodynamic and kinetic studies of cadmium adsorption from aqueous solution onto rice husk. Brazilian J Chem Eng 2010;27:347–55. doi:10.1590/S0104-66322010000200013.

[58] Huang Y, Li S, Chen J, Zhang X, Chen Y. Adsorption of Pb(II) on mesoporous activated carbons fabricated from water hyacinth using H 3 PO 4 activation: Adsorption capacity, kinetic and isotherm studies. Appl Surf Sci 2014;293:160–8. doi:10.1016/j.apsusc.2013.12.123.

[59] Mittal A, Malviya A, Kaur D, Mittal J, Kurup L. Studies on the adsorption kinetics and isotherms for the removal and recovery of Methyl Orange from wastewaters using waste materials. J Hazard Mater 2007;148:229–40. doi:10.1016/j.jhazmat.2007.02.028.

[60] Qiu H, Lv L, Pan BC, Zhang QJ, Zhang WM, Zhang QX. Critical review in adsorption kinetic models. J Zhejiang Univ Sci A 2009;10:716–24. doi:10.1631/jzus.A0820524.

[61] Fierro V, Torné-Fernández V, Montané D, Celzard A. Adsorption of phenol onto activated carbons having different textural and surface properties. Microporous Mesoporous Mater 2008;111:276–84. doi:10.1016/j.micromeso.2007.08.002.

[62] Basha S, Murthy ZVP, Jha B. Sorption of Hg(II) onto Carica papaya: Experimental studies and design of batch sorber. Chem Eng J 2009;147:226–34. doi:10.1016/j.cej.2008.07.005.

[63] Şengil IA, Özacar M, Türkmenler H. Kinetic and isotherm studies of Cu(II) biosorption onto valonia tannin resin. J Hazard Mater 2009;162:1046–52. doi:10.1016/j.jhazmat.2008.05.160.

[64] Olu-Owolabi BI, Diagboya PN, Adebowale KO. Evaluation of pyrene sorption-desorption on tropical soils. J Environ Manage 2014;137:1–9. doi:10.1016/j.jenvman.2014.01.048.

[65] Li Y, Du Q, Liu T, Sun J, Jiao Y, Xia Y, et al. Equilibrium, kinetic and thermodynamic studies on the adsorption of phenol onto graphene. Mater Res Bull 2012;47:1898–904. doi:10.1016/j.materresbull.2012.04.021.

[66] Liu Z, Zhang FS. Removal of lead from water using biochars prepared from hydrothermal liquefaction of biomass. J Hazard Mater 2009;167:933–9. doi:10.1016/j.jhazmat.2009.01.085.

[67] Inyang M, Gao B, Ding W, Pullammanappallil P, Zimmerman AR, Cao X. Enhanced lead sorption by biochar derived from anaerobically digested sugarcane bagasse. Sep Sci Technol 2011;46:1950–6. doi:10.1080/01496395.2011.584604.

[68] Goel J, Kadirvelu K, Rajagopal C, Kumar Garg V. Removal of lead(II) by adsorption using treated granular activated carbon: Batch and column studies. J Hazard Mater 2005;125:211–20. doi:10.1016/J.JHAZMAT.2005.05.032.

[69] Largitte L, Laminie J. Modelling the lead concentration decay in the adsorption of lead onto a granular activated carbon. J Environ Chem Eng 2015;3:474–81. doi:10.1016/J.JECE.2014.12.020.

[70] Lodeiro P, Herrero R, Sastre de Vicente ME. Batch desorption studies and multiple sorption-regeneration cycles in a fixed-bed column for Cd(II) elimination by protonated Sargassum muticum. J Hazard Mater 2006;137:1649–55. doi:10.1016/j.jhazmat.2006.05.003.

Chapter 4 Removal of Pb (II) ions from aqueous solution using magnetic hemp and maple microwave pyrolysis biochars: A comparative study

Abstract

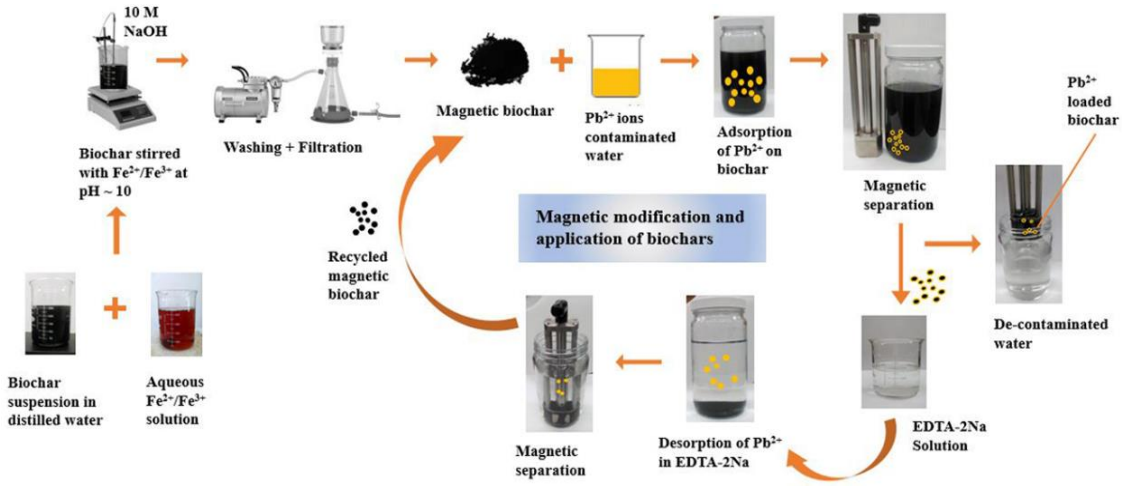

Figure 4-1 *Graphical abstract of the modification and application of biochars*

This research evaluates and compares two microwave pyrolyzed biochars produced from agricultural biomass (shredded hemp stalk) vs woody biomass (maple wood chips) for the removal of Pb (II) from aqueous solution in a batch adsorption study. Biochars were produced by microwave pyrolysis of 1.5 kg of each biomass at an average temperature of 600 ˚C in a stainless steel 309 reactor and then magnetized by mixing aqueous Fe^{3+}/Fe^{2+} solutions with aqueous biochar suspensions, followed by treatment with NaOH. The magnetic biochars were characterized and the effects of pH, adsorbent dose, temperature, contact time and initial concentration of Pb (II) solution on their adsorption performance were investigated. The physico-chemical properties of the biochars significantly influence their adsorption capacities. For the cation and system under investigation, the adsorption capacity of magnetic hemp

biochar was higher than that of magnetic maple biochar. The higher adsorption efficiency of hemp biochar was correlated to its higher polarity index, pH and zeta potential. Results from kinetics data show that the mechanism for the adsorption of Pb (II) by both adsorbents follows a pseudo-second-order (PSO) kinetic model. Isotherm modelling indicates that Freundlich model best described the uptake of Pb (II) by magnetic hemp adsorbent while the loading of Pb (II) onto magnetic maple adsorbent is best characterized by Langmuir model.

Keywords: Magnetic separation; biochar adsorbent; wastewater purification; heavy metals; lead, kinetics, isotherm.

4.1. Introduction

Water pollution from Pb (II) ions has been one of the most discussed topics over the years. Heavy metal ions, particularly those of Pb from industrial effluents and mine waters have attracted researchers' attention. This is because they have a very long residence time, hence the tendency to accumulate in aquatic organisms and are transferred to human beings in the food chains. These ions are highly toxic to the human bodies [1] and have been reported to decrease the activities of enzymes and kidney functions as well as cause neuromuscular difficulties [2]. Lead poison from drinking water has been reported; hence the need to capture these heavy metal ions from wastewater [3,4].

Various technologies have been explored for the removal of these metal ions including adsorption, chemical precipitation, ion exchange, etc. [5]. Adsorption is widely accepted among these technologies because it is the most cost effective and efficient [6,7]. Residue generation from adsorption is comparatively low and the used adsorbents can be regenerated [8]. Different adsorbents have been applied for the

adsorption of these metal ions, but carbon-based adsorbents have been proven to be most efficient. Activated carbon has been the widely used carbon-based adsorbent for the adsorption of heavy metal ions at trace levels for several years [9]. However, water purification using activated carbon is expensive due to the cost of producing activated carbon. Hence, recent research activities have been focused on producing a low-cost adsorbent like biochar. Several studies have demonstrated that biochars can successfully remove heavy metal ions from wastewater and be used also as a remedy for immobilization of heavy metal ions in metal polluted soil [10–12]. Biochars are readily accessible at lower cost with favorable chemical and physical surface characteristics; hence a promising adsorbent for adsorbing metal ions from aqueous systems.

Biochar is a fine-grained, highly porous and carbon-rich substance derived by thermally degrading biomass in a system with limited oxygen condition. Their surface area and highly porous structure contribute to their high adsorption capacities. They possess various surface oxygen-containing functional groups (e.g. ketone, phenolic groups, carboxyl, hydroxyl, aldehyde) hence, their affinity to heavy metal ions is very strong [13–15].

Biochars are usually produced by gasification, slow pyrolysis and fast pyrolysis of biomass [16,17]. Fast pyrolysis requires a biomass moisture contents of less than 10% and adequate energy to power the process. In this process, the biomass is converted to bio-oil and biochar [18]. Some of the biomass (10–25 %) feedstock is converted to gas which can be recycled and used for process heating. Various biomass has been explored for biochar production including sludge [19], algal biochar [20,21], diary manure [11,14], corn cobs and stover [17], crop residues [22], etc. Oak bark and Oak

wood biochars from fast pyrolysis have been used for the removal of lead from aqueous solutions [13]. To the best of our knowledge, no study has compared the adsorption of Pb ions from aqueous systems by a biochar derived from an agricultural biomass (hemp stalks) against a woody biomass (maple chips), especially when these biochars are prepared by microwave-assisted pyrolysis and not the conventional method of pyrolysis.

Practical industrial applications of biochars for water treatment have been limited because it is difficult to regenerate the spent biochars from aqueous system by the conventional methods; filtration and centrifugation. A different separation technique using magnetic field has been proven to be an effective method for separating solid-liquid phase in aqueous solutions [23]. It was convenient to use a low internal or external magnetic field to isolate the magnetic biochars from aqueous system. However, the process of magnetic modification of adsorbents for water and wastewater remediation is a new subject of research [24,25]. A few authors have investigated the application of magnetic bio-sorbents for water purification. These includes magnetically modified spent coffee grounds [26], magnetic *Saccharomyces cerevisiae* [27], magnetized sugarcane bagasse [28], slowly pyrolyzed magnetic biochar [29], magnetic oak bark and oak wood biochars from fast pyrolysis [30], and review papers on magnetic materials for wastewater purifications [31,32].

The limited investigations on the use of biochars (modified or unmodified) for water purification have all been done with biochar prepared by conventional method of biomass pyrolysis. Hence, it is necessary to examine the adsorption performance of magnetically modified biochars prepared by microwave-assisted pyrolysis of biomass. A low magnetic field strength can manipulate magnetic biochar easily, enabling easy

recovery of the spent biochars from the aqueous system which contains high suspended solids, oil and grease. With the conventional separation technique (filtration), these impurities cause carbon fouling which usually lead to frequent separation and regeneration. Magnetic separation enables easy isolation of adsorbent and washing before redispersion of the adsorbent [25].

Therefore, this study reports the successful magnetic modification of microwave pyrolyzed biochars from an agricultural biomass (hemp) and woody biomass (maple). This was required to prevent the usual filter media clog during adsorbent filtration. The hemp and maple feed stock (1.5 kg each) were pyrolyzed in a microwave batch reactor separately at a residence time of 1.5 h and an average temperature of 600 $^{\circ}$C. Microwave-assisted pyrolysis was chosen over the conventional pyrolysis method because it is not only energy efficient but also ensures rapid heating, reduces residence time and it is easier to control. The biochars were chemically modified before magnetization via two simple steps: (1) oxidation of the biochars with H_2O_2 to increase oxygen-containing surface functional groups, hence enhance its affinity for heavy metal ions. (2) magnetization of biochars through co-precipitation to attach the magnetic iron particles to the surface of the oxidized biochars. This makes separation of the used adsorbent from aqueous system easier. The adsorption characteristics of Pb (II) ions onto the different magnetic biochars were examined in a batch mode and compared. Adsorption kinetics and isotherm, adsorbent dose, pH dependence of Pb (II) ions onto the biochars from aqueous solution were examined. The sorption isotherms were fitted with Langmuir, Freundlich and Temkin models. The pseudo-first-order (PFO) and pseudo-second-order (PSO) kinetic models were used to fit the kinetic data. Multiple regeneration effects on the biochars' sorption performance and their magnetization properties were also studied.

4.2. Material and Methods

4.2.1. Materials and Chemicals

The shredded hemp stalk was sourced from Plains hemp, Manitoba, Canada while the sugar maple chips were purchased from Montana Grilling Gear, USA. The chemicals used were all reagent grades. Ferric sulfate (>96%), ferrous Sulfate (98%), Sodium Nitrate and EDTA-2Na were bought from Alfa Aesar, USA. A 30% H_2O_2 solution, Pb $(NO_3)_2$, Granular NaOH, NaOH (0.01 M) and HNO_3 (0.01 M) solutions were purchased from Fisher Scientific. The standard Pb (II) solution (1.000 g L^{-1}) was prepared by dissolving the right amounts of Pb $(NO_3)_2$ salt in a given volume of distilled water. The reagents were used as received without further purification.

4.2.2. Pyrolysis of Biomass

The biochars were produced in a custom-built cylindrical stainless steel 309 reactor. Microwave was used to pyrolyze 1.5 kg of each biomass as received with a 2.7 kW microwave power an average temperature of 600 ˚C. The reaction time was 1.5 h [33]. The purchase biomass had a moisture content between 9 – 11%. The produced hemp and maple biochars were then milled, followed by sieving to 200 - 300 µm particle size for use.

4.2.3. H_2O_2 Oxidation of Biochars

4.2.3.1. Pre-treatment of Biochars

The 200 - 300 µm biochar powder were thoroughly washed with distilled water and dried overnight at 105 ˚C in a temperature-controlled oven. Dried biochars were stored in sealed containers and used to synthesize the modified biochars.

4.2.3.2. H_2O_2 Oxidation of Hemp and Maple Biochars

Approximately 55g of each pre-treated biochar powder was soaked in 350 mL of 30% H_2O_2 solution and stirred for 6 h with a magnetic stirrer at 300 rpm and 24±1 ˚C temperature. After the H_2O_2 impregnation, samples were vacuum filtered and washed thoroughly with distilled water followed by ethanol. The H_2O_2 oxidized biochars were dried in an air oven at 60 ˚C for 24 h before magnetization.

4.2.4. Magnetization of H_2O_2 Oxidized Biochars

The oxidized biochars were magnetized as described by Nakahira et al [34]. In summary, 15g of each oxidized biochars were suspended in 150 mL distilled water. A fresh solution of ferrous sulfate was prepared by dissolving 6.00 g of $FeSO_4.7H_2O$ in 45 mL distilled water. Another separate solution of ferric sulfate was prepared by dissolving 5.55g of $Fe_2(SO4)_3.nH_2O$; (n = 6 - 9) in 390 mL distilled water. The prepared Fe solutions were combined and vigorously stirred at 25 – 30 ˚C. The solution of $Fe^{2+}/Fe^{3+}SO4^{2-}$ formed was slowly added into the earlier prepared suspension of oxidized biochars at room temperature and stirred slowly for 30 mins. At this point, aqueous NaOH (10 M) was added dropwise to the $BC/Fe^{3+}/Fe^{2+}$ suspension to increase the pH to approximately 10 – 11. The biochar in Fe solution was then stirred for another 60 minutes and aged for 24 h at room temperature. After 24 h, the solution was filtered and the magnetized biochars washed thoroughly with distilled water followed by ethanol and dried at 50 ˚C overnight.

4.2.5. Adsorbents Characterization

The surface functional groups of the magnetized biochars were identified with FT-IR. A NEXUS 470 spectrophotometer (Nicolet Thermo Instruments, Canada) was used to record the FT-IR spectra after blending KBr with the chars. An Auto-sorb instrument (Belsorp-Max BEL Inc, Osaka, Japan) was used to determine the BET surface area of

the biochars. Before and after Pb (II) adsorption, the biochar surface morphology and chemical compositions were analyzed by SEM and EDS respectively. A JEOL JSM-6400 Scanning Electron Microscope equipped with an EDAX Genesis 4000 Energy Dispersive X-ray (EDS) analyzer was used. Before observation in the microscope, biochar samples were coated with carbon using an Edwards 306A carbon coater.

A Lake Shore 7304 Vibrating Sample Magnetometer (VSM) was used to perform the hysteresis measurement. The magnetic property of magnetic particles is represented by plots of magnetization (M) versus field strength (H) given in the hysteresis loop. The saturation magnetization of the magnetic biochars were determined from the hysteresis curve. A Bruker D8 Advance spectrometer was used to measure the X-ray powder patterns of the magnetic biochars. The fine powder samples were packed into the circular well on the sample-holder and placed on the sample stage for measurement. The program EVA (Bruker) was used to analyze and refine the raw data obtained from the spectrometer. Thermogravimetric analysis (TGA) of the magnetic adsorbents were performed using SDT Q600 by TA Instruments, USA fitted with nitrogen gas supply. The equipment operates between 10 °C to 800 °C at 10 °C min^{-1} heating rate. The biochars zeta potentials were measured on a zeta potential analyzer (ZetaPlus, Brookhaven Instruments Corporation, USA).

4.2.6. Batch Adsorption Study

The suitability of the magnetic biochars to remediate heavy metal ion contaminated water was evaluated using Pb (II) as the pollutant. A solution of Pb (II) with varying concentrations were prepared by diluting the standard solution accordingly. The desired solution pH was achieved by adding HNO_3 (0.01M) or NaOH (0.01M) as required. The batch adsorption experiments were carried out using 40 mL solution at 20 mg L^{-1} initial concentration and initial pH of 5.0. The adsorbent dose was 0.02 g

per 40 mL of Pb solution in a vial on a temperature-controlled shaker (SWB25, Thermo Electron Corporation, Germany). The agitation speed of the system was 130 rpm. The effects of pH, adsorbent dose, temperature, contact time and initial solution concentration on the adsorption process were evaluated. The concentration of Pb (II) in the filtrate after sorption was determined with ICP-OES (VISTA-MPX Axial, Varian Inc, USA). The percent Pb (II) ions removed from solution R (%) was determined with **equation 4.1**.

$$R = \frac{(C_i - C_e)}{C_i} \times 100 \qquad \textit{Equation 4.1}$$

where C_i(mg L^{-1}) and C_e(mg L^{-1}) are the initial concentration and equilibrium concentration of the solution respectively. The amount of Pb (II) ions loading onto the biochars (Q) was calculated with **equation 4.2**.

$$Q = \frac{(C_i - C_e)}{m} \times V \qquad \textit{Equation 4.2}$$

where Q (mg g^{-1}) is the amount of Pb (II) ions adsorbed on per gram of the biochar, m (g) is the mass of biochar, V (L) is the volume of the Pb (II) ions solution.

4.2.6.1. Adsorbent Separation Study

Separation of the spent magnetic biochars from solution using a magnetic field was investigated in a batch experiment. A 500 mL capacity glass vial (dia. = 6.5 cm) was filled with 250 mL distilled water. Then 125 mg of biochars was added into water-containing vial. After 5 minutes of agitating the biochar suspension with a Barnant mixer series 20 agitators at a speed of 100 rpm, the vial was withdrawn and a magnetic jig purchased from Industrial Magnetics, Inc (ON/OFF Magnetic Jig, JP155R) was inserted in the suspension to create a magnetic field. The depth of the biochar suspension when the magnetic jig was inserted at the center of the vial was 8.0 cm. A repeat trial was performed by creating an external magnetic field, in which case, the

vial containing the suspension was gently placed on the surface of the jig. When the biochar particles in solution have been magnetized by the jig, a certain volume (20 mL) of the remediated solutions were collected at intervals from a marked spot in the vial (6.0 cm from the base). The water sample was withdrawn via a needle and syringe for turbidity test using a turbid meter (Hach 2100Q Portable Turbidimeter).

4.2.6.2. Regeneration of Adsorbents

For the adsorbent regeneration study, magnetic biochars were loaded with Pb (II) at these operating conditions: fixed adsorbent dose – 1.0 g L^{-1}, initial concentration of Pb (II) solution – 20 mg L^{-1}, pH - 5, contact time 2 h, temperature - 25 ˚C. The Pb-loaded biochars was filtered under vacuum and washed thoroughly with distilled water, followed by drying overnight at 60 ˚C in an air oven.

Batch desorption study was undertaken with a fixed dose of the Pb-loaded magnetic biochars (1.0 g L^{-1}) in EDTA-2Na (0.1 mol L^{-1}) solution. This was performed at 25 ˚C during 2 h contact time. After the agitation, the biochar-EDTA solution was filtered using quantitative filter paper under vacuum. The cake was washed thoroughly with distilled water until neutral pH and dried at 60 ˚C overnight before use in the next adsorption–desorption cycle. The filtrate, EDTA-2Na solution was analyzed for Pb (II) concentration using ICP-OES to quantify the desorbed amount of Pb (II) during regeneration.

4.3. Results and Discussion

4.3.1. Characterization of Magnetic Biochar Adsorbents

The physio-chemical properties of the magnetic biochars were characterized to determine their functional groups, surface morphology, surface area and porosity,

chemical composition, moisture and ash content, as well as pH and point of zero charge.

4.3.1.1. BET and Elemental Analysis

From the observed pH of adsorbents, the magnetic hemp biochar (MHBC) is an alkaline material while the maple (MMBC) adsorbent is slightly acidic with BET surface area of 83.76 m^2 g^{-1} and 75.99 m^2 g^{-1} respectively as shown in **Table 4.1**.

Considerably higher pH and point of zero charge values were observed for MHBC than MMBC. Furthermore, MHBC also has a higher carbon composition than MMBC.

In comparison, the higher nitrogen contents of MHBC suggests that hemp biochar may also have a higher oxygen content associated with the nitro (-NO_3) functional group as shown by FT-IR (**Figure 4-4**). This deduction, combined with the observed higher N content of MHBC (Table 4.1), means that the polarity index (N/C, O/C and (O+N)/C ratios) of MHBC will be higher than that of MMBC. Thus, magnetic hemp biochar is likely to present a relatively more hydrophilic and polar structure than magnetic maple biochar [35].

One parameter that accounts for the surface phenomena of particles such as deposition and agglomeration of particles including their stability is the zeta-potential [36]. This parameter can be used to estimate how particle charge affects aggregation behavior of ions with respect to the adsorbents during adsorption. Both modified biochars showed negative zeta potential charge values that should be favorable to the attraction between adsorbent's active sites and positively charge heavy metal ions, resulting in electrostatic interaction [37]. The zeta potentials for the magnetic hemp and maple adsorbents were - 45.3 mV and -16.84 mV respectively. This demonstrates that MHBC has a higher and much more negative zeta potential charge than MMBC, thus there

will be a greater attraction between the hemp adsorbent's active sites and positively charged heavy metal ions. The very high percent Fe composition of both adsorbents confirmed a successful magnetization.

Table 4.1 *Characteristics of magnetic maple and hemp biochars*

Parameter	*Units*	*Values*	
		Magnetic maple biochar	**Magnetic hemp biochar**
BET surface area	$m^2\ g^{-1}$	75.99	83.76
Total pore volume	$cm^3\ g^{-1}$	0.11	0.14
Zeta Potential (pH = 5.8)	mV	- 16.84	- 45.30
pH_{pzc}		6.04	6.61
pH		5.95	9.05
Ash content	%	56.18	44.97
Moisture Content	%	2.77	3.13
C	%	54.03	58.94
N	%	0.3886	0.6324
N/C		0.0072	0.011
Fe	%	16.24	13.66

4.3.1.2. Morphology and Chemical Composition of Biochar

The SEM micrograph of the unmodified biochar adsorbents, before and after adsorption were taken at 1500 magnification. The micrograph as shown in **Figure 4-2** showed that unmodified hemp biochar surface is irregular, uneven, heterogenous which could impact on the Pb (II) sorption process [38]. The magnetic hemp biochar surface was coarse with some hairy-like particles and irregular crevices with varying dimensions. It is believed that this observation may indicate the presence of various pores for the transport of heavy metal ions to active sites for adsorption.

On the other hand, SEM image of unmodified maple biochar showed a vessel structure running at different directions in different layers. Similar SEM results have been

reported for a maple biochar produced using microwave [39]. These vessels were well organized and regular in shape. The maple biochar maintained these regular-shaped vessels after magnetic modification but with hair-like particles on the surfaces like what was observed on modified hemp biochar.

These particles on the surfaces of these magnetic chars may be attributed to the iron oxide particles that are fused or bonded to the biochar's surface

The SEM images after metal adsorption also show some crevices on the spent hemp adsorbents. A look at the micrographs of **Figure 4-3** show that the surface of the hemp biochar after adsorbing Pb (II) ions were more disaggregated with an increased surface roughness. The spent magnetic maple biochar equally shows increasingly rough surface with debris in the well-structured vessels.

These observed changes in the char surfaces of the adsorbents may be connected to the adsorption processes effects on the adsorbents as the aqueous metal solution interacts with the biochar particles.

It is believed that during batch adsorption at a constant agitation, the surface cavities of the adsorbents may have acted as paths for the Pb (II) ions in aqueous solution, thereby providing the ions easy access to the meso-pores where adsorption and chemical interactions occur between the ions and adsorbent's functional groups on the active sites [40].

The observed bright spots in the micrographs of the modified and spent adsorbents, also indicates that some degree of conductivity exist as a result of the presence of metals. The observation from the SEM micrograph demonstrates that the microstructures of biochars depends on biomass species.

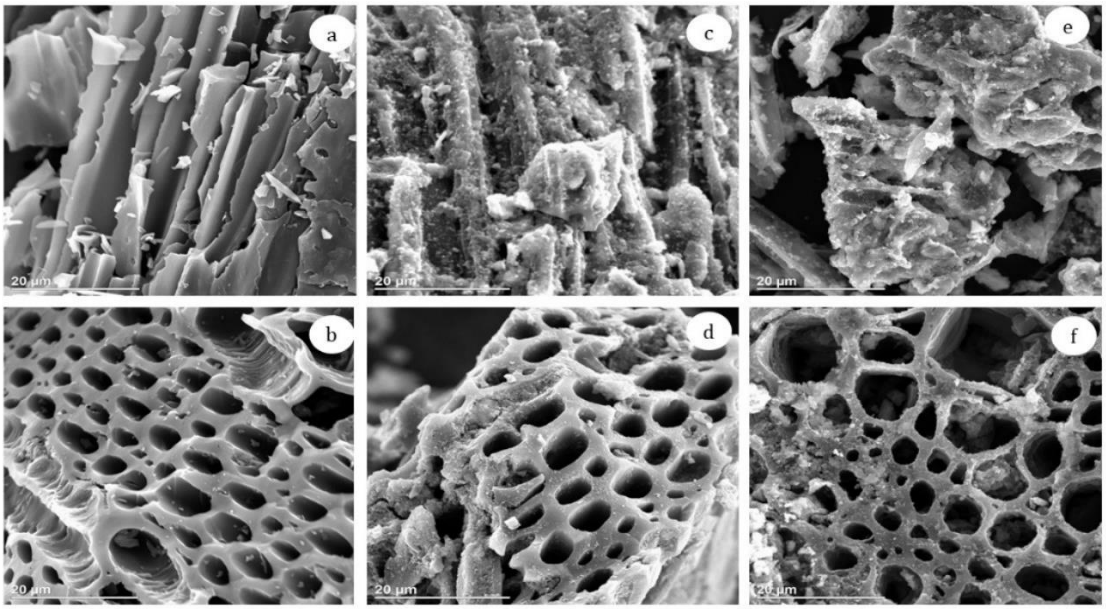

Figure 4-2 *SEM micrograph of biochars (a) unmodified hemp x1500 (b) unmodified maple x1500 (c) magnetic hemp x1500 (d) magnetic maple x1500 (e) Pb-loaded magnetic hemp x1500 (f) Pb-loaded magnetic maple x1500*

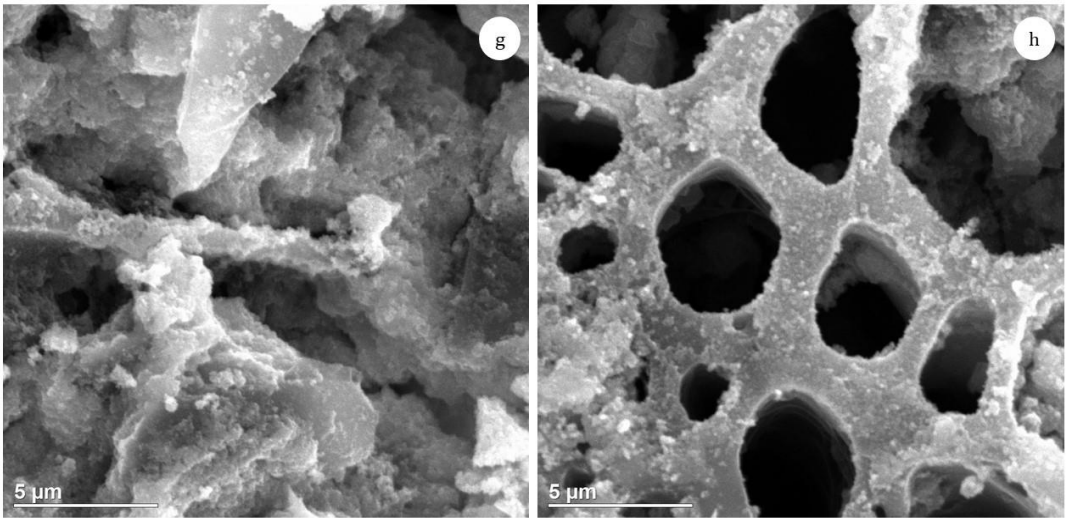

Figure 4-3*: SEM micrographs of spent biochars (g) Pb-loaded magnetic hemp x4500 (h) Pb-loaded magnetic maple x4500*

The EDS analyses of both biochars chemical compositions were examined and their spectra are given in **Figure 4-4**. The analyses indicate that the modified hemp biochar has a relatively high carbon content (74.5%), oxygen content of 11.9%, iron content

of 12.4% and trace amounts of other heteroatoms. On the other hand, magnetic maple had a lower carbon content after modification (48.8%), 17.6% oxygen and a relatively higher iron content (32.9%). The abrupt jump in iron contents of both biochars following magnetization thus confirmed that the modification was successful.

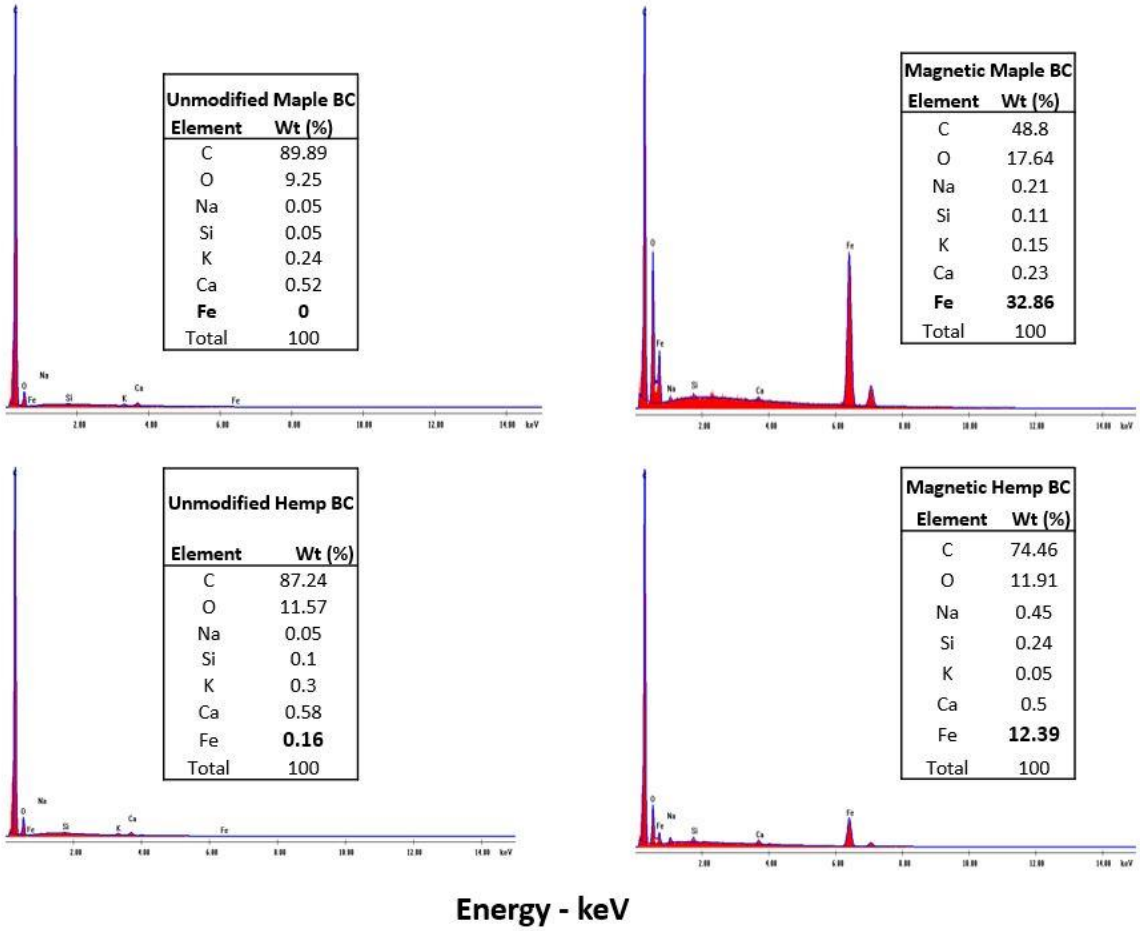

***Figure 4-4**: EDS spectra of biochars before and after magnetic modification*

The adsorbents' EDS spectra after Pb (II) ions adsorption are given in **Figure 4-5**. In Figure 4.5, the spectra of both biochars adsorption process showed peaks for Pb (II) ions after adsorption, thereby confirming the ions' presence on the surface of the modified biochar after adsorptions were carried out. It should be noted that the iron contents of the used biochars were lower than those of modified but unused biochars

given in **Figure 4-4**. The observed changes may be connected to the effects of the step where the biochars were washed and filtered which may have resulted in component losses due to Fe leaching, thus changing the biochar composition. The results of the EDS spectra of both adsorbents before and after metal ions removal further confirmed the fact that these magnetic adsorbents were able to successfully adsorbed Pb (II) ions from aqueous solution.

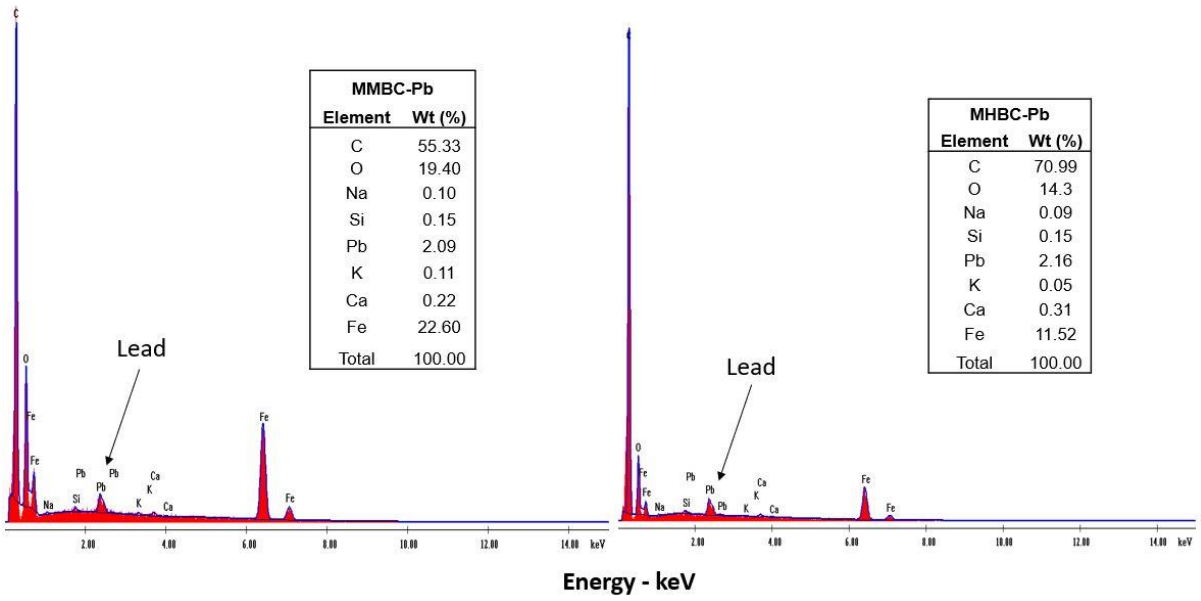

***Figure 4-5**: EDS spectra of magnetic maple and magnetic hemp biochars respectively after Pb (II) removal (Left - Right)*

4.3.1.3. FT-IR Characterization

As shown in the FT-IR spectra of the biochars **Figure 4-6**, the main peaks of both biochars did not show any obvious or marked difference between the two kinds of magnetic chars. The FTIR spectra of the biochars are shown in the region of 4000 – 500 cm^{-1}. The peaks corresponding to 1800 - 1685 cm^{-1} wavenumber region is assigned to C=O stretching vibrations due to esters, carboxylic acids, anhydrides and ketones. The peak at 1600 cm^{-1} is attributed to C=C [41]. When Saligna wood chips was used

as biomass for biochar production, similar results were observed [42]. Additionally, similar results were reported for maple biochar produced by micro-wave assisted pyrolysis[39]. The C-H presence signifies that the cellulose of the pyrolysis feedstocks was not entirely carbonized during biochar production and the C=C bond is attributed to the aromatic rings of lignin. The bands at 650 cm^{-1} and 1470 cm^{-1} are assigned to Fe-O and nitro ($-NO_3$) functional group respectively [43].

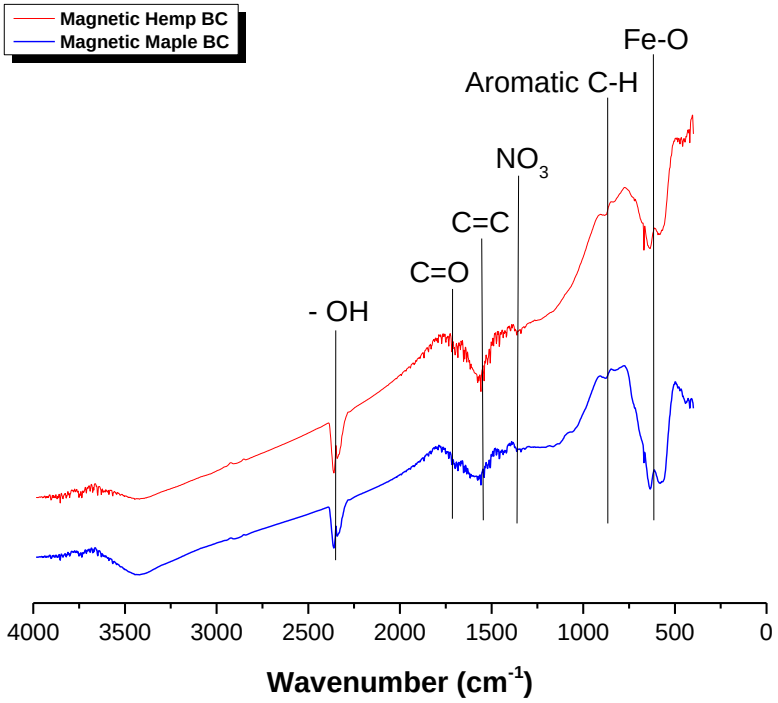

Figure 4-6 *FTIR spectra of biochars before and after magnetic modification*

4.3.1.4. Vibrating Sample Magnetometry

The applicability of ferromagnetic materials depends on their characteristics. These characteristics are given by their hysteresis loop obtained as the magnetization (M) of these materials is plotted against a field strength. At 27˚C, vibrating sample magnetometry (VSM) was used to perform the adsorbents magnetization characteristics as shown in **Figure 4-7**. The saturation magnetization values for both

magnetic hemp (MHBC) and magnetic maple (MMBC) biochars were 10.7 and 9.30 emu/g respectively. These high saturation values may be attributed to the high weight fraction of iron oxide particles contained in the biochars' hybrid particles as shown in **Table 4.1**. The nature and type of biochar also determines the steps in the biochar's magnetization process.

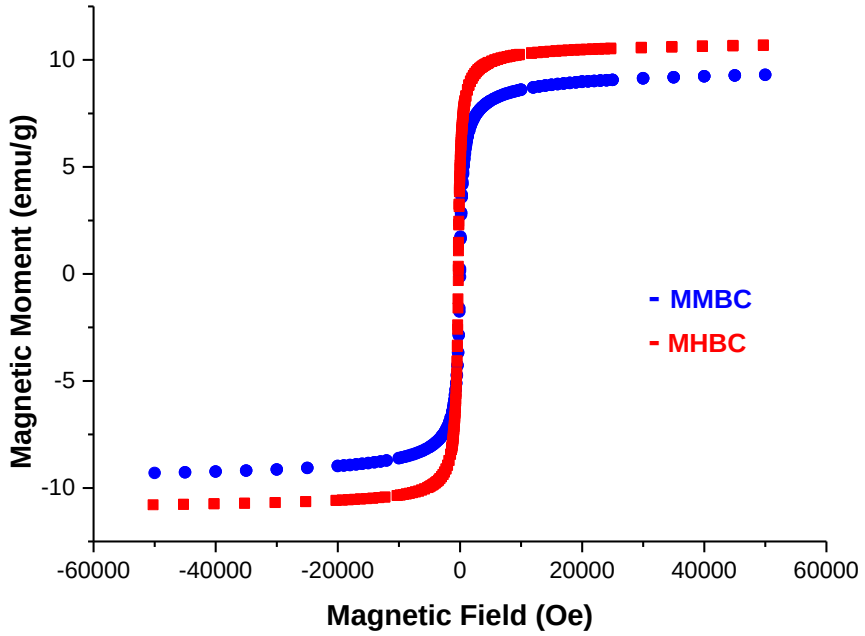

Figure 4-7 *Magnetic moment of magnetic biochars at 27 ˚C*

Various oxygen-containing functional groups are present on biochar surface. These includes alcohol, pyrone, carboxylic acid, anhydride, hydroxy, quinone, ether, ketone, lactone [44]. During microwave-assisted pyrolysis of the hemp and maple biomass, substantial quantities of oxygen; 11.57% and 9.25% respectively; were left in the biochars as given by EDS analysis of **Figure 4-4**. This depends largely on the pyrolysis operating conditions; temperature and time. In addition to the functional groups, there are acidic, basic, hydrophilic and hydrophobic sites found throughout the pore's

surfaces and subsurface volume of biochars. The properties and contributions of these functional groups are affected by the type of feedstock and pyrolysis conditions. These variables include pyrolysis temperature and time, reactor configuration, operating power which affects rate of heat transfer and feedstock particle size distribution [44]. Phenolic hydroxyls and carboxylic functional groups have acidic functions. Other groups such as quinines, lactones, ethers and anhydrides carry electron lone pairs which can serve as Lewis bases, thereby forming co-ordinate bonds with metal cations. Since some oxygen-containing hydrophilic functional groups are present throughout the biochars, water molecules travel easily into the solid regions thus cause swelling [45]. Therefore, metal cations bind with sorption sites below the surface and, sometimes, throughout substantial parts of the solid region [44,45].

4.3.1.5. X-Ray Powder Diffraction

The XRD patterns for MHBC and MMBC are shown in **Figure 4-8**. Multiple sharp iron oxide phase peaks were seen in the 2θ range of 20–80˚ for both magnetic adsorbents. These show the presence of crystallinity in phases available in both magnetic biochars. The peaks cantered at 30.16˚ in MMBC and 30.48˚ in MHBC are attributed to Fe_3O_4 [46], while those at 35.54˚ in MMBC and 35.82˚ in MHBC are due to γ-Fe_2O_3 [46]. The small peaks at 43.30˚ and 43.46˚ confirmed the existence of cubic iron oxide particles on both MMBC and MHBC surfaces respectively [47]. The Peaks at 57.32˚ and 62.82˚ in MMBC are assigned to Fe_2O_4 (magnetite). The MHBC peaks at 57.52˚ and 63.02˚ are assigned to Fe_2O_4 (magnetite).

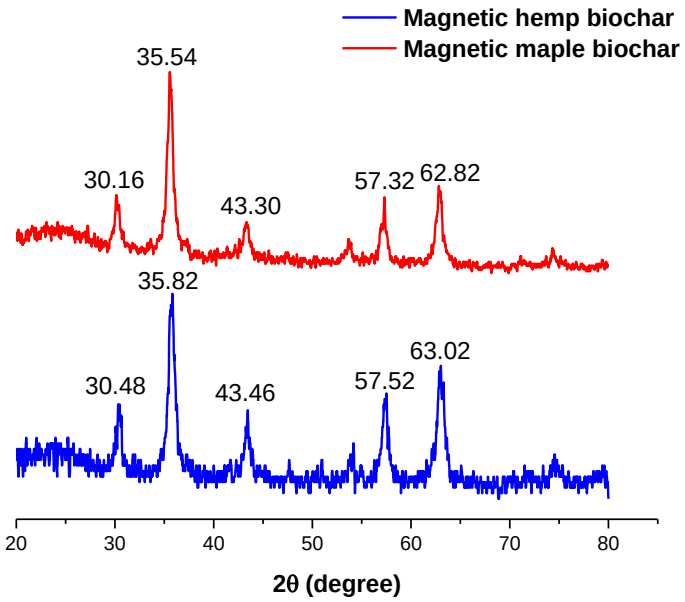

Figure 4-8 *Powder XRD of magnetic hemp and maple biochars*

4.3.1.6. Thermogravimetric Analysis

The weight loss of the magnetic biochars in a controlled atmosphere when there is a change in temperature was quantified. The temperature profile as shown in **Figure 4-9** provides data on the chemical components of the biochars such as fixed carbon, moisture content, ash content and volatile components of the adsorbents. The TGA analysis of the magnetic biochars in **Figure 4-9** shows weight loss in two regions - I and II. In region (I) which occurred from 20 to 100 ˚C may be connected to weight loss as a result of water molecules elimination. Nearly 5.0 % of weight loss occurred in this region. The eliminated water molecules could have probably been hydrogen bonded to biochars surface or water that was absorbed [48,49]. Region (II) happened from 100 to 800 ˚C and may be associated with the volatile organic components that were still present on biochar surface after pyrolysis being removed following their decomposition. This second region accounts for 22.5% approximately.

The total loss in weight of the biochars from thermal decomposition was about 27.5%. This result shows that the magnetic biochars were composed of approximately 70% stable carbon under the thermal decomposition

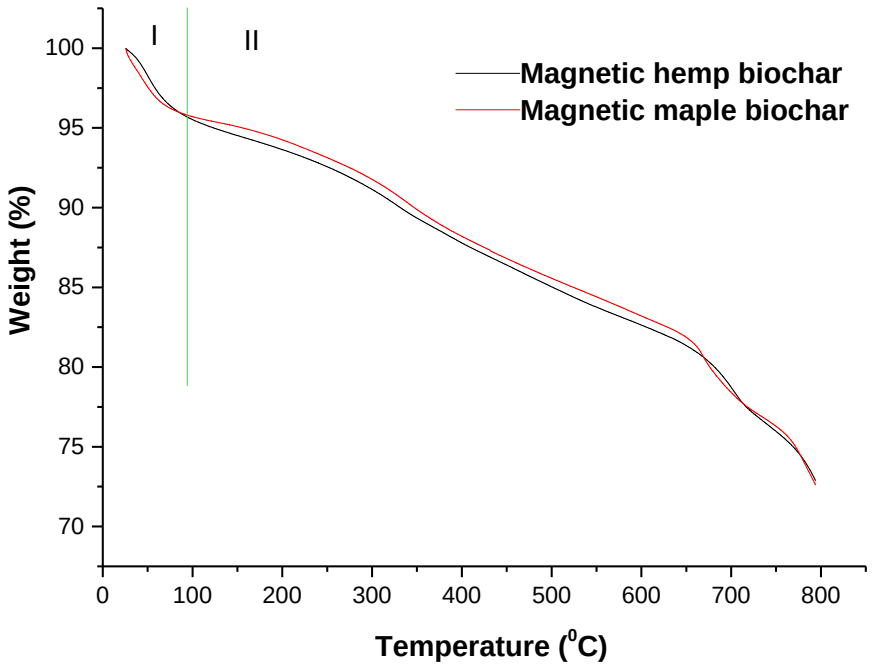

Figure 4-9 *Thermogravimetric analysis of magnetic biochars under N_2*

4.3.2. Adsorption Behavior

4.3.2.1. Effects of Adsorbent Dose

Adsorbent dose is one of the parameters that significantly affect the adsorption process in an aqueous system [50]. This parameter determines the adsorption capacity of an adsorbent for a given initial adsorbate concentration [51]. A study was therefore performed on the effects of adsorbents dose on the performance of both magnetic biochars as shown in **Figure 4-10**. An increase in the dose of both biochars resulted in an increase in percentage of Pb (II) ions removal. At a slightly higher biochar dose of 0.6 g L^{-1}, the percent of metal ions removed was very high for both biochars although

hemp performed better than maple under the same condition. The high Pb (II) removal efficiency at higher adsorbent doses may be attributed to enough active sites available on the adsorbents' surface. As expected, at lower adsorbent doses, the percent Pb (II) ions removal was lower possibly as a result of the progressive saturation of these available active sites. In **Figure 4-10**, it can be noticed that the amount of Pb (II) ions adsorbed per unit mass of adsorbent decreased significantly as the adsorbents' dose was increased. This observation may be connected to the active adsorption sites remaining fallow or unsaturated in the adsorption process. The trend of these results have been reported for the adsorption of heavy metals using biochars [52]. Looking at the biochars performance as shown in **Figure 4-10**, it was decided that it is efficient to use an adsorbent dose of 0.5 g L^{-1} for further studies.

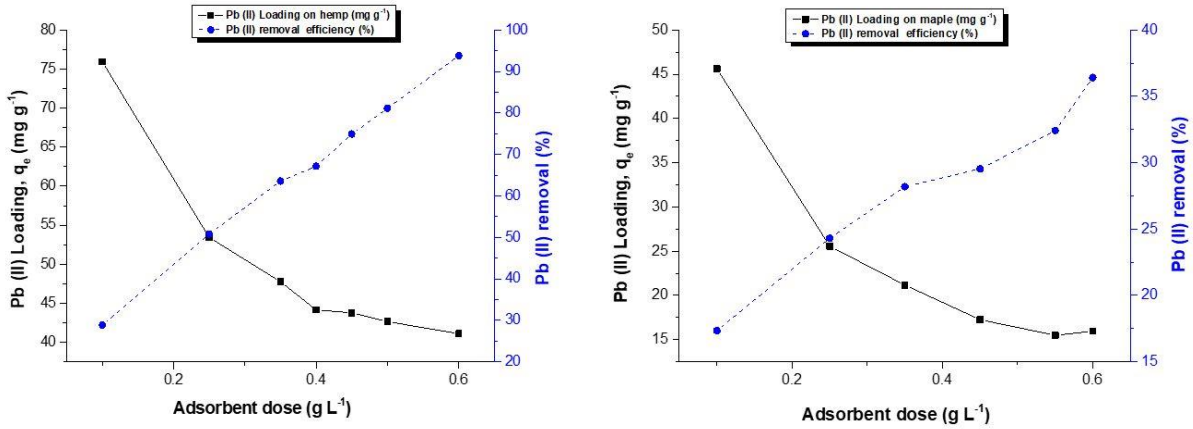

Figure 4-10 *Effects of biochar dose on Pb (II) loading per unit mass (Continuous line) and on Pb (II) removal percent (Dash line): MHBC (left), MMBC (right).*

4.3.2.2. Effects of pH on Adsorption

The removal of Pb (II) ions from aqueous systems strongly depends on the pH of the solution. The metal pollutant ions speciation varies with the pH of solution. Secondly, the biochar functions differently under various pH conditions. To evaluate this complex interaction on Pb (II) adsorption, the pH of a 20 mg/L solution was varied

between 2 to 7 and results shown in **Figure 4-11**. As expected, at high pH values the highest Pb (II) adsorption occurred. Furthermore, the results showed that adsorption also depends strongly on the type of biochar. The Pb (II) adsorption was significantly higher for MHBC than MMBC under all the pH conditions. The evaluation was carried out at pH values below the point at which the metal ions will hydrolyze and precipitate from its solution, which is estimated to be 7.7 for $Pb(OH)_2$ [30]. Pb (II) can form different hydrolysis products which may be present in different amounts under various conditions. In dilute aqueous solutions, Pb (II) hydrolysis products form at pH values above 6.0 [13]. At pH between 2 – 6, Pb^{2+} species are pre-dominant. At higher pH values, other species ($PbOH^+$) may exist [13].

The amount of Pb (II) removed by the adsorbents was very low at an initial pH value below 3. It then increases sharply within the next 4 pH points, **Figure 4-11**. At the lower pH values, the higher concentration of protons (H_3O^+) are in competition with Pb (II) ions for the adsorbents active sites. [53,54]. Higher pH (pH > 3) values are more favorable to the deprotonation of the biochars phenolic, carboxylic acid, hydroxyl and other acidic groups, thus making biochars surface negatively charged. These negative charges are formed on both biochar and ferric oxide/Fe_3O_4 surfaces. The negative surface charges increase electrostatic attraction and decreases repulsions between Pb (II) ions and active sites, hence enhances the Pb (II) ions adsorption. On the other hand, positive sites are dominant on the biochar surfaces at lower pH values and causes electrostatic repulsions between the biochar surface and Pb (II) ions.

It was reported that at initial pH of 8.0, metal is removed by both adsorption and precipitation caused when – OH forms $Pb(OH)_2$ (s) [55]. This could be one of the factors behind the higher performance of MHBC over MMBC. This is explained in

detailed in **section 4.3.3.2**. The point of zero surface charge, pH_{ZPC}, for the MHBC and MMBC were 6.61 and 6.04 respectively. Furthermore, the pH of the biochars as shown in **Table 4.1** were 9.05 and 5.95 for MHBC and MMBC respectively. At higher pH values, Pb (II) ions will replace protons from the magnetic adsorbent's surfaces. The highest adsorption of Pb^{2+} took place at the highest pH values. At this pH, the oxygen-containing function groups in the biochars will be deprotonated and become negatively charged. These negatively charged active sites have columbic attraction for free Pb^{2+} ions and other hydrated Pb cationic species.

In order to correlate Pb (II) ions removal efficiency with the adsorption process, the equilibrium and kinetic studies were performed at an initial solution pH of 5.0.

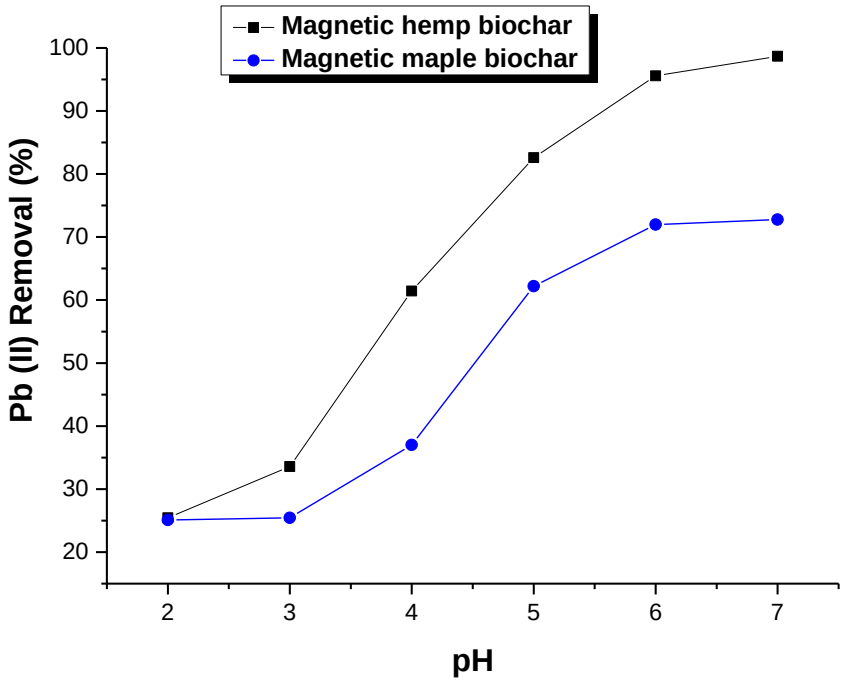

Figure 4-11 *Effects of pH on adsorption of Pb (II) ions from aqueous solution at 25 ˚C*

4.3.2.3. Effects of Temperature on Adsorption

The effects of temperature on the adsorption of Pb (II) ions from aqueous solution by both magnetic biochars are shown in **Figure 4-12**. The studies were performed by varying the temperature of a 20 mg/L solution from 25 to 65 ˚C a pH of 5.0. An adsorbent dose of 0.5 g/L was used during the 2 hours experimental run. The removal of Pb (II) ions from solution increased as the temperature was increased from 25 to 35 ˚C. This result indicates that the adsorption of Pb (II) by these magnetic adsorbents is an endothermic process [4]. At temperatures higher than 35 ˚C, there were no marked difference in percentage metal removal. Hence, an optimum temperature of 35 ˚C was selected for Pb (II) ions adsorption onto both MHBC and MMBC.

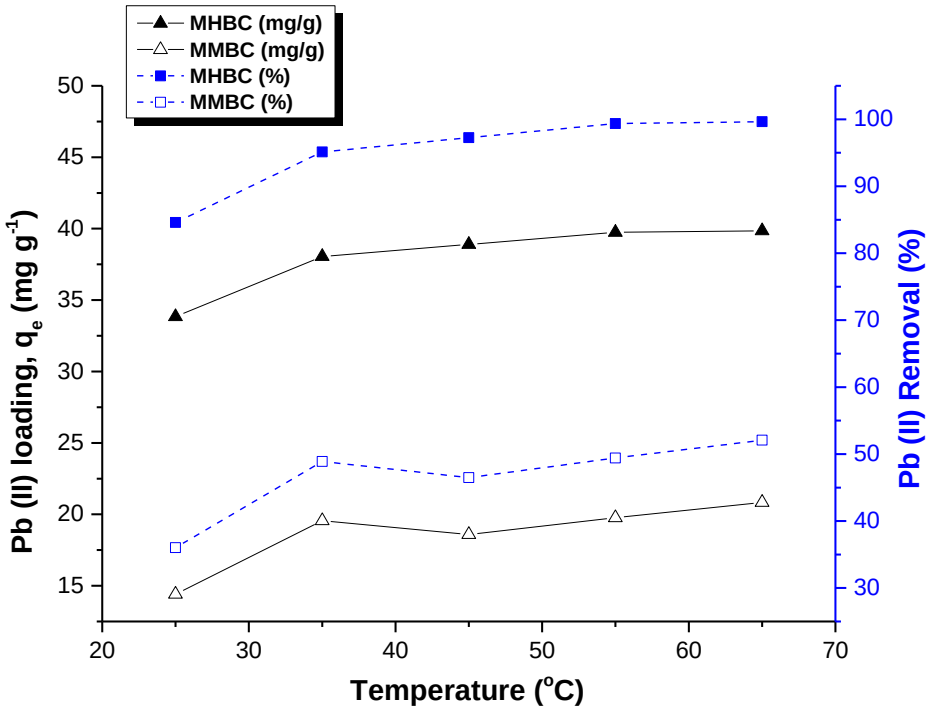

Figure 4-12 *Effects of temperature on the adsorption of Pb (II) ions onto magnetic biochars*

4.3.3. Adsorption Kinetics and Isotherms

4.3.3.1. Adsorption Kinetics

The effects of contact time on the percentage removal of Pb (II) ions from aqueous system by magnetic biochars were evaluated at a pH of 5 and results shown in **Figure 4-13**. This study was performed at 35 ˚C using 20 mg L^{-1} metal ion concentration in a 40 mL Pb ion-biochar system at 130 rpm and the quantity of biochar used was 0.02 g. The Pb ions adsorption kinetic profiles by the magnetic biochars as shown in **Figure 4-13** indicates that both adsorbents removed the metal ions via two stages. A fast metal adsorption occurred within 60 minutes of adsorbate-adsorbent contact. After the first 60 minutes, a slow phase of metal ions uptake occurred from 90 min until 240 min when a quasi-stabilized state or equilibrium was assumed to have been reached. The Pb ion loading onto the chars after 240 min were 41.08 mg g^{-1} and 15.50 mg g^{-1} for MHBC and MMBC respectively.

The two-phase kinetic profile for Pb (II) ions adsorption by both magnetic biochars may be attributed to the types and nature of available surface-active sites for sorption. At the outset of the adsorption process when the adsorbate-adsorbent contact is first established, there are many readily available active sites for adsorption to take place. Hence, the fast Pb (II) ions uptake observed. However, as the adsorption process proceeds and unoccupied active sites are reduced, the adsorption rate decreased as a result of a combination of factors.

The slower adsorption rate may be attributed to factors such as reduction in the number of active sites available for metal ions to occupy as well as electrostatic repulsion between the adsorbed metal ions and the in-coming adsorbates. As expected, the remaining available active sites were occupied at a much slower rate compared to the

beginning when there were many active sites for adsorption. This two-phase trend in adsorption kinetics have been reported by several authors [4,50,56–58].

Furthermore, **Figure 4-13** demonstrates that the Pb (II) ions loading i.e. the amount of Pb^{2+} ions removed from solution per gram of adsorbent was much higher for MHBC compared to MMBC under the same conditions. This marked difference in the magnetic biochars adsorption performance could be explained by the properties of the biochars surfaces. Adsorption strongly depends on the chemical or/and physical characteristics of adsorbent, which have an influence on the adsorption mechanism. The elemental analysis of MHBC (**Table 4.1**) indicates that its carbon, nitrogen and possibly oxygen contents are higher than those in MMBC. Therefore, it was established that the surface of MHBC may contain a greater amount of polar functional groups responsible for binding the Pb (II) ions to the biochar surface.

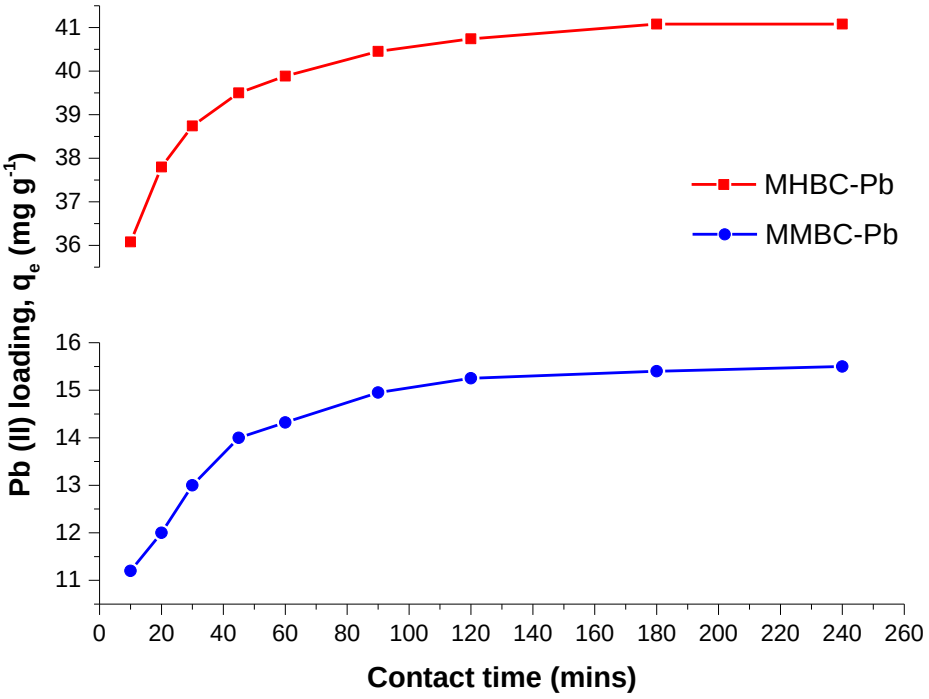

Figure 4-13 *Effects of contact time on Pb (II) loading onto magnetic biochars*

The Pb (II) ions loading onto the modified biochars were modelled with two adsorption kinetics models namely - pseudo fist order (PFO) and pseudo second order (PSO) kinetic models (see the supplementary document for details). These models were evaluated by a non-linear trial and error procedure. This method calculates the parameters of the isotherm model by minimizing the coefficient of determination between the experimental data and models using the solver add-in in Microsoft excel [59,60].

To determine the goodness of fit of the isotherms to the experimental data with a non-linear regression, it is required that error functions be defined in order to fit the model parameters with the experimental data. Here in, reduced Chi square test (ε^2), adjusted coefficient of determination (adj. R^2), and the root mean square error (RMSE) were used as error parameters for the models. These parameters were determined according to equations (B4.7 and B4.8) in Appendix B.

4.3.3.1.1. Pseudo First and Second Order Kinetic Modelling

The plots of **Figure 4-14** show the PFO and PSO kinetic models for Pb (II) ion uptake by MHBC and MMBC adsorbents. The models' parameters with their corresponding error functions are presented in **Table 4.2**. An evaluation of Figure 4.14 and Table 4.2 indicates that the kinetics of Pb (II) ions sorption from solution by both adsorbents could be described by the pseudo second order model.

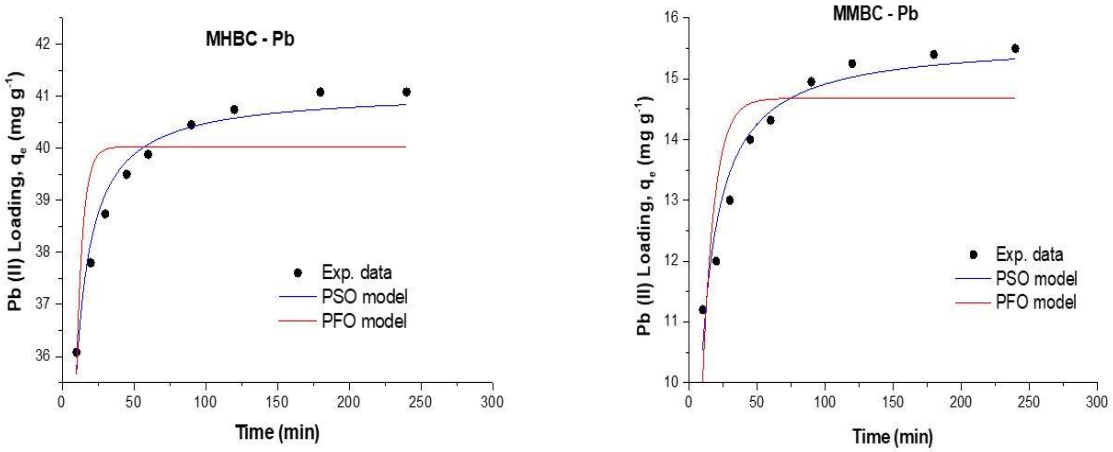

Figure 4-14 *Effect of contact time on Pb (II) ions loading on biochars at 35 ˚C*

Furthermore, PSO calculated parameter ($q_{e,model}$) matches the data obtained from the experimental results analysis closely. From **Table 4.2**, PSO model predicted a metal loading ($q_{e,cal}$) of 40.83 mg/g for MHBC while the experimentally determined value was 41.08 mg/g at the operating conditions. Similarly, the PSO estimated value for MMBC was 15.63 mg/g while the experimentally determined value was 15.50 mg/g. Additionally, for the PSO, the adjusted R^2 is high while the reduced root mean square and reduced chi-square are values are low for both adsorbents. With these observations, it shows that PSO is a better fit with the experimental data than PFO model. Based on the kinetic modelling results, the rate limiting step during Pb (II) ions uptake by the magnetic adsorbents from aqueous solution has a chemisorption rate-controlling mechanism [61]. This involves electron transfer or electron sharing between the adsorbate (Pb^{2+}) and biochar adsorbents.

Table 4.2 *PFO and PSO Kinetic parameters for Pb (II) ions uptake by magnetic biochars*

Kinetic Models	***Parameters***	***Adsorbents***	
Pseudo First Order (PFO)		MMBC - Pb	MHBC - Pb
	$q_{e,\ cal}$ (mg g^{-1})	14.68	40.02
	K_1 (min^{-1})	0.115	0.221
	adj. R^2	0.629	0.599
	ε^2	0.909	1.138
	RMSE	0.873	0.94
Pseudo Second Order (PSO)			
	$q_{e,\ cal}$ (mg g^{-1})	15.63	40.83
	K_2 (g mg^{-1} min^{-1})	0.013	0.016
	adj. R^2	0.932	0.962
	ε^2	0.166	0.107
	RMSE	0.359	0.289

4.3.3.2. Adsorption Equilibrium Studies and Isotherms

Equilibrium studies for the adsorption of Pb (II) ions from solution by the magnetic adsorbents were performed. The studies considered a range of initial solution concentration from 5 mg L^{-1} to 500 mg L^{-1} at an initial pH of 5 and 35 ˚C using adsorbent dose of 0.5 g L^{-1}. From the experimental results as shown in **Figure 4-15**, magnetic biochar from agricultural biomass (MHBC) had a higher adsorption capacity for removing Pb^{2+} from aqueous solution than a magnetic biochar obtained from woody biomass (MMBC). The maximum adsorption performance for Pb^{2+} determined from experimental data based on the amount removed at equilibrium time of 2 hours were 59.06 and 54.50 mg/g for MHBC and MMBC respectively. This difference in the adsorption performance by the biochars could be attributed to several factors. Firstly, it was established earlier in this thesis (**sections 4.3.1.1** and **4.3.3.1**) that

MHBC has a higher polarity index than MMBC based on their physical/chemical characteristics. Therefore, the hemp biochar may possess a larger quantity of highly polar surface functional groups that binds Pb^{2+} ions onto the adsorbent surface easily. Secondly, the pH for both magnetic biochars are 9.05 and 5.95 for MHBC and MMBC respectively (**Table 4.1**). This means that hemp biochar is slightly basic while maple biochar is slightly acidic. It is therefore assumed that as hemp adsorbent was in contact with the solution, it quickly altered the initial pH of the metal solution from the slightly acidic condition (pH – 5) to a basic condition. At about pH of 8.0, metal ions are removed by both adsorption and precipitation caused when – OH forms $Pb(OH)_2$ (s) [55]. Hence, precipitation may have enhanced the capacity of MHBC to remove Pb from solution. The third factor may be attributed to the zeta potentials of the adsorbents. While MHBC has a zeta potential of – 45.30 mV, MMBC has a zeta potential of -16.84 mV. The much higher zeta potential of MHBC may have equally influenced the adsorption process since it affects the particles surface charge, agglomeration, deposition and stability [36]. When the biochar adsorbent was immersed into the aqueous metal solution in its powdered form and agitated in the batch adsorption process, the interaction between the biochar surface and the adsorbate (Pb^{2+}) in the aqueous system depends on several factors governed by not only the pH of the aqueous system but also the nature and type of potential or charge on the biochar surface. Thus, the more negative zeta potential charge of MHBC surface may have caused a greater attraction between the hemp active sites and positively charged Pb^{2+} ions.

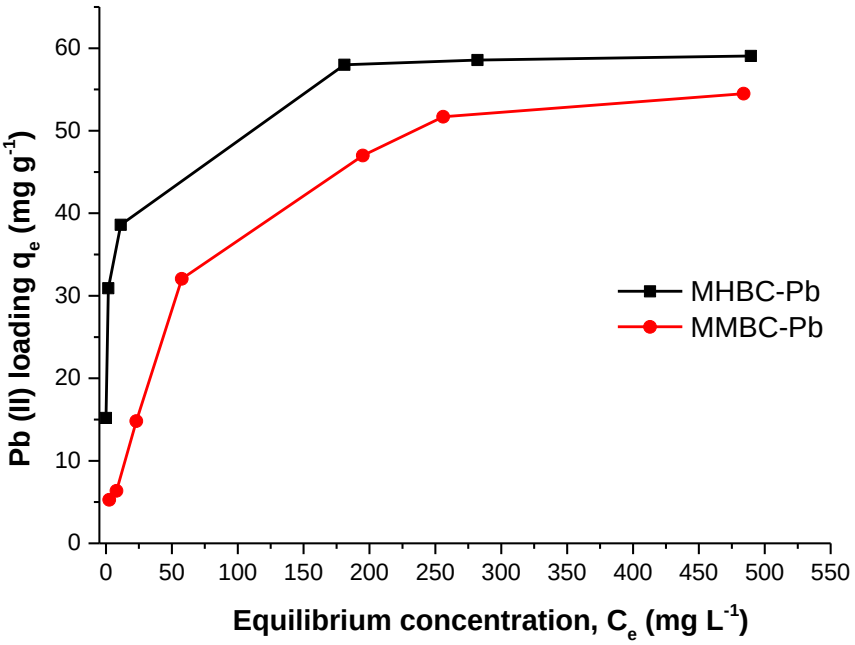

Figure 4-15 *Comparison of adsorption performance of magnetic hemp and maple biochars*

The adsorption process by was characterized by Freundlich, Langmuir and Temkin isotherm models. These models were evaluated by a non-linear approach which uses trial and error. This method minimizes the coefficient of determination between experimental data and isotherm models to determine the isotherm parameters with the aid of an add-in solver in Microsoft excel [59,60].

The isotherms for Pb (II) ions adsorption by both adsorbents are shown in **Figure 4-16**. From the isotherm plots, the model parameters were determined and given in **Table 4.3**.

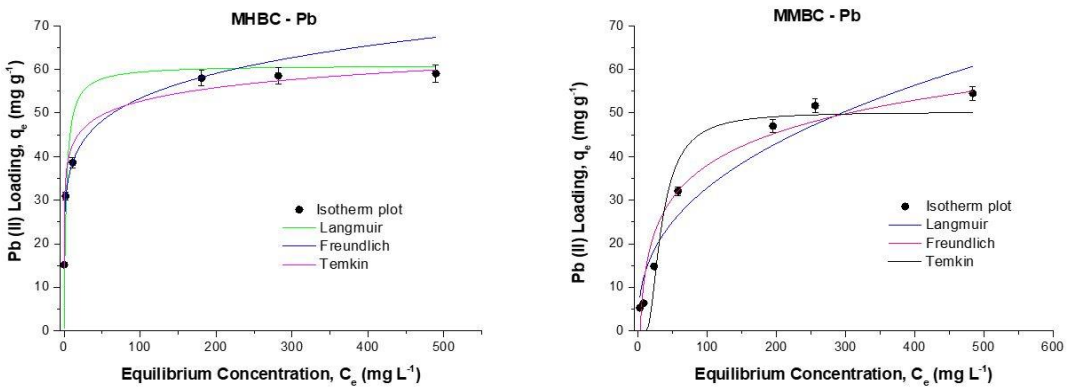

***Figure 4-16**: Freundlich, Langmuir and Temkin adsorption isotherms for Pb (II) ions on biochars*

An exponential distribution of active sites across the adsorbent as well as energies-heterogeneous surface is the assumption of the Freundlich isotherm model [62]. Related to the capacity of adsorbents to remove Pb (II) ion from solution is the Freundlich constant (K_F). This parameter was found to be 27.15 and 5.46 (mg g^{-1})(L mg^{-1})$^{1/n}$ respectively for MHBC and MMBC respectively. The higher K_F value for MHBC suggests that based on the assumption of Freundlich model, the uptake of Pb (II) from solution was successful. Another Freundlich parameter "n" which relates to the intensity of the adsorption by adsorbent was found to be 6.81 and 2.57 for MHBC and MMBC respectively; which is higher for hemp magnetic biochar. Thus, it indicates that Pb (II) ions were more favorably adsorbed from solution by MHBC adsorbent.

Further comparison of the best fit from the three isotherm models to the experimental data from MHBC batch adsorption studies was carried out based on the statistical parameters obtained from the models in supplementary file. These parameters are the reduced chi-square test (ε^2), adjusted coefficient of determination (adj. R^2) and the root mean square error (RMSE) as given in **Table 4.3**. From this analysis, the adsorption of Pb (II) ions from aqueous solution by modified hemp biochar (MHBC) was best described by the Freundlich model. In describing the MHBC adsorption process, the

adj. R^2 value from Freundlich model fitting was 0.99 which was higher than the corresponding values from the Langmuir and Temkin models. This demonstrates that the Freundlich model fits the adsorption experimental data better than the Langmuir and Temkin models for the removal of Pb (II) ions from aqueous system. Furthermore, the values of the two error parameters, ε^2 and RMSE are significantly the lowest for Freundlich isotherm model as compared to the Langmuir and Temkin isotherms. Therefore, the Freundlich model is the best among the three isotherms to characterize the uptake of Pb (II) ions from solution by the MHBC adsorbent.

The assumption of Langmuir model is that the binding sites on adsorbents' surface is homogeneous with equivalent adsorption energies. It also assumes no interaction between adsorbed ions. The Langmuir constant "K_L" is the energy constant which relates to the heat of adsorption while "q_{max}" indicates the maximum adsorption capacity of each adsorbent [63]. For the Pb (II) ions loading, the Langmuir constant values were 0.367 L mg^{-1} and 0.0164 L mg^{-1} for MHBC and MMBC respectively. This indicates that Pb (II) ions uptake onto the surface of the MHBC has a comparatively lower heat of adsorption. The Langmuir adsorption capacity constants for the adsorbents were 61.00 mg g^{-1} and 58.45 mg g^{-1} for MHBC and MMBC respectively. This value is an indication of the maximum amount of Pb (II) ions that can load onto the magnetic biochars. Thus, it implies that the loading of Pb (II) onto magnetic hemp biochar was higher than that of magnetic maple biochar. The possible reasons for this observation have been explained earlier in this thesis.

In describing the adsorption by MMBC, the three isotherms were also fitted with the experimental data and the obtained parameters also given in **Table 4.3**. From the parameters of table 4.3, Langmuir model characterizes the loading of Pb (II) onto

MMBC better than those of the other two isotherm models as its adj. R^2 value is the highest (0.99), while the values of ε^2 and RMSE are also the lowest for MMBC. Therefore, the Langmuir isotherm model is the best amongst the three models to describe the adsorption of Pb (II) by magnetic maple biochar.

Here in, the dimensionless separation factor R_L value for both adsorbents is between 0 and 1, since their $K_L > 0$, thereby indicating that the adsorption process was favorable.

Table 4.3 *Isotherm parameters for adsorption of Pb (II) ions onto Magnetic biochars*

Isotherm Models	***Parameters***	***MHBC - Pb***	***MMBC - Pb***
Experimental	q_{exp} (mg g^{-1})	59.06	54.50
Langmuir	q_{max} (mg g^{-1})	61.00	58.45
	K_L (L mg^{-1})	0.367	0.0164
	adj. R^2	0.76	0.99
	ε^2	100.20	4.01
	RMSE	8.17	1.69
Freundlich	K_F (mg g^{-1})(L $mg^{-1})^{1/n}$	27.15	5.46
	n	6.81	2.57
	adj. R^2	0.99	0.93
	ε^2	1.15	32.59
	RMSE	0.88	4.83
Temkin	A_T (L mg^{-1})	1110.60	308.15
	b_T	565.01	237.86
	adj. R^2	0.96	0.94
	ε^2	12.97	28.00
	RMSE	2.94	4.47

The Langmuir adsorption capacity, "q_{max}" of the magnetic adsorbents for Pb (II) adsorption determined in this research was compared with those reported by other

authors. The comparison was with other studies that used magnetic biochars and commercial activated carbon as adsorbents for removing Pb (II) from aqueous solution. The comparison is given in **Table 4.4**. In **Tables 4.4**, the Langmuir adsorption capacity of the adsorbents used in this study for the adsorption of Pb (II) ions was within the range of values obtained by other authors on the application of magnetic biochars and commercial activated carbon as adsorbents. Thus, the magnetic biochars employed in this study were excellent adsorbents for removing Pb (II) ions from aqueous systems as their adsorption parameters and characteristics are well within the range of the performance of reported magnetically modified biochars and commercial activated carbon adsorbents.

Table 4.4: *Langmuir adsorption capacities of magnetic biochars versus other biochars/activated carbon for Pb (II) removal from solution*

Adsorbents	***Medium***	***pH***	***Temp. (˚C)***	***Conc. range (mg/L)***	***Surface area (m^2/g)***	***Max. Loading Capacity q_{max} (mg/g)***	***Ref.***
Magnetic microwave pyrolyzed hemp biochar	Aqueous solution	***5.0***	***35***	***5-500***	***83.8***	***61.00***	This study[1]
Magnetic microwave pyrolyzed maple biochar	Aqueous solution	***5.0***	***35***	***5-500***	***75.99***	***58.45***	This study[1]
Magnetic oak wood char	Aqueous solution	5.0	35	1-100	6.1	9.49	[64]
Pine wood char	Aqueous solution	5.0	25	1-100	2.04	11.30	[13]
Rice husk biochar	Synthetic	5.0	35	5 - 40	n/a	2.25	[65]
DAWC (digested dairy waste biochar)	Aqueous solution	5.0	22	5-600	555.2	51.38	[66]
Commercial activated carbon	Aqueous solution	5.0	30	1-150	1058	47.20	[67]
Commercial granular activated carbon (GAC)	Aqueous solution	5.0	40	1-60	1000	10.80	[68]
Commercial activated carbon (CGAC)	Aqueous solution	7.2	30	100-1000	n/a	5.95	[69]

[1]The values in bold and italics are results obtained in this study

4.3.4. Regeneration of Magnetic Adsorbents

4.3.4.1. Recycling Adsorbents for Pb (II) Ions Adsorption

A study was performed at 25 ˚C to regenerate the adsorbents via adsorption-desorption cycles. During the adsorption step, the Pb-loaded adsorbents were prepared using adsorbent dose of 1.0 g L^{-1}, 2 hours contact time, concentration of Pb (II) solution was 20 mg L^{-1} at an initial pH of 5.0. In the desorption step, the prepared Pb-loaded adsorbents were desorbed using 0.1 mol L^{-1} EDTA-2Na solution with a solid/liquid ratio of 10 g L^{-1} and 2 hours contact time.

This process was necessary to remove the heavy metals from wastewater streams and maximize the use and benefits of the adsorbents. At the conditions stated above, the magnetic biochars were recycled and used five times. For MHBC, the adsorption efficiency for the 5 cycles were 99.9, 92.9, 88.2, 73.2, 71.4 respectively as given in **Figure 4-17**. Similarly, for MMBC, the corresponding cycle efficiencies were 65.1, 64.0, 62.2, 59.0, 57.5 in that order as shown in **Figure 4-18**. This decrease in sorption performance of the adsorbents after successive reuse may be connected to the regeneration process of the adsorbents, which is believed to alter their porous structures and eventually leading to the loss or blockage of adsorption sites [70]. Comparing the results of **Figure 4-17** and **4-18**, the performance of MHBC in removing Pb (II) from aqueous solution after five cycles was better than that of MMBC. The modified hemp biochar still maintained a satisfactory 70% and above removal efficiency for Pb (II) ions against the 57% removal efficiency of MMBC. This indicates that MHBC is a renewable absorbent and has a greater potential to be used multiple times for remediating lead contaminated water than MMBC.

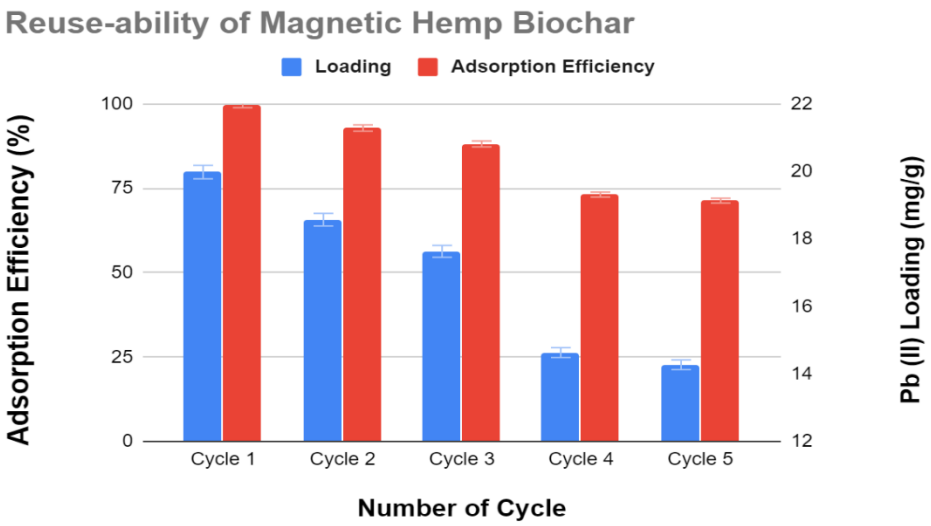

Figure 4-17 *Pb (II) ions removal efficiency by regenerated MHBC*

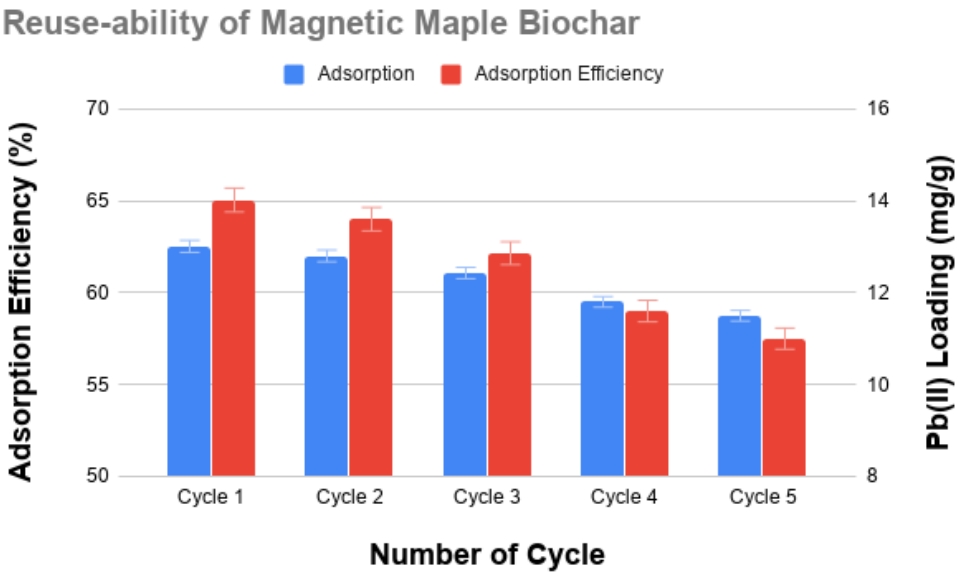

Figure 4-18*: Pb (II) ions removal efficiency by regenerated MMBC*

4.3.4.2. Separation of Magnetic Biochars from Aqueous Solution

An appropriate method of separating the adsorbents from solution after each use was investigated using a magnetic field. An adsorbent dose of 0.5 g/L in distilled water was used and at different separation times (1, 5, 10, 20 and 30 min) as presented in **Figure 4-19** and **Figure 4-20** for MHBC and MMBC respectively. In the study, both internal and external magnetic fields were applied in separating the adsorbents from solution.

Internal magnetic field is created when the magnetic jig is inserted into the biochar suspension while an external magnetic field is created by placing the biochar suspension on the magnetic jig. In **Figure 4-19**, the suspension of MHBC had a turbidity of 456 NTU at the beginning. During the first 1 minute of having the MHBC suspension in a magnetic field, there was a significant decreased in turbidity of the biochar suspension to 154 NTU and 111 NTU as a result of the influence of the external and internal magnetic fields respectively. The suspension turbidity was further decreased after 30 minutes in the fields to 19.9 NTU and 8.79 NTU for the external and internal field respectively. In the case of MMBC as shown in **Figure 4-20**, the initial turbidity of the suspension immediately after agitation was 56.3 NTU. The turbidity value of the magnetic maple biochar was significantly lower when compared to magnetic hemp biochar in suspension. The substantial disparity in the dispersion of these adsorbents powder in distilled water may be connected to their zeta potentials which affects the adsorbents surface phenomena such as particles agglomeration and surface charge [36]. The MHBC powder with a more negative zeta potential, - 45.3 mV was observed to be easily and well dispersed in distilled water more than the MMBC with zeta potential of – 16.8 mV. This difference in the adsorbents dispersion further adds credence to the higher adsorption performance of MHBC over MMBC in removing Pb (II) from aqueous system. The initial 56.3 NTU of MMBC suspension was reduced to 16.0 and 6.32 NTU by the external and internal magnetic fields respectively. At the end of the 30 minutes separation time, the external magnetic field was able to reduce the turbidity of MMBC suspension to 0.83 NTU while the internal magnetic field created by inserting the magnetic jig reduced the suspension turbidity to 0.51 NTU. To put this in perspective, the turbidity of a good drinking water is estimated to be between 0.02 to 1.0 NTU.

These observations demonstrate that it is possible to separate the Pb-loaded magnetic biochars from aqueous solution within a short time using a low magnetic field strength. As expected, the separation using an internal magnetic field was more effective in the recovery of the used adsorbents because the internal field strength created by the magnetic jig was stronger without the interfering barrier from the glass vial and could therefore attract the biochar particles easily.

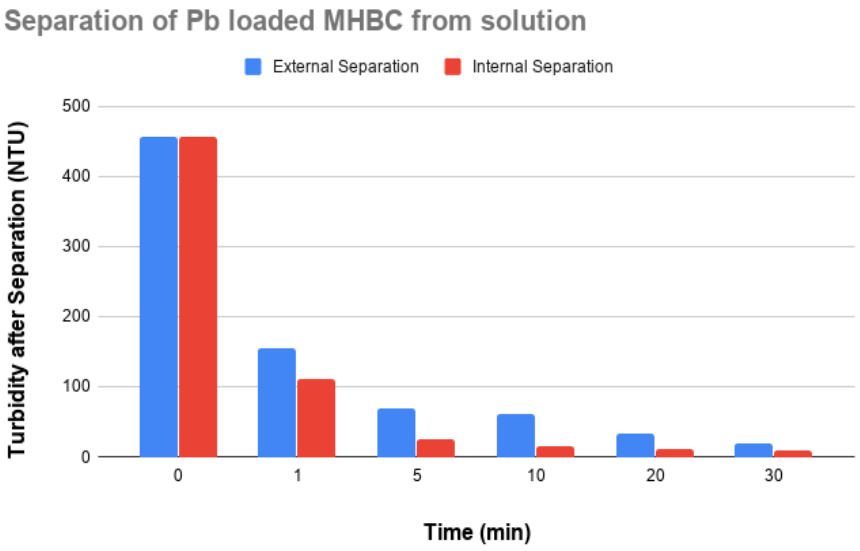

Figure 4-19 Magnetic separation performance of MHBC

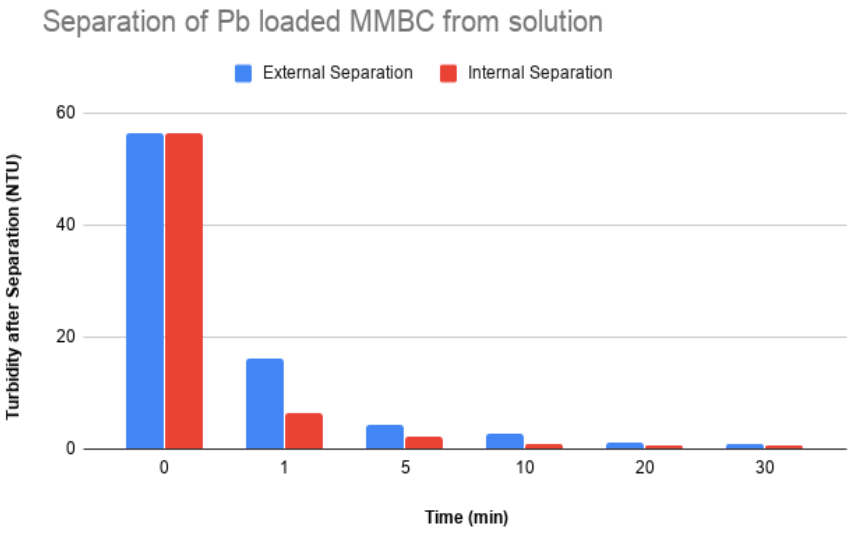

Figure 4-20: Magnetic separation performance of MMBC

4.4. Conclusions

Microwave was used to pyrolyze agricultural biomass (hemp stalk) and woody biomass (maple chips) to produce biochar. These biochars were oxidized using 30% H_2O_2 solution to enhance their adsorption performance followed by magnetic modification to enable easy adsorbent recovery from aqueous solution after adsorption. The capacities of these magnetic biochars to remove Pb (II) from aqueous solution was investigated and compared. Although both biochars were effective in remediating lead ions-contaminated wastewater, magnetic biochar obtained from hemp biomass performed better. It was established that the higher adsorption capacity of magnetic hemp biochar (MHBC) over magnetic maple biochar (MMBC) may be attributed to three factors. Firstly, MHBC possesses more polar surface functional groups that bind Pb^{2+} strongly and easily. Secondly, chemical precipitation contributed to the adsorption of Pb (II) by MHBC in aqueous solution. Thirdly, since MHBC has a more negative zeta potential charge, there may be a greater attraction between its active sites and the positively charged cation.

The kinetic modelling indicates that the process of adsorbing Pb (II) onto both magnetic biochars follows a pseudo-second-order (PSO) kinetics model. In the isotherm studies, it was observed that the sorption of Pb (II) by MHBC is best described by Freundlich model whereas the adsorption of the same Pb (II) by MMBC is best characterized by Langmuir model. The magnetic biochars were manipulated easily using a low strength internal or external magnetic field, thereby enabling an easy recovery of the spent adsorbents from aqueous system. This research has successfully demonstrated that magnetic biochars could be used to remediate lead contaminated water particularly when such water is high in suspended particles, grease and oil impurities which may cause carbon fouling of the filtration units leading to frequent

separation/regeneration treatments. Separation by a magnetic field was very simple and could enable easy isolation and washing of the spent biochars before redispersion.

4.5. References

[1] Volesky B, Holan+ ZR. REVIEW Biosorption of Heavy Metals. Biotechnol Prog 1995;11:235–50.

[2] Seiler HG, Sigel H, Sigel A. Handbook on toxicity of inorganic compounds 1988.

[3] Li K, Wang X. Adsorptive removal of Pb(II) by activated carbon prepared from Spartina alterniflora: Equilibrium, kinetics and thermodynamics. Bioresour Technol 2009;100:2810–5. doi:10.1016/J.BIORTECH.2008.12.032.

[4] Li Y, Chen MD, Wan X, Zhang L, Wang X, Xiao H. Solvent-free synthesis of the cellulose-based hybrid beads for adsorption of lead ions in aqueous solutions. RSC Adv 2017;7:53899–906. doi:10.1039/c7ra09592a.

[5] Demirbas A. Heavy metal adsorption onto agro-based waste materials: A review. J Hazard Mater 2008;157:220–9. doi:10.1016/J.JHAZMAT.2008.01.024.

[6] Bailey SE, Olin TJ, Bricka RM, Adrian DD. A review of potentially low-cost sorbents for heavy metals. Water Res 1999;33:2469–79. doi:10.1016/S0043-1354(98)00475-8.

[7] Dupont L, Guillon E. Removal of hexavalent chromium with a lignocellulosic substrate extracted from wheat bran. Environ Sci Technol 2003;37:4235–41. doi:10.1021/es0342345.

[8] Yu JX, Wang LY, Chi RA, Zhang YF, Xu ZG, Guo J. Competitive adsorption of Pb2+ and Cd2+ on magnetic modified sugarcane bagasse prepared by two simple steps. Appl Surf Sci 2013;268:163–70. doi:10.1016/j.apsusc.2012.12.047.

[9] McDowall DJ, Gupta BS, Stannett VT. Grafting of vinyl monomers to cellulose by ceric ion initiation. Prog Polym Sci 1984;10:1–50. doi:10.1016/0079-6700(84)90005-4.

[10] Chen X, Chen G, Chen L, Chen Y, Lehmann J, McBride MB, et al. Adsorption of copper and zinc by biochars produced from pyrolysis of hardwood and corn straw in aqueous solution. Bioresour Technol 2011;102:8877–84. doi:10.1016/J.BIORTECH.2011.06.078.

[11] Xu X, Cao X, Zhao L, Wang H, Yu H, Gao B. Removal of Cu, Zn, and Cd from aqueous solutions by the dairy manure-derived biochar. Environ Sci Pollut Res 2013;20:358–68. doi:10.1007/s11356-012-0873-5.

[12] Inyang M, Gao B, Yao Y, Xue Y, Zimmerman AR, Pullammanappallil P, et al. Removal of heavy metals from aqueous solution by biochars derived from anaerobically digested biomass. Bioresour Technol 2012;110:50–6. doi:10.1016/J.BIORTECH.2012.01.072.

[13] Mohan D, Pittman CU, Bricka M, Smith F, Yancey B, Mohammad J, et al. Sorption of arsenic, cadmium, and lead by chars produced from fast pyrolysis of wood and bark during bio-oil production. J Colloid Interface Sci 2007;310:57–73. doi:10.1016/J.JCIS.2007.01.020.

[14] Cao X, Ma L, Gao B, Harris W. Dairy-Manure Derived Biochar Effectively Sorbs Lead and Atrazine. Environ Sci Technol 2009;43:3285–91. doi:10.1021/es803092k.

[15] Park JH, Choppala GK, Bolan NS, Chung JW, Chuasavathi T. Biochar reduces the bioavailability and phytotoxicity of heavy metals. Plant Soil 2011;348:439–51. doi:10.1007/s11104-011-0948-y.

[16] Brewer CE, Schmidt-Rohr K, Satrio JA, Brown RC. Characterization of biochar from fast pyrolysis and gasification systems. Environ Prog Sustain Energy 2009;28:386–96. doi:10.1002/ep.10378.

[17] Mullen CA, Boateng AA, Goldberg NM, Lima IM, Laird DA, Hicks KB. Bio-oil and bio-char production from corn cobs and stover by fast pyrolysis. Biomass and Bioenergy 2010;34:67–74. doi:10.1016/J.BIOMBIOE.2009.09.012.

[18] Dinesh Mohan * , † , ‡, and CUPJ†, § PHS. Pyrolysis of Wood/Biomass for Bio-oil: A Critical Review 2006. doi:10.1021/EF0502397.

[19] Lu H, Zhang W, Yang Y, Huang X, Wang S, Qiu R. Relative distribution of Pb2+ sorption mechanisms by sludge-derived biochar. Water Res 2012;46:854–62. doi:10.1016/J.WATRES.2011.11.058.

[20] BIRD MI, WURSTER CM, DE PAULA SILVA PH, PAUL NA, DE NYS R. Algal biochar: effects and applications. GCB Bioenergy 2012;4:61–9. doi:10.1111/j.1757-1707.2011.01109.x.

[21] Bird MI, Wurster CM, de Paula Silva PH, Bass AM, de Nys R. Algal biochar – production and properties. Bioresour Technol 2011;102:1886–91. doi:10.1016/J.BIORTECH.2010.07.106.

[22] Xu R, Xiao S, Yuan J, Zhao A. Adsorption of methyl violet from aqueous solutions by the biochars derived from crop residues. Bioresour Technol 2011;102:10293–8. doi:10.1016/J.BIORTECH.2011.08.089.

[23] Chang YC, Chang SW, Chen DH. Magnetic chitosan nanoparticles: Studies on chitosan binding and adsorption of Co(II) ions. React Funct Polym 2006;66:335–41. doi:10.1016/j.reactfunctpolym.2005.08.006.

[24] Faulconer EK, von Reitzenstein NVH, Mazyck DW. Optimization of magnetic powdered activated carbon for aqueous Hg(II) removal and magnetic recovery. J Hazard Mater 2012;199–200:9–14. doi:10.1016/J.JHAZMAT.2011.10.023.

[25] Mohan D, Sarswat A, Singh VK, Alexandre-Franco M, Pittman CU. Development of magnetic activated carbon from almond shells for trinitrophenol removal from water. Chem Eng J 2011;172:1111–25. doi:10.1016/J.CEJ.2011.06.054.

[26] Safarik I, Horska K, Svobodova B, Safarikova M. Magnetically modified spent coffee grounds for dyes removal. Eur Food Res Technol 2012;234:345–50. doi:10.1007/s00217-011-1641-3.

[27] Patzak M, Dostalek P, Fogarty R V., Safarik I, Tobin JM. Development of magnetic biosorbents for metal uptake. Biotechnol Tech 1997;11:483–7. doi:10.1023/A:1018453814472.

[28] Yamamura APG, Yamaura M, Costa CH. Magnetic biosorbent for removal of uranyl ions. Int J Nucl Energy Sci Technol 2011;6:8. doi:10.1504/IJNEST.2011.039243.

[29] Zhang M, Gao B, Varnoosfaderani S, Hebard A, Yao Y, Inyang M. Preparation and characterization of a novel magnetic biochar for arsenic removal. Bioresour Technol 2013;130:457–62. doi:10.1016/j.biortech.2012.11.132.

[30] Mohan D, Kumar H, Sarswat A, Alexandre-Franco M, Pittman CU. Cadmium and lead remediation using magnetic oak wood and oak bark fast pyrolysis bio-chars. Chem Eng J 2014;236:513–28. doi:10.1016/J.CEJ.2013.09.057.

[31] Ambashta RD, Sillanpää M. Water purification using magnetic assistance: A review. J Hazard Mater 2010;180:38–49. doi:10.1016/J.JHAZMAT.2010.04.105.

[32] Safarik I, Horska K, Pospiskova K, Safarikova M. Magnetically Responsive Activated Carbons for Bio - and Environmental Applications. Int Rev Chem Eng 2012;4:346–52.

[33] Salema AA, Afzal MT, Bennamoun L. Pyrolysis of corn stalk biomass briquettes in a scaled-up microwave technology. Bioresour Technol 2017;233:353–62. doi:10.1016/j.biortech.2017.02.113.

[34] NAKAHIRA A, NISHIDA S, FUKUNISHI K. Synthesis of Magnetic Activated Carbons for Removal of Environmental Endocrine Disrupter Using Magnetic Vector. J Ceram Soc Japan 2006;114:135–7. doi:10.2109/jcersj.114.135.

[35] Bogusz A, Oleszczuk P, Dobrowolski R. Application of laboratory prepared and commercially available biochars to adsorption of cadmium, copper and zinc ions from water. Bioresour Technol 2015;196:540–9. doi:10.1016/j.biortech.2015.08.006.

[36] Alkan M, Karadaş M, Doğan M, Demirbaş Ö. Zeta potentials of perlite samples in various electrolyte and surfactant media. Colloids Surfaces A Physicochem Eng Asp 2005;259:155–66. doi:10.1016/j.colsurfa.2005.02.024.

[37] Boonamnuayvitaya V, Chaiya C, Tanthapanichakoon W, Jarudilokkul S. Removal of heavy metals by adsorbent prepared from pyrolyzed coffee residues and clay. Sep Purif Technol 2004;35:11–22. doi:10.1016/S1383-5866(03)00110-2.

[38] Ge X, Wu Z, Wu Z, Yan Y, Cravotto G, Ye BC. Microwave-assisted modification of activated carbon with ammonia for efficient pyrene adsorption. J Ind Eng Chem 2016;39:27–36. doi:10.1016/j.jiec.2016.05.003.

[39] Li N, Xia Q, Niu M, Ping Q, Xiao H. Immobilizing Laccase on Different Species Wood Biochar to Remove the Chlorinated Biphenyl in Wastewater. Sci Rep 2018;8. doi:10.1038/s41598-018-32013-0.

[40] Pezoti O, Cazetta AL, Bedin KC, Souza LS, Martins AC, Silva TL, et al. NaOH-activated carbon of high surface area produced from guava seeds as a high-efficiency adsorbent for amoxicillin removal: Kinetic, isotherm and thermodynamic studies. Chem Eng J 2016;288:778–88. doi:10.1016/j.cej.2015.12.042.

[41] Coates J. Interpretation of Infrared Spectra, A Practical Approach. Encycl Anal Chem 2006:10815–37. doi:10.1002/9780470027318.a5606.

[42] Chia CH, Gong B, Joseph SD, Marjo CE, Munroe P, Rich AM. Imaging of mineral-enriched biochar by FTIR, Raman and SEM-EDX. Vib Spectrosc 2012;62:248–57. doi:10.1016/j.vibspec.2012.06.006.

[43] Wang C, Wang H. Pb(II) sorption from aqueous solution by novel biochar loaded with nano-particles. Chemosphere 2018;192:1–4. doi:10.1016/j.chemosphere.2017.10.125.

[44] Mohan D, Sharma R, Singh VK, Steele P, Pittman CU. Fluoride Removal from Water using Bio-Char, a Green Waste, Low-Cost Adsorbent: Equilibrium Uptake and Sorption Dynamics Modeling. Ind Eng Chem Res 2012;51:900–14. doi:10.1021/ie202189v.

[45] Mohan D, Rajput S, Singh VK, Steele PH, Pittman CU. Modeling and evaluation of chromium remediation from water using low cost bio-char, a green adsorbent. J Hazard Mater 2011;188:319–33. doi:10.1016/j.jhazmat.2011.01.127.

[46] Wang H, Hu Y, Jiang Y, Qiu L, Wu H, Guo B, et al. Facile synthesis and excellent recyclable photocatalytic activity of pine cone-like Fe3O4@Cu2O/Cu porous nanocomposites. Dalt Trans 2013;42:4915–21. doi:10.1039/c2dt32290k.

[47] Korobeinyk A V., Whitby RLD, Niu JJ, Gogotsi Y, Mikhalovsky S V. Rapid assembly of carbon nanotube-based magnetic composites. Mater Chem Phys 2011;128:514–8. doi:10.1016/j.matchemphys.2011.03.038.

[48] Li X, Wu D, Wang J, Zhu W, Luo Y, Han C, et al. Synthesis of large-sized mesoporous silica spheres by pseudomorphic transformation of commercial silica spheres. Microporous Mesoporous Mater 2016;226:309–15. doi:10.1016/j.micromeso.2016.02.010.

[49] Ali RM, Hamad HA, Hussein MM, Malash GF. Potential of using green adsorbent of heavy metal removal from aqueous solutions: Adsorption kinetics, isotherm, thermodynamic, mechanism and economic analysis. Ecol Eng 2016;91:317–32. doi:10.1016/j.ecoleng.2016.03.015.

[50] El-Ashtoukhy ESZ, Amin NK, Abdelwahab O. Removal of lead (II) and copper (II) from aqueous solution using pomegranate peel as a new adsorbent. Desalination 2008;223:162–73. doi:10.1016/j.desal.2007.01.206.

[51] Aydin H, Bulut Y, Yerlikaya Ç. Removal of copper (II) from aqueous solution by adsorption onto low-cost adsorbents. J Environ Manage 2008;87:37–45. doi:10.1016/j.jenvman.2007.01.005.

[52] Pellera FM, Giannis A, Kalderis D, Anastasiadou K, Stegmann R, Wang JY, et al. Adsorption of Cu(II) ions from aqueous solutions on biochars prepared from agricultural by-products. J Environ Manage 2012;96:35–42. doi:10.1016/j.jenvman.2011.10.010.

[53] Wang ZX, Li G, Yang F, Chen YL, Gao P. Electro-Fenton degradation of cellulose using graphite/PTFE electrodes modified by 2-ethylanthraquinone. Carbohydr Polym 2011;86:1807–13. doi:10.1016/j.carbpol.2011.07.021.

[54] Iqbal M, Saeed A, Kalim I. Characterization of adsorptive capacity and investigation of mechanism of Cu2+, Ni2+ and Zn2+ adsorption on mango peel waste from constituted metal solution and genuine electroplating effluent. Sep Sci Technol 2009;44:3770–91. doi:10.1080/01496390903182305.

[55] Mohan D, Kumar H, Sarswat A, Alexandre-Franco M, Pittman CU. Cadmium and lead remediation using magnetic oak wood and oak bark fast pyrolysis bio-chars. Chem Eng J 2014;236:513–28. doi:10.1016/J.CEJ.2013.09.057.

[56] Ibrahim MNM, Ngah WSW, Norliyana MS, Daud WRW, Rafatullah M, Sulaiman O, et al. A novel agricultural waste adsorbent for the removal of lead (II) ions from aqueous solutions. J Hazard Mater 2010;182:377–85. doi:10.1016/j.jhazmat.2010.06.044.

[57] Feng N, Guo X, Liang S. Adsorption study of copper (II) by chemically modified orange peel. J Hazard Mater 2009;164:1286–92. doi:10.1016/j.jhazmat.2008.09.096.

[58] Iqbal M, Schiewer S, Cameron R. Mechanistic elucidation and evaluation of biosorption of metal ions by grapefruit peel using FTIR spectroscopy, kinetics and isotherms modeling, cations displacement and EDX analysis. J Chem Technol Biotechnol 2009;84:1516–26. doi:10.1002/jctb.2212.

[59] Wong YC, Szeto YS, Cheung WH, McKay G. Adsorption of acid dyes on chitosan - Equilibrium isotherm analyses. Process Biochem 2004;39:695–704. doi:10.1016/S0032-9592(03)00152-3.

[60] Brown AM. A step-by-step guide to non-linear regression analysis of experimental data using a Microsoft Excel spreadsheet. Comput Methods Programs Biomed 2001;65:191–200. doi:10.1016/S0169-2607(00)00124-3.

[61] Kumar PS, Ramakrishnan K, Kirupha SD, Sivanesan S. Thermodynamic and kinetic studies of cadmium adsorption from aqueous solution onto rice husk. Brazilian J Chem Eng 2010;27:347–55. doi:10.1590/S0104-66322010000200013.

[62] Hashemian S, Salari K, Salehifar H, Atashi Yazdi Z. Removal of azo dyes (violet b and violet 5r) from aqueous solution using new activated carbon developed from orange peel. J Chem 2013;2013. doi:10.1155/2013/283274.

[63] Hashemian S, Salari K, Yazdi ZA. Preparation of activated carbon from agricultural wastes (almond shell and orange peel) for adsorption of 2-pic from aqueous solution. J Ind Eng Chem 2014;20:1892–900. doi:10.1016/j.jiec.2013.09.009.

[64] Mohan D, Kumar H, Sarswat A, Alexandre-Franco M, Pittman CU, Mohan D. Cadmium and lead remediation using magnetic oak wood and oak bark fast pyrolysis bio-chars. Chem Eng J 2014;236:513–28. doi:10.1016/j.cej.2013.09.057.

[65] Liu Z, Zhang FS. Removal of lead from water using biochars prepared from hydrothermal liquefaction of biomass. J Hazard Mater 2009;167:933–9. doi:10.1016/j.jhazmat.2009.01.085.

[66] Inyang M, Gao B, Yao Y, Xue Y, Zimmerman AR, Pullammanappallil P, et al. Removal of heavy metals from aqueous solution by biochars derived from anaerobically digested biomass. Bioresour Technol 2012;110:50–6. doi:10.1016/j.biortech.2012.01.072.

[67] Largitte L, Gervelas S, Tant T, Dumesnil PC, Hightower A, Yasami R, et al. Removal of lead from aqueous solutions by adsorption with surface precipitation. Adsorption 2014;20:689–700. doi:10.1007/s10450-014-9613-0.

[68] Machida M, Aikawa M, Tatsumoto H. Prediction of simultaneous adsorption of Cu(II) and Pb(II) onto activated carbon by conventional Langmuir type equations. J Hazard Mater 2005;120:271–5. doi:10.1016/j.jhazmat.2004.11.029.

[69] Kannan N, Veemaraj T. Removal of lead(II) ions by adsorption onto bamboo dust and commercial activated carbons - A comparative study. E-Journal Chem 2009;6:247–56. doi:10.1155/2009/515178.

[70] Lodeiro P, Herrero R, Sastre de Vicente ME. Batch desorption studies and multiple sorption-regeneration cycles in a fixed-bed column for Cd(II) elimination by protonated Sargassum muticum. J Hazard Mater 2006;137:1649–55. doi:10.1016/j.jhazmat.2006.05.003.

Chapter 5 Conclusions

5.1. General Summary

Studies have shown that the properties of biochar do not only depend on the types of feedstock but also on the production methods and conditions. Biochars are produced by pyrolysis of biomass with microwave-assisted pyrolysis being a more efficient thermochemical process for biochar production. This is the first study where biochars produced by microwave-assisted pyrolysis at pilot scale is used for the adsorption of Pb^{2+} ions from synthetic wastewater.

Modification methods especially chemical methods improve the surface properties of biochars. Acidic modification generates extensive oxygenated functional groups, while alkaline modification produces high ratios of surface aromaticity and Nitogen/Carbon (N/C). A major challenge with the practical wastewater treatment using biochar is the difficulty encountered in isolating and recycling the spent biochars from aqueous solution by the traditional methods of filtration and centrifugation. This is one of the few studies where magnetic separation method has been demonstrated to be a potential technique for solid-liquid phase separation. The used biochars were recovered from aqueous solution by simple magnetic field. Making biochars magnetic has helped in the recovery of the biochars following metal adsorption.

In this study, the biochars were produced by microwave-assisted pyrolysis of biomass at a pilot scale in a custom-built microwave reactor. These biochars were converted to magnetic biochars via hydrogen peroxide oxidation followed by chemical co-precipitation of iron oxides onto the biochars. The modification reduced the BET surface area of the biochars due to the iron oxides formation. The magnetic biochars effectively adsorbed Pb^{2+} ions from aqueous solution. The adsorption efficiencies of

the adsorbents in removing Pb^{2+} ions from aqueous solution and their magnetic separation performances were still very satisfactory after 5 regeneration cycles.

In a comparative study, microwave was used to pyrolyze agricultural biomass (hemp stalks) and woody biomass (maple wood chips) to produce biochars. The capacities of these magnetic biochars to remove Pb^{2+} from aqueous solution was investigated and compared. Although both biochars were effective in remediating lead ions-contaminated synthetic wastewater, magnetic biochar obtained from hemp biomass performed better. It was established that the higher adsorption capacity of magnetic hemp biochar (MHBC) over magnetic maple biochar (MMBC) may be attributed to three factors. Firstly, MHBC possesses more polar surface functional groups that bind Pb^{2+} strongly and easily. Secondly, chemical precipitation contributed to the adsorption of Pb^{2+} by MHBC in aqueous solution. Thirdly, since MHBC has a more negative zeta potential charge, there may be a greater attraction between its active sites and the positively charged cation.

The kinetic modelling indicates that the process of adsorbing Pb^{2+} ions onto both magnetic biochars follows a pseudo-second-order (PSO) kinetics model. The isotherm studies showed that the adsorption of Pb^{2+} by MHBC is best described by Freundlich model whereas the adsorption of the same Pb^{2+} by MMBC is best characterized by Langmuir model.

The magnetic biochars were manipulated easily using a low strength internal or external magnetic fields, thereby enabling an easy recovery of the spent adsorbents from aqueous solution. This research has successfully demonstrated that magnetic biochars could be used to remediate lead ions-contaminated water particularly when such water is high in suspended particles, grease and oil impurities which may cause

carbon fouling of the filtration units leading to frequent separation/regeneration treatments. Separation by a magnetic field was very simple and could enable easy isolation and washing of the spent biochars before redispersion. The magnetic biochars are green-based, renewable and cost-effective absorbents that could be used to remediate lead ions-contaminated water.

5.2. Recommendations for future work

Biochars have potential for metal ions adsorption and have received increasing attention during the past decade. However, studies are mostly at a lab scale, focusing on adsorption of single metal ions from synthetic aqueous solution. In natural waters, heavy metal ions often co-exist with other pollutants, hence there is a competition for adsorption sites on biochar surface between metal ions and other ions or organic pollutants in the system.

The publications on the competitive adsorption of heavy metal ions from contaminated water using modified biochar is limited. Further competitive adsorption studies are necessary to accurately estimate metal ions sorption capacity of biochars in natural environments. This is necessary particularly when such biochars are produced by microwave-assisted pyrolysis.

Presently, no study has reported the use of biochars to remove heavy metal ions from polluted wastewater for field application. The actual metal ions-contaminated water is more complicated than the synthetic wastewater used by current studies. To ensure the suitability of biochars to remediate contaminated wastewater, using physicochemical conditions to simulate polluted water or employing actual industrial contaminated wastewater for studies is very important.

The amount of biochar required for water treatment could be reduced by an economical biochar regeneration, thereby decreasing the cost of wastewater treatment. This study has shown that Pb-loaded biochar could be regenerated using 0.1 M EDTA-2Na solution, with a very high Pb (II) ions desorption efficiency and low loss of Fe. Further studies on biochar regeneration using different eluants are required to develop suitable methods to simultaneously achieve metal ions desorption and retain the adsorption capacity of the biochar.

Furthermore, future studies should address other aspects of biochar application such as the disposal of metal-loaded biochars.

Finally, the reported studies on biochar application have examined the adsorption performance of biochar in a batch mode experiment. Further studies should therefore investigate the potential of biochars to remove heavy metal ions from ions-contaminated water in a continuous system.

Appendix A: Supplementary Data for Chapter 3.

1. Adsorbent data

Table A3.1: Mass of materials used for magnetic modification of hemp biochar

Mass of Iron salts (g)		*BC mass (g)*	*Water Vol. (ml)*	*Water Vol. (ml)*	*Water Vol. (ml)*	*ID*
$FeSO_4.7H_2O$	$Fe_2(SO_4)_3.nH_2O$		BC Suspension	$Fe_2(SO_4)_3.nH_2O$ solution	$FeSO_4$ Solution	
3.00	2.78	15	150	390	45	MHBC-1
6.00	5.55	15	150	390	45	MHBC-2
9.00	8.33	15	150	390	45	MHBC-3
12.00	11.10	15	150	390	45	MHBC-4

2. Adsorption Isotherm Models

The Langmuir isotherm model assumes that sorption occurs at specific sites, which are distributed uniformly across the adsorbent's surface [1–3]. The non-linear presentation of the equation is given in **equation A3.1**

$$q_e = \frac{q_m K_L C_e}{1+K_L C_e} \qquad \textit{Equation A3.3}$$

where q_e (mg g^{-1}) is the equilibrium metal ion loading onto the adsorbent, C_e (mg L^{-1}) is the concentration of metal ion in the solution at equilibrium, q_m (mg g^{-1}) is the adsorbent's monolayer adsorption capacity also known as q_{max}. K_L (L mg^{-1}) is the Langmuir adsorption constant related to the free energy of adsorption of adsorbent [4]. An essential characteristic of the Langmuir equation, a dimensionless separation factor R_L is given by **equation A3.2** [5]

$$R_L = \frac{1}{(1+C_0 K_L)} \qquad \textit{Equation A3.4}$$

where C_0 (mg L^{-1}) is the highest initial Pb (II) ion concentration. The value of R_L describes the isotherm type and the nature of the interaction: irreversible (R_L = 0),

favorable ($0 < R_L < 1$), unfavorable ($R_L > 1$), linear ($R_L = 1$). From **equation A3.2**, the sorption system would be favorable if $K_L > 0$.

The Freundlich model assumes a heterogeneous sorption surface area and active sites with varying energy based on a multi-layer sorption process. The adsorption intensity of the adsorbate on adsorbent is estimated by the Freundlich isotherm [6]. The non-linear form of the model is shown in **equation A3.3**.

$$q_e = K_F(C_e)^{1/n} \qquad \textit{Equation A3.5}$$

where K_F (mg g^{-1}) is the Freundlich constant related to the adsorption capacity, C_e (mg L^{-1}) is the equilibrium concentration of metal ions solution, 1/n is an empirical parameter that varies with the heterogeneity of the adsorbent material and it is related to the material's adsorption intensity [3,4].

Different from Langmuir and Freundlich models, the Temkin model takes into account the interactions between adsorbates and adsorbents and assumes that the adsorption free energy is a function of the surface coverage [7]. The Temkin isotherm model is given by **equation A3.4**.

$$q_e = \frac{RT}{b_T} In(A_T C_e) \qquad \textit{Equation A3.6}$$

where A_T is an equilibrium binding constant which corresponds to the maximum binding energy, b_T is the Temkin constant, T (K) is the temperature, and R is the ideal gas constant (8.315 J mol^{-1} K^{-1}).

Dubinin-Redushkevich (D-R) model assumes no homogeneous surface of the adsorbent [8] and is given by **equation A3.5**.

$$q_e = q_D exp\{-B_D[RT\ In(1 + \frac{1}{C_e})]^2\} \qquad \textit{Equation A3.7}$$

where q_D is the D-R isotherm constant, B_D is constant relating to the mean free energy of adsorption per mole of the adsorbate as it is travels to the surface of the absorbent from an infinite distance in the solution.

3. Non-linear regression analysis

Non-linear regression was used to evaluate all the parameters for the models. To evaluate the fitting of the models to the experimental data, the optimization procedure requires an error function to be defined. The adjusted coefficient of determination (adj. R^2), root mean square error (RMSE) and the reduced chi-square (ε^2) test were used to measure the goodness-of-fit. RMSE [9] is shown in **equation A3.6**.

$$RMSE = \sqrt{\frac{1}{m-p}\sum_{i=1}^{m}(Q_i - q_i)^2} \qquad \textit{Equation A3.8}$$

where Q_i is the measured experimental data, q_i is the isotherm model's calculated value corresponding Q_i , m is the number of data points evaluated, p is the number of parameters in the regression model. Smaller RMSE value indicates a better curve fitting.

The reduced chi-square test function [10] is shown as **equation A3.7**.

$$\varepsilon^2 = \frac{1}{v}\sum_{i=1}^{m}\frac{(Q_i - q_i)^2}{Q_i} \qquad \textit{Equation A3.9}$$

where $v = m - p$ is the degree of freedom, Q_i is the equilibrium capacity obtained from experiment, q_i is the equilibrium capacity obtained from isotherm model. If the data from model are very close to the experimental data, ε^2 will be a small number.

4. Adsorption isotherms

The Freundlich isotherm assumes an energies-heterogeneous surface and exponential distribution of adsorption sites across the adsorbent [11]. The Freundlich constant (K_F) is related to the adsorption capacity for Pb (II) ion from solution by MHBC-3 adsorbent

and was found to be 27.15 (mg g^{-1})(L mg^{-1})$^{1/n}$. This high value indicates that based on the Freundlich model assumption, the loading of Pb (II) was successful. Additionally, the Freundlich constant (n) is related to the intensity of adsorption and found to be 6.81which is high and shows that Pb (II) ion is favorably adsorbed by MHBC-3 adsorbent.

From **Table 3.4**, the Freundlich adjusted coefficient of determination, adj. R^2 value is 0.99, which is the highest among the 3 models. This indicates that the Freundlich isotherm fits the experimental adsorption data better than the Langmuir and Temkin models for Pb (II) ions adsorption. In addition, the values for the two error parameters, RMSE and ε^2 are significantly lower for the Freundlich model than for the Langmuir and Temkin models. Hence the Freundlich isotherm is the better isotherm for the description of Pb (II) ions sorption by the MHBC-3 adsorbent.

5. FT-IR spectra of biochars

The FT-IR spectra of the magnetic hemp biochar and regenerated biochar as shown in (**Figure A3.1**) showed that all active functional groups including the peak at 650 cm^{-1} assigned to Fe-O were intact; thus, the regeneration process did not significantly affect the magnetic properties of the adsorbent.

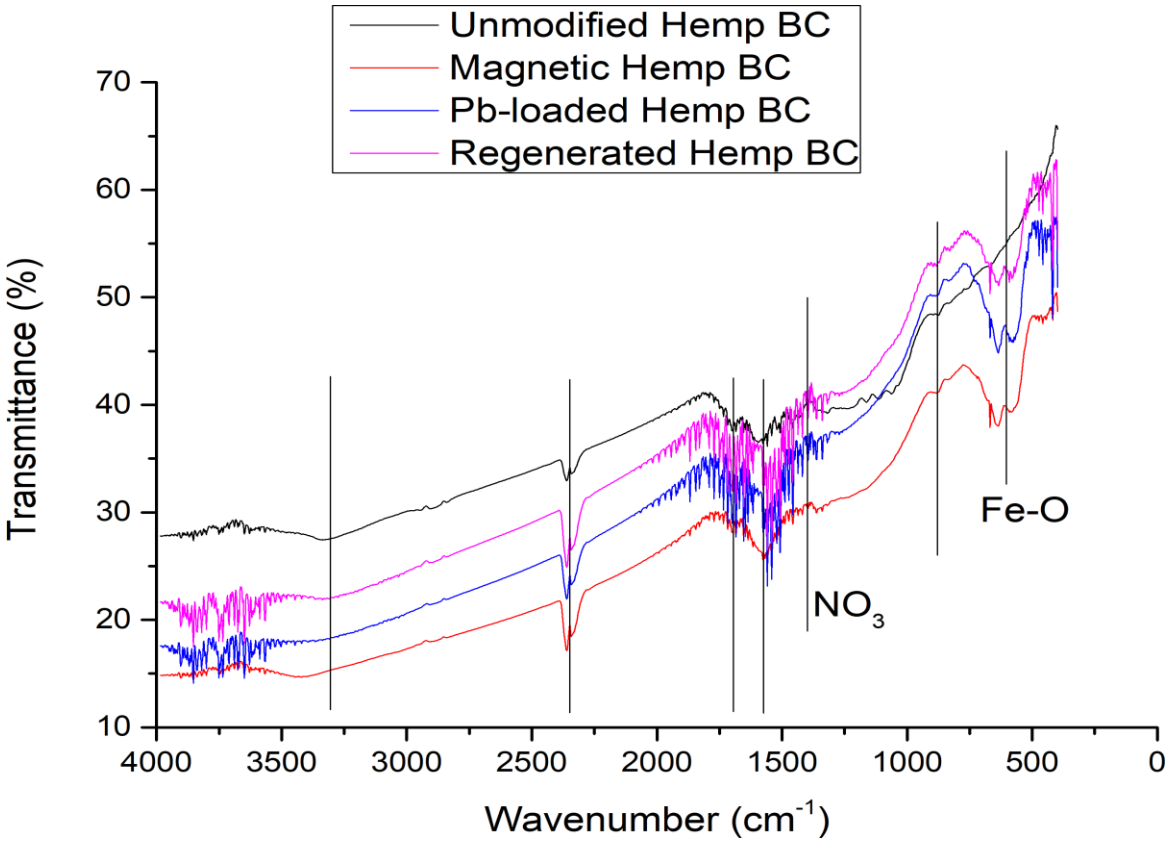

Figure A3.1*: FTIR spectra of the magnetic hemp biochar and regenerated biochar*

References

[1] Basha S, Murthy ZVP, Jha B. Sorption of Hg(II) onto Carica papaya: Experimental studies and design of batch sorber. Chem Eng J 2009;147:226–34. doi:10.1016/j.cej.2008.07.005.

[2] Langmuir I. The adsorption of gases on plane surfaces of glass, mica and platinum. J Am Chem Soc 1918;40:1361–403. doi:10.1021/ja02242a004.

[3] Asuquo ED, Martin AD. Sorption of cadmium (II) ion from aqueous solution onto sweet potato (Ipomoea batatas L.) peel adsorbent: Characterisation, kinetic and isotherm studies. J Environ Chem Eng 2016;4:4207–28. doi:10.1016/j.jece.2016.09.024.

[4] Sari A, Mendil D, Tuzen M, Soylak M. Biosorption of Cd(II) and Cr(III) from aqueous solution by moss (Hylocomium splendens) biomass: Equilibrium, kinetic and thermodynamic studies. Chem Eng J 2008;144:1–9. doi:10.1016/j.cej.2007.12.020.

[5] McKay G. Adsorption of dyestuffs from aqueous solutions with activated carbon I: Equilibrium and batch contact-time studies. J Chem Technol Biotechnol 2007;32:759–72. doi:10.1002/jctb.5030320712.

[6] Athar M, Farooq U, Aslam M, Salman M. Adsorption of Pb(II) ions onto biomass from Trifolium resupinatum: equilibrium and kinetic studies. Appl Water Sci 2013;3:665–72. doi:10.1007/s13201-013-0115-0.

[7] Deng S, Ting YP. Fungal biomass with grafted poly(acrylic acid) for enhancement of Cu(II) and Cd(II) biosorption. Langmuir 2005;21:5940–8. doi:10.1021/la047349a.

[8] Dubinin MM. The potential theory of adsorption of gases and vapors for adsorbents with energetically nonuniform surfaces. Chem Rev 1960;60:235–41. doi:10.1021/cr60204a006.

[9] Chen Z, Ma W, Han M. Biosorption of nickel and copper onto treated alga (Undaria pinnatifida): Application of isotherm and kinetic models. J Hazard Mater 2008;155:327–33. doi:10.1016/j.jhazmat.2007.11.064.

[10] Ho YS, Chiu WT, Wang CC. Regression analysis for the sorption isotherms of basic dyes on sugarcane dust. Bioresour Technol 2005;96:1285–91. doi:10.1016/j.biortech.2004.10.021.

[11] Hashemian S, Salari K, Salehifar H, Atashi Yazdi Z. Removal of azo dyes (violet b and violet 5r) from aqueous solution using new activated carbon developed from orange peel. J Chem 2013;2013. doi:10.1155/2013/283274.

Appendix B: Supplementary Data for Chapter 4.

1. Adsorption kinetic models

The processes governing the mechanism of metal removal from solution in a batch mode is identified by the adsorption kinetics of the system. The kinetic data help to determine the rate-limiting step in the adsorption process. The two sorption kinetic models used in this study to evaluate the kinetics of Pb (II) loading onto the magnetic biochars were the pseudo-first order (PFO) and pseudo-second order (PSO) kinetic models.

The non-linear versions of these kinetic models, PFO and PSO are given in **equations B4.1** and **B4.2** respectively [1].

$$q_t = q_e(1 - e^{-K_1 t}) \qquad \textit{Equation B4.1}$$

$$q_t = \frac{K_2 q_e^2 t}{1 + K_2 q_e t} \qquad \textit{Equation B4.2}$$

where q_e (mg g^{-1}) and q_t (mg g^{-1}) are the adsorption capacities at equilibrium and at any given time, t during the process respectively, K_1 (min^{-1}) and K_2 (g mg^{-1} min^{-1}) are the rate constants of PFO and PSO kinetic models respectively.

2. Sorption isotherm models

The isotherm study was performed by shaking 0.02 g of the adsorbents with 40 mL of Pb (II) solution at different initial concentrations. The isotherms for Pb (II) adsorption by biochars were characterized by fitting the Langmuir, Freundlich, Temkin models with the data from experimental trials.

The Langmuir isotherm is based on the assumption that adsorption process happens at specific sites that are uniformly distributed across the adsorbent's surface area [2–4]. The non-linear form of Langmuir model is presented in **equation B4.3**.

$$q_e = \frac{q_m K_L C_e}{1+K_L C_e}$$ *Equation B4.3*

where q_e (mg g^{-1}) is the metal ion uptake by adsorbent at equilibrium, q_m (mg g^{-1}) is the adsorbent's monolayer adsorption capacity also called q_{max}, C_e (mg L^{-1}) is the equilibrium concentration of metal ion in the solution, K_L (L mg^{-1}) is the Langmuir adsorption constant related to the adsorbent's free energy of adsorption [5]. A very important characteristic of the Langmuir model is a dimensionless separation factor, R_L as given by **equation B4.4** [6]

$$R_L = \frac{1}{(1+C_0 K_L)}$$ *Equation B4.4*

where C_0 (mg L^{-1}) is the highest initial metal ion concentration. The nature of the interaction and isotherm type depends the value of R_L. Favorable ($0 < R_L < 1$), unfavorable ($R_L > 1$), linear ($R_L = 1$), irreversible ($R_L = 0$). From **equation B4.4**, the adsorption process most likely be favorable if $K_L > 0$.

The Freundlich isotherm assumes that the adsorption surface area is heterogeneous with varying energies of active sites distributed randomly on adsorbent's surface. It assumes a multi-layer adsorption process. The Freundlich model estimates the adsorption intensity of the adsorbate on adsorbent [7]. The non-linear version of the model is given by **equation B4.5**.

$$q_e = K_F (C_e)^{1/n}$$ *Equation B4.5*

where C_e (mg L^{-1}) is the metal solution's equilibrium concentration, K_F (mg g^{-1}) is the Freundlich constant related to the adsorbent's adsorption capacity, 1/n is an empirical parameter related to the material's adsorption intensity and it varies with the heterogeneity of the adsorbent material [4,5].

The Temkin isotherm accounts for the interactions between adsorbents and adsorbates. It assumes that the free energy of adsorption is a function of the surface coverage [8]. The Temkin model is given in **equation B4.6**.

$$q_e = \frac{RT}{b_T} In(A_T C_e) \qquad \textit{Equation B4.6}$$

where b_T is the Temkin constant, T (K) is the temperature, A_T is an equilibrium binding constant corresponding to the maximum binding energy and R is the ideal gas constant (8.315 J mol^{-1} K^{-1}).

3. Non-linear regression analysis

The parameters for the models were evaluated using the non-linear regression analysis. The adjusted coefficient of determination (adj. R^2), root mean square error (RMSE) and the reduced chi-square (ε^2) test were the parameters used to determine the goodness-of-fit of the model to the experimental data. RMSE [9] is presented by **equation B4.7**.

$$RMSE = \sqrt{\frac{1}{m-p}\sum_{i=1}^{m}(Q_i - q_i)^2} \qquad \textit{Equation B4.7}$$

where Q_i is the experimentally determined data, q_i is the isotherm model's calculated value corresponding Q_i , p is the number of parameters in the regression model while m is the number of data points evaluated. A Smaller value of RMSE indicates a better fitting of model with the experimental data.

The reduced chi-square test function [10] is given in **equation B4.8**.

$$\varepsilon^2 = \frac{1}{v}\sum_{i=1}^{m}\frac{(Q_i - q_i)^2}{Q_i} \qquad \textit{Equation B4.8}$$

where $v = m - p$ is the degree of freedom, q_i is the equilibrium capacity calculated from isotherm model, Q_i is the equilibrium capacity determined from experimental

data. If data from model are closely fit the experimental data, the value of ε^2 will also be a small number.

References

[1] Asuquo E, Martin A, Nzerem P, Siperstein F, Fan X. Adsorption of Cd(II) and Pb(II) ions from aqueous solutions using mesoporous activated carbon adsorbent: Equilibrium, kinetics and characterisation studies. J Environ Chem Eng 2017;5:679–98. doi:10.1016/j.jece.2016.12.043.

[2] Basha S, Murthy ZVP, Jha B. Sorption of Hg(II) onto Carica papaya: Experimental studies and design of batch sorber. Chem Eng J 2009;147:226–34. doi:10.1016/j.cej.2008.07.005.

[3] Langmuir I. The adsorption of gases on plane surfaces of glass, mica and platinum. J Am Chem Soc 1918;40:1361–403. doi:10.1021/ja02242a004.

[4] Asuquo ED, Martin AD. Sorption of cadmium (II) ion from aqueous solution onto sweet potato (Ipomoea batatas L.) peel adsorbent: Characterisation, kinetic and isotherm studies. J Environ Chem Eng 2016;4:4207–28. doi:10.1016/j.jece.2016.09.024.

[5] Sari A, Mendil D, Tuzen M, Soylak M. Biosorption of Cd(II) and Cr(III) from aqueous solution by moss (Hylocomium splendens) biomass: Equilibrium, kinetic and thermodynamic studies. Chem Eng J 2008;144:1–9. doi:10.1016/j.cej.2007.12.020.

[6] McKay G. Adsorption of dyestuffs from aqueous solutions with activated carbon I: Equilibrium and batch contact-time studies. J Chem Technol Biotechnol 2007;32:759–72. doi:10.1002/jctb.5030320712.

[7] Athar M, Farooq U, Aslam M, Salman M. Adsorption of Pb(II) ions onto biomass from Trifolium resupinatum: equilibrium and kinetic studies. Appl Water Sci 2013;3:665–72. doi:10.1007/s13201-013-0115-0.

[8] Deng S, Ting YP. Fungal biomass with grafted poly(acrylic acid) for enhancement of Cu(II) and Cd(II) biosorption. Langmuir 2005;21:5940–8. doi:10.1021/la047349a.

[9] Chen Z, Ma W, Han M. Biosorption of nickel and copper onto treated alga (Undaria pinnatifida): Application of isotherm and kinetic models. J Hazard Mater 2008;155:327–33. doi:10.1016/j.jhazmat.2007.11.064.

[10] Ho YS, Chiu WT, Wang CC. Regression analysis for the sorption isotherms of basic dyes on sugarcane dust. Bioresour Technol 2005;96:1285–91. doi:10.1016/j.biortech.2004.10.021.

Curriculum Vitae

Candidates full name:

Patrick Muesi Godwin

Universities attended:

University of New Brunswick, 2018 – 2020

M.ScE Candidate, Department of Chemical Engineering

University of Manchester, United Kingdom, 2013 – 2017

M.Eng (Hons), Department of Chemical Engineering

Publications:

Godwin P, Pan Y, Xiao H, Afzal MT. Progress in the preparation and application of modified biochar for improving heavy metal ion removal from wastewater. J Bioresour Bioprod 2019;4:31–42. doi:10.21967/JBB.V4I1.180.

Co-authored Publications:

Ni S, Zhang H, Godwin PM, Dai H, Xiao H. ZnO nanoparticles enhanced hydrophobicity for starch film and paper. Mater Lett 2018;230:207–10. doi:10.1016/j.matlet.2018.07.075.

Zhong Y, Godwin PM, Jin Y, Xiao H. Biodegradable Polymers and Green-based Antimicrobial Packaging Materials: A mini-review. Adv Ind Eng Polym Res 2019. doi:10.1016/J.AIEPR.2019.11.002.

Work Experience:

Junior Process Engineer, INVISTA, United Kingdom, (July 2015 – Sept. 2016)

Associate Process Engineer, J.D. Irving, Limited, Canada, (Jan. 2020 – April 2020)